UNIVERSITY OF LONDON THESIS

Degree PhD Year 2007 Name of Author MANI, Alireza

Cardiac rhythm abnormalities in cirrhosis

by

Alireza Mani

A thesis submitted in the fulfilment of the requirements for the degree of
Doctor of Philosophy (Ph.D.)

from

University College London
(UCL)
University of London

ProQuest LLC
789 East Eisenhower Parkway
P.O. Box 1346
Ann Arbor, MI 48106-1346

Declaration

I, Alireza Mani, confirm that the work presented in this thesis is the result of my own independent investigation carried out at the University College London. Where information has been derived from other sources, I confirm that this has been indicated in the thesis.

Signed

Date: 12 December 2007

ABSTRACT

Liver cirrhosis is associated with cardiovascular dysfunction including decreased heart rate variability and impaired acceleration of the heart rate in response to sympathetic activation (chronotropic incompetence). In this thesis, the hypothesis that increased formation of reactive nitrogen species in cirrhosis causes nitration or S-nitrosation of cardiac proteins and leads to impaired chronotropic function was assessed in an experimental model of cirrhosis. Cardiac chronotropic responsiveness to ß-adrenergic stimulation was assessed *in vitro* using spontaneous beating rat isolated atria. A novel mass spectrometric method was developed for dynamic assessment of nitration reactions based on the nitration of deuterium-labelled *para*-hydroxyphenyl acetic acid. Nitration of cardiac proteins was measured by mass spectrometry and located by immunogold electron microscopy. Marked impairment of chronotropic responses of isolated atria to isoproterenol was observed in rats with cirrhosis, which normalized after the administration of N-acetylcysteine (a scavenger of reactive oxygen and nitrogen species) or L-NAME (a nitric oxide synthase inhibitor). The levels of protein-bound nitrotyrosine in atrial tissue increased from 16 ± 1 to 23 ± 3 pg/g tyrosine in rats with cirrhosis, and decreased to 15 ± 1 and 17 ± 1 pg/g after treatment with L-NAME and N-acetylcysteine, respectively ($P<0.05$). Immunogold electron microscopy demonstrated increased nitration of filaments and mitochondria in the atria of rats with cirrhosis. A chemiluminescence-based method was developed to stabilise and measure S-nitrosothiols in tissues. There was no difference in cardiac S-nitrosothiols following induction of cirrhosis, and neither N-acetylcysteine nor L-NAME had any effect on the cardiac levels of S-nitrosothiols. Autonomic regulation of cardiac function was assessed by analysis of heart rate variability in anesthetized rats using Fast Fourier Transformation. Heart rate variability analysis showed impaired sympathovagal balance towards increase of cardiac sympathetic activity in rats with cirrhosis ($P<0.05$). However there was no change in the sympathovagal balance following N-acetylcysteine or L-NAME adminstration in cirrhotic rats. In conclusion, abnormal cardiac chronotropic function in cirrhosis is associated with increased nitration of cardiac proteins. Two independent treatments (N-acetylcysteine and L-NAME) that decrease nitration of cardiac proteins led to normalization of cardiac responses. Nitration of critical proteins in cardiac tissue may lead to abnormal cardiac function.

ACKNOWLEDGEMENTS

I wish to thanks my supervisor, Kevin Moore for the considerable time and care that he has devoted to my progress at all times during my staying in London.

Thanks are due to Sara Montagnese, Marsha Morgan, Richard Ollosson, Silvia Ippolito, Ahmad R. Dehpour, David Harry, Nelson Orie, Jim Owen, Pat Blake, Mohammad R. Ebrahimkhani, Leonard Damelin and Martin Hughes for their invaluable support and friendship.

I acknowledge the award of a travelling fellowship by the Wellcome Trust UK

And again special thanks must go to Tara, Jelveh, Sotoodeh and Mohammad, for their love and support

STATEMENT OF ORIGINALITY

The projects described in this thesis were designed and performed by myself except as stated below:

In chapter 4, the electron microscopy images were prepared by Mr Innes R Clatworthy (Electron Microscopy Unit, Hampstead Campus, UCL, London).

The human study presented in chapter 5 was performed in collaboration with Dr Marsha Y Morgan and Dr Sara Montagnese (Department of Medicine, Hampstead Campus, UCL, London). The electrophysiological data from patients with cirrhosis were recorded by Dr Sara Montagnese (chapter 5). Mr Clive Jackson (Department of Neurophysiology, Royal Free Hospital NHS Trust, London) prepared the software to detect R-R intervals which was used for heart rate variability analysis from human electrophysiological recordings (chapter 5). The plasma levels of inflammatory cytokines in patients with cirrhosis were measured by Dr Robert Stephens (Institute of Child Health, UCL, London).

LIST OF CONTENTS

LIST OF FIGURES

LIST OF TABLES

Chapter 1: Cardiovascular dysfunction in liver cirrhosis

1.1 Cirrhosis

Liver cirrhosis is defined as a diffuse process with fibrosis and nodule formation in the liver (Sherlock and Dooley 2002). Liver injury leading to hepatic fibrosis occurs in response to a variety of insults, which trigger a wound healing-like reaction. During chronic liver injury, *hepatic stellate cells* become activated and express a combination of matrix metalloproteinases which have the ability to induce global changes in the liver extra-cellular matrix. This pattern is characterised by increased degradation of the sub-endothelial basement membrane, loss of normal liver architecture, and inhibition of degradation of liver collagen (Friedman 2007). Chronic liver injury leading to hepatic cirrhosis occurs in response to a variety of insults including chronic viral hepatitis (HBV, HCV), alcohol misuse, metabolic disorders (e.g. haemochromatosis and Wilson's disease), prolonged cholestasis (e.g. primary biliary cirrhosis), autoimmune hepatitis and fatty liver disease.

1.2 Consequences of liver cirrhosis

Cirrhosis has certain clinical and pathological associations such as splenomegaly, ascites, oesophageal varices, hepatic encephalopathy, impaired coagulation and hypoalbuminemia. Cirrhosis results in two major events: *portal hypertension* and *hepato-cellular failure*. Prognosis and treatment depend on the magnitude of these two factors (Sherlock and Dooley 2002).

***Portal hypertension*:** Portal hypertension is the most common and lethal complication of chronic liver diseases; it is responsible for the development of oesophageal varices, variceal haemorrhage, ascites, splenomegaly and renal dysfunction observed in patients with cirrhosis. Portal hypertension is defined by a pathologic increase in portal pressure, in which the pressure gradient between the portal vein and inferior vena cava (the portal pressure gradient) is increased above the upper limit of 5 mm Hg (Bosch et al. 2007). Portal hypertension becomes clinically significant when the portal pressure gradient increased above the threshold value of 10 mm Hg (e.g. formation of varices) or 12 mm Hg (e.g. variceal bleeding, ascites). Portal pressure gradient values between 6 and 10 mm Hg represent sub-clinical portal hypertension in humans (Bosch et al. 2007). Portal pressure gradient is determined be the product of blood flow and

vascular resistance to portal blood flow and aggravated by an increased portal venous inflow.

Increased resistance to sinusoidal blood flow in cirrhosis represents not only disruption of liver's vascular structure by liver disease (e.g. fibrosis) but also a dynamic component resulting from the active contraction of vascular smooth muscles, myo-fibroblasts, and hepatic stellate cells (Bosch et al. 2007). Active contraction is caused by decreased intra hepatic production of vasodilators such as nitric oxide (NO) and by increased release of endogenous vasoconstrictors such as endothelins (Leivas et al. 1998). Apart from increased hepatic vasculature resistance in cirrhosis, increased portal venous inflow secondary to *splanchnic vasodilatation* usually aggravates elevation of portal pressure (Figure 1.1).

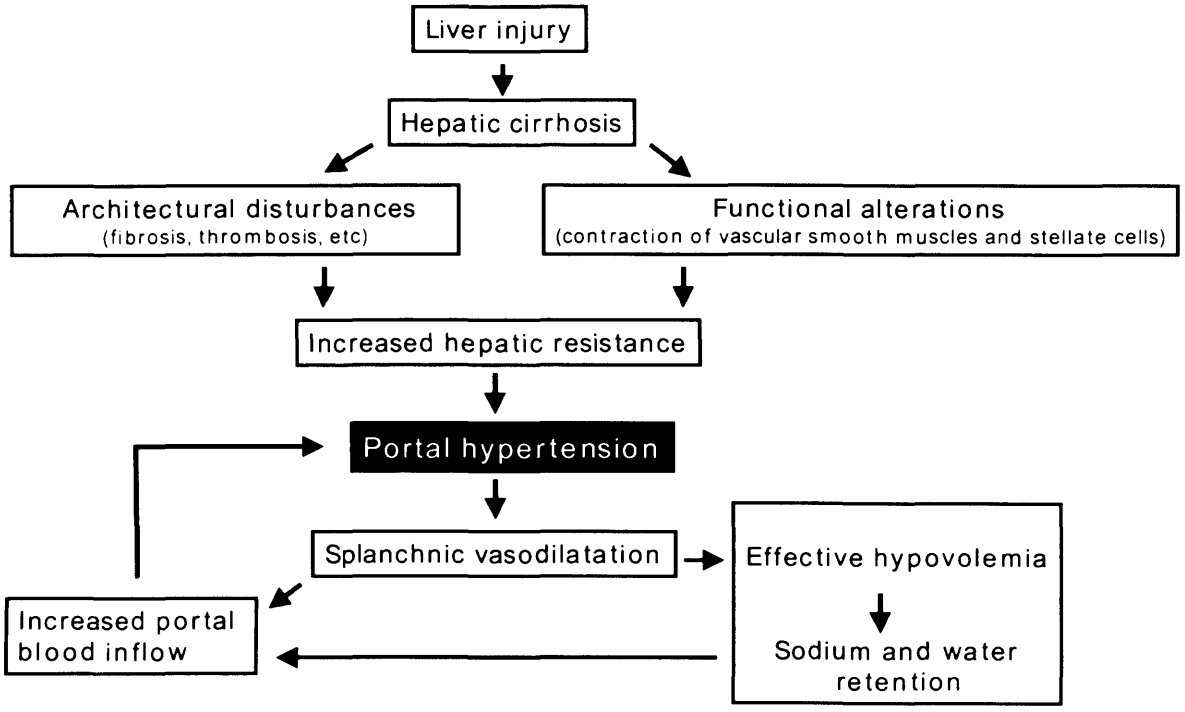

Figure 1.1. Schematic representation of the pathophysiology of portal hypertension in hepatic cirrhosis.

***Splanchnic vasodilatation*:** An increased portal venous inflow is characteristically observed in advanced stages of portal hypertension and is the result of marked arteriolar dilatation in the splanchnic organs draining into the portal vein (Bosch and Garcia-Pagan 2000). The increased blood flow contributes to the portal hypertensive syndrome. Different mechanisms have been suggested to explain the development of these haemodynamic changes. Initial studies focused on the potential role of increased levels of circulating vasodilators. Several candidate mediators have been proposed, most of them being vasodilator of splanchnic origin that undergo hepatic metabolism and accumulate in systemic circulation when hepatic uptake is reduced in liver disease or during portosystemic shunting. Splanchnic vasodilatation present in portal hypertension is likely to be multi-factorial in origin, being promoted in part by an excessive release of glucagon, nitric oxide (NO), carbon monoxide, endocannabinoids and other vasoactive mediators. In addition, experimental studies suggest that when one of the vasoactive mediators is chronically inhibited, the enhancement of other vasoactive pathways may prevent the correction of splanchnic vasodilation (Fernandez et al. 1996).

Glucagon: Many studies have demonstrated that plasma glucagons levels are elevated in patients with cirrhosis and experimental models of portal hypertension. Hyper-glucagonemia results, in part, form a decreased hepatic clearance of glucagons, but more importantly from an increased formation of glucagons by pancreatic cells (Gomis et al. 1994). The support for a role of glucagons in modulating splanchnic blood flow comes from physiologic studies showing that in rats with experimental portal hypertension, normalizing circulating glucagon levels by administering anti-glucagon antibodies or infusing somatostatin partially reverses the increase in splanchnic blood flow, a response that can be specifically blocked by the concomitant infusion of glucagon (Benoit et al. 1986; Kravetz et al. 1988). Glucagon might promote vasodilatation by a dual mechanism: Relaxing the vascular smooth muscle and decreasing its sensitivity to endogenous vasoconstrictors such as norepinephrine, angiotensin II and vasopressin (Pizcueta et al. 1991; Wiest et al. 2001). The role of glucagon in the splanchnic hyperemia of portal hypertension provides a rationale for the use of somatostatin and its analogues to treat portal hypertension (Bosch et al. 2007).

Nitric Oxide (NO): Experimental studies of specific NO synthase (NOS) inhibitors have shown that NO is involved in the regulation of splanchnic and systemic hyperdynamic circulation in portal hypertension (the chemistry and physiological aspects of NO is reviewed in chapter 1.4). Inhibition of NOS in portal hypertensive rats reverses the vascular hypo-responsiveness to vasoconstrictors that develops in this model where is thought to contribute to systemic and splanchnic vasodilatation (Sieber and Groszmann 1992a,b). In addition, increased synthesis of NO has been demonstrated *in vitro* in perfused mesenteric artery preparations from portal hypertensive rats (Hori et al. 1998). The finding of increased serum and urinary concentrations of nitrite and nitrate in patients with cirrhosis, which are end-products of NO oxidation, also supports a role for NO in the genesis of the circulatory disturbances of portal hypertension (Guarner et al. 1993).

The role of different isoforms of NOS in increased NO synthesis in cirrhosis is controversial (see Farzaneh-Far and Moore 2001 for review). In portal hypertensive animals, increased NO synthesis by eNOS in the splanchnic circulation precedes the development of hyperdynamic circulation and is mostly due to an up-regulation of endothelial NOS (eNOS) catalytic activity, rather than eNOS over-expression (Wiest et al. 1999). Factors likely to activate eNOS include shear stress and pro-inflammatory mediators (Farzaneh-Far and Moore 2001). Indeed, eNOS phosphorylation by Akt seems to be the mechanism of the initial up-regulation of eNOS activity (Iwakiri et al. 2002). Later on, other mechanisms become important, including an enhanced signalling of the molecular chaperone heat shock protein 90 (Hsp90) (Garcia-Cardena et al. 1998; Shah et al. 1999). In addition, in cirrhotic rats with ascites, it was shown that bacterial translocation further increased eNOS activity in the mesenteric artery, probably in response to increased levels of tumor necrosis-α (TNF-α). TNF-α production was associated with elevated levels of tetrahydrobiopterin (BH4), a TNF-α-stimulated cofactor and enhancer of eNOS-derived NO biosynthesis and NOS activity (Wiest et al. 1999). Fig. 1.2 summarises the involvement of NO in genesis of splanchnic and hyperdynamic circulation in cirrhosis.

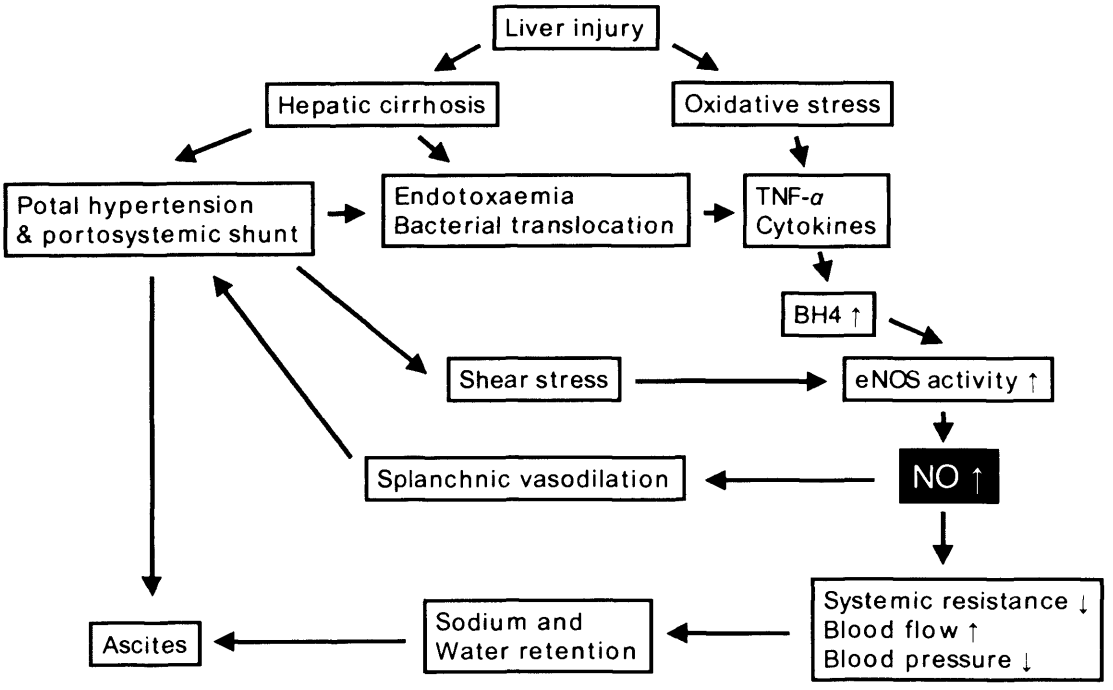

Figure 1.2. Nitric oxide over-production in cirrhosis. Liver injury results in increased nitric oxide synthesis by eNOS through a variety of mechanisms. Once underway, this process is reinforced by the effects of shear stress on endothelium which increases eNOS activity.

Nitric oxide paradox in cirrhosis: Nitric oxide displays an astonishing array of biological functions. In liver disease, one or more of these functions may be disturbed by either too much production of NO or too little. Systemically, increased synthesis of NO is a major contributing factor in the establishment of the splanchnic vasodilatation and hyperdynamic circulation in cirrhosis. On the other hand, NO plays a protective role in maintaining the patency of the hepatic microvasculature and local deficiency of NO in the liver may contribute to portal hypertension. Alterations in eNOS-derived NO synthesis in the intrahepatic microcirculation and in the splanchnic and systemic vasculature are strikingly opposite. Liver cirrhosis is associated with endothelial dysfunction and deficiency of endothelial NO release in hepatic sinusoids (Loureiro-Silva et al. 2003). Deficiency of NO in the microcirculation results in impaired vasoregulation and enhanced vasoconstriction, leading to increased vascular tone. In

contrast, the splanchnic and systemic vasculature exhibit increased endothelial NO synthesis. This increase in eNOS-derived NO-synthesis leads to arterial vasodilation and plays a crucial role in the development of the hyperdynamic circulation and its subsequent lethal complications of chronic liver diseases. It is the up-regulation of the endothelial NO-synthesizing machinery in the splanchnic and systemic circulation that complicates the use of nitrovasodilators for the delivery of NO to the intrahepatic microcirculation. Any systemic administration of NO-donors (e.g. organic nitrates) will have a more marked and detrimental effect in the splanchnic and systemic circulation than a beneficial effect in the intrahepatic circulation. Therefore, the development of liver specific NO-donors will be of great importance for optimizing therapy of liver cirrhosis.

Carbon monoxide: Recent studies have shown an increased expression and activity of inducible form of Haem oxygenase (HO), in splanchnic tissues form animals with portal hypertension (Fernandez and Bonkovsky 1999). In addition, the simultaneous inhibition of NOS and HO has been shown to completely reverse the reduced vasoconstrictor response to vasoconstrictors in the mesenteric vascular bed (Fernandez et al. 2001).

Endocannabinoids: Recent data suggest a role for endocannabinoids in the hyperdynamic circulation of portal hypertension (Batkai et al. 2001; Ros et al. 2002; Moezi et al. 2006). Increased levels of the endogenous cannabinoid anandamide (arachidonyl ethanolamide) have been found in the monocyte fraction of blood from cirrhotic humans and rats, and an increased expression of the cannabinoid receptor (CB1) was found in hepatic human endothelial cells (Batkai et al. 2001). In addition, CB1 receptor blockade has been found to reduce portal blood flow and pressure and increase arterial pressure in cirrhotic rats (Batkai et al. 2001; Ros et al. 2002). The mechanism of action is not well understood. It has been suggested that it could be due to, at least in part, to an increased NO production, mediated by the activation of CB1 or Vanilloid (VR1) receptors (Moezi et al. 2006).

Other vasoactive mediators: Several other circulating vasodilators such as prostacyclin (PGI_2), calcitonin gene-related polypeptide (CGRP), and adenosine have been implicated in splanchnic vasodilatation (Bosch et al. 2007). Altogether, these data suggest that the splanchnic vasodilatation is likely to be multi-factorial in origin

and coupling of several vasoactive systems may cause the splanchnic vasodilatation seen in portal hypertensive states.

***Hyperdynamic circulation in cirrhosis*:** It appears that the haemodynamic changes in cirrhosis begin in the splanchnic circulation, at some early stage in the natural history of patients with cirrhosis and portal hypertension. At some further stage, the *hyperdynamic circulation* becomes clinically evident. The Oxford Textbook of Medicine describes the clinical features hyperdynamic circulation as flushed extremities, bounding pulses and capillary pulsations in cirrhosis which is associated with systemic hypotension, tachycardia, elevated cardiac output and reduced total systemic vascular resistance (Sherlock 1986). In 1988, Schrier and colleagues proposed the *'peripheral arterial vasodilatation hypothesis'* to account for this hyperdynamic circulation as well as the initiation of sodium and water retention in cirrhosis (Schrier et al. 1988). Thereafter, Vallance and Moncada (1991) suggested a mechanism by which enodtoxaemia induces NO over-production and peripheral vasodilatation in patients with liver disease. Their hypothesis was based on data provided by other experiments: (1) NO synthesis is induced in the endothelium and smooth muscle when vascular tissue is exposed to endotoxin or cytokines *in vitro* (Beasley 1990). (2) Infusion of endotoxin in humans leads to the gradual appearance of peripheral vasodilatation (Suffredini et al. 1989). (3) Inhibitors of NOS increase blood pressure of patients with septic shock (Petros et al. 1991) and (4) High circulating levels of endotoxin are found in cirrhotic patients with or without clinical evidence of infection (Lumsden et al. 1988). Evidence supporting a role for NO has been obtained from various experimental models of cirrhosis. For example, administration of NOS inhibitors to cirrhotic rats increases systemic vascular resistance, thus modulating hyperdynamic circulation (Calver et al. 1994). Moreover, the production of NO is observed to increase in cirrhotic patients by using various parameters including increased plasma nitrate + nitrite (NO end products) and urinary cGMP levels (Fernandez-Rodriguez et al. 1997). As mentioned above several other circulating vasodilators (e.g. endocannabinoids, glucagon and CGRP) may also be implicated in the peripheral vasodilatation observed in cirrhosis. Overall, peripheral vasodilatation in cirrhosis activates three major *compensatory* mechanisms (see Dagher and Moore 2001 for review):

1. Renin-angiotensin-aldosterone system: This leads to water and salt retention and exacerbate accumulation of fluids in the peritoneum (*Ascites*).

2. Sympathetic nervous system. This impairs the renal auto-regulatory mechanism which regulates kidney perfusion.

3. Stimulation of arginine vasopressin (AVP) release from the pituitary gland: This can lead to impaired solute-free water excretion by the kidney and *dilutional hyponatremia,* a complication in patients with advance cirrhosis.

These compensatory mechanisms along with oxidative stress (see below) are major cause of renal vasoconstriction in cirrhosis (Dagher and Moore 2001). Renal impairment in most patients with cirrhosis is secondary to functional abnormalities that occur in response to a severe systemic vasodilatation which triggers an intense compensatory neuro-hormonal response causing sodium retention, solute-free water retention and finally, severe renal vasoconstriction. *Hepatorenal syndrome* is the end of the spectrum of functional renal abnormalities by a severe vasoconstriction of the renal circulation. It seems that the pathogenesis of hyperdynamic circulation is complex with several non-linear interactions between vascular and neural mechanisms.

***Role of oxidative stress in the pathogenesis of hyperdynamic circulation*:** Administration of low molecular weight thiols (e.g. N-acetylcysteine and lipoic acid) prevents the development of hyperdynamic circulation in rat models of portal hypertension (Fernando et al. 1998; Marley et al. 1999). Since low molecular weight thiols have antioxidant properties, these observations suggest that oxidative stress may have a role in the pathogenesis of hyperdynamic circulation in cirrhosis. A marked overproduction of F_2-isoprostanes has also been reported in experimental models as well as patients with cirrhosis (Fernando et al. 1998; Marley et al. 1999; Holt et al. 1999). Isoprostanes are a group of vaso-active compounds which derived from the free radical oxidation of arachidonic acid (Morrow et al. 1992). In a landmark study Holt et al., (1999) observed that N-acetylcysteine ameliorates renal dysfunction and survival rate in patients with hepatorenal syndrome, suggesting a relationship between oxidative stress and pathogenesis of hyperdynamic circulation. The mechanism of how low molecular weight thiols such as N-acetylcysteine and lipoic acid improve the

haemodynamic abnormalities in cirrhosis is not well understood. However it was postulated that N-acetylcysteine might enhance cell redox status and cellular rodox signalling (see chapter 1.8).

1.3 Cardiac dysfunction in cirrhosis

Cirrhosis is known to be associated with numerous cardiac abnormalities, but only until relatively recently did the development of techniques for precisely measuring cardiovascular variables allow determination of the extent of these anomalies. Cardiac abnormalities in cirrhosis include:

1. Chronotropic incompetence
1. High cardiac output at rest but blunted contractile responsiveness to physical or pharmacological stimuli (this phenomenon has been controversially termed *cirrhotic cardiomyopathy*).
3. Prolongation of QT interval
4. Decreased heart rate variability (HRV).

1.3.1 Chronotropic incompetence

Chronotropic incompetence in cirrhosis is defined as impaired acceleration of heart rate in response to physiological stimuli (see Zambruni et al. 2006 for review). Although resting tachycardia is a feature of the hyperdynamic circulatory syndrome, maneuvers leading to either activation of the sympathetic nervous system (or alter the sympathovagal balance in favour of the sympathetic system) such as Valsalva maneuver, tilting, ice-cold skin stimulation and physical exercise, do not evoke an adequate acceleration of heart rate (Bernardi et al. 1987; Lee et al. 1990; Bernardi et al 1991, Wong 2001). Impaired chronotropic responses can be observed in patients with cirrhosis regardless of the aetiology of cirrhosis, and its prevalence increases with the disease severity (Bernardi et al 1991). Accordingly, the dose of ß-agonists (such as isoproterenol) required to increase heart rate by 25 beats/min increases by threefold with respect to healthy subjects (Ramond et al. 1986). Likewise, in rats with biliary cirrhosis, a four fold increase in the dose of isoproterenol was needed to elicit a 10% increase in basal heart rate compared with sham-operated animals (Lee et al. 1990).

Whether and to what extent abnormal chronotropic responses have a clinical impact in patients with cirrhosis is unknown. Recent studies on the haemodynamic abnormalities associated with renal failure precipitated by spontaneous bacterial

peritonitis (Ruiz-del-Arbol et al. 2003; Ruiz-del-Arbol et al. 2005) suggest that chronotropic incompetence may play an important role in the pathophysiology of such complications. Contrary to preconceived ideas, renal failure precipitated by spontaneous bacterial peritonitis is not associated with a significant drop in peripheral vascular resistance, but is associated with a reduction in cardiac output. Since cardiac output is the product of heart rate and the stroke volume (cardiac output = heart rate x stroke volume), there may be two causes for this reduction of cardiac output, such as impaired heart contractility or impaired heart rate acceleration. What is certain is that heart rate failed to increase in these patients, even in the face of a dramatic activation of sympathetic nervous system (Ruiz-del-Arbol et al. 2003; Ruiz-del-Arbol et al. 2005). A similar haemodynamic abnormality has been reported in paracentesis-induced circulatory dysfunction. In fact, even though a further reduction in peripheral vascular resistance actually occurred, a striking feature was that cardiac index did not increase at all. Again, one possible reason for this was that heart rate did not show any significant acceleration (Ruiz-del-Arbol et al. 1997). Possibly, these reports are the first to demonstrate how chronotropic incompetence can assume clinical relevance in patients with cirrhosis.

The mechanism of chronotropic incompetence in cirrhosis is not well understood. Mani et al. (2002) have previously reported that, NO plays a dual role in the regulation of the sino-atrial pacemaker cells and this may have a role in the pathophysiology of chronotrpic incompetence in rats with biliary cirrhosis. We have further investigated this which is presented in Chapter 4.

1.3.2 "Cirrhotic cardiomyopathy"

This syndrome was first described in the late 1960s, although for many years, it was mistakenly attributed to latent or sub-clinical alcoholic cardiomyopathy (see Lee et al. 2007 for review). In 1953, Kowalski and Abelmann showed that an increased cardiac output, decreased blood pressure, and total peripheral resistance along with a prolonged QT interval were present in alcoholic cirrhosis. In another study, Regen et al. (1969) injected angiotensin (a potent vasoconstrictor) into ten alcoholic cirrhotic patients and noted a rise in cardiac output and stroke volume; however it was significantly less than the effect in healthy controls. Subsequent studies in human and animal models with non-alcoholic cirrhosis, dating from the mid-1980s showed a

similar pattern of increased baseline cardiac output with blunted response to physical or pharmacological stress (see Lee et al. 2007 for review). Although nowadays presence of cardiac dysfunction in cirrhosis is considered to be a well-described clinical entity, however the term "cirrhotic cardiomyopathy" is still controversial.

Left ventricular hypertrophy has been reported in patients and rats with cirrhosis (Pozzi et al. 1997; Inserte et al. 2003). Histomorphometric analysis revealed a significant increase in cell volume of cardiomyocytes from the left ventricle of cirrhotic rats, but no differences in myocardial collagen content (Inserte et al. 2003). Echocardiography data in patients has also shown an increase in left ventricle wall thickness in cirrhotic patients with ascites (Pozzi et al. 1997). Left ventricular wall thickness in this patient population probably reflects an adaptive change in response to hyperdynamic circulation and not necessarily the presence of cardiomyopathy (Inserte et al. 2003). However, elevated circulating levels of brain natriuretic peptide (BNP; the gene of which is predominantly expressed in failing cardiomyocytes) has been reported in cirrhosis (Henriksen et al. 2003), which most likely reflects increased cardiac ventricular generation of these peptides and thus indicates the presence of myocardial dysfunction.

Studies on isolated papillary muscle from rats with cirrhosis have shown a blunted inotropic response upon stimulation with ß-adrenergic agonists (Ma et al. 1996; Liu et al. 2000). In contrast, studies on isolated perfused hearts pereparations (at constant pressure), were unable to detect any contractility dysfunction in experimentally induced cirrhosis (Inserte et al. 2003; Mani and Moore, unpublished). The differences in the perfused heart and papillary muscle studies can be explained in part by the different influence of left ventricular hypertrophy in both models. In the papillary muscle model, generated tension is calculated by dividing generated force by cross-sectional muscle area. In the presence of hypertrophy, cross-sectional area is greater, and, for the same contractile force, generated tension will be smaller. In contrast, in the isolated heart model generated pressure, instead of tension, is analyzed. According to the Laplace law, wall tension in the intact heart is calculated as the product of pressure by cavity radius divided by wall thickness. Because cavity radius in cirrhotic and control hearts are equal, by applying the Laplace formula, generated wall tension in cirrhotic model is reduced by ~ 20 % with respect to hearts from control rats. In

other words, because, in cirrhotic rats, higher ventricular mass produces the same total work, work produced by unit of myocardial mass is smaller (Inserte et al. 2003).

Lee and colleagues have extensively studied the mechanism of cardiac dysfunction in cirrhotic rats using isolated papillary muscle (Ma et al. 1996; Liu et al. 2000; Liu et al. 2001; Gaskari et al. 2005). In their model, blunted inotropic response to adrenergic stimulation in cirrhotic rats has been shown to be a reversible phenomenon. Thus, pre-incubation of the papillary muscle with NOS inhibitors, haem oxygenase inhibitors as well as CB1 receptor antagonists normalizes the inotropic responsiveness to adrenergic stimulation in bile duct ligated rats (Liu et al. 2000; Liu et al. 2001; Gaskari et al. 2005). Based on these studies it has been suggested that over-activity of NO, carbon monoxide and endocannabinoid systems might have a role in the genesis of cardiac inotropic dysfunction in cirrhosis. Considering the undeniable interrelation of these systems, further studies are required to elucidate the complex mechanism of the observed effects.

Overall, it seems that cirrhosis is associated with a decrease in responsiveness of both cardiomyocytes and sino-atrial pacemaker cells to adrenergic stimulation. However whilst, a moderate left ventricular hypertrophy compensates for the blunted inotropic response, there is no such compensatory mechanism in pacemaker cells. This makes chronotropic incompetence a prominent feature in cardiac abnormalities observed in cirrhosis.

1.3.3 Prolongation of QT interval

The electrocardiographic QT interval reflects ventricular repolarization. Several studies have reported a high prevalence of prolonged QT interval in patients with cirrhosis. Several investigations have shown that QT interval prolongation increases with the severity of liver disease, but can also occur in patients with well-compensated cirrhosis (Bernardi et al. 1998; Bal and Thuluvath 2003). The mechanisms leading to QT interval prolongation in cirrhosis are unknown. The recent finding that QT interval prolongation correlates with circulating concentrations of BNP suggests that a sub-clinical cardiomyopathy may be responsible for its development (Henriksen et al 2003). Over all, the QT interval is further prolonged by transjugular intrahepatic portosystemic shunt (TIPS) (Trevisani et al. 2003) and is

shortened or normalized by acute administration of beta-blockers (Henriksen et al. 2004), chronic NO synthesis blockade (Tavakoli et al. 2007) and liver transplantation (Garcia-Gonzalez et al. 1999; Bal and Thuluvath 2003). However, the clinical interpretation of the QT interval prolongation in cirrhosis remains unclear.

1.3.4 Decreased heart rate variability

Spontaneous variations in heart rate have been known since the advent of experimental physiology in the early 1700s however it is only since the development of modern computational methods that we have been able to study heart rate variability. Normally, heart rate varies beat to beat which reflects the complex interplay between the autonomic nervous system and the heart (Fig. 1.3A). Loss of heart rate variability (HRV) and increased heart rate regularity is a common feature of systemic inflammatory conditions such as endotoxaemia and liver failure (Mani et al. 2006a; Fleisher et al. 2000). Previous studies have shown that indices of depressed heart rate variability in patients with liver failure correlate not only with the extent of disease progression, but also predict the adverse outcomes in this patient's population (Fleisher et al. 2000). For instance Fleisher et al. (2000), have shown that heart rate variability was significantly lower in the non-survivor patients awaiting liver transplantation than the survivors. The mechanism of decreased heart rate variability in cirrhosis remains unclear. However in chronic liver disease there is an increased incidence of autonomic neuropathy (Hendrickse et al, 1992) and increased circulary concentration of pro-inflammatory cytokines (Tilg et al. 1992; Genesca et al. 1999), both of which may impact upon this dynamic relationship (Fig 1.3B). Chapter 5 and 6 provide the background information and experimental set up to study the mechanism of decreased heart rate variability in patients and rats with cirrhosis.

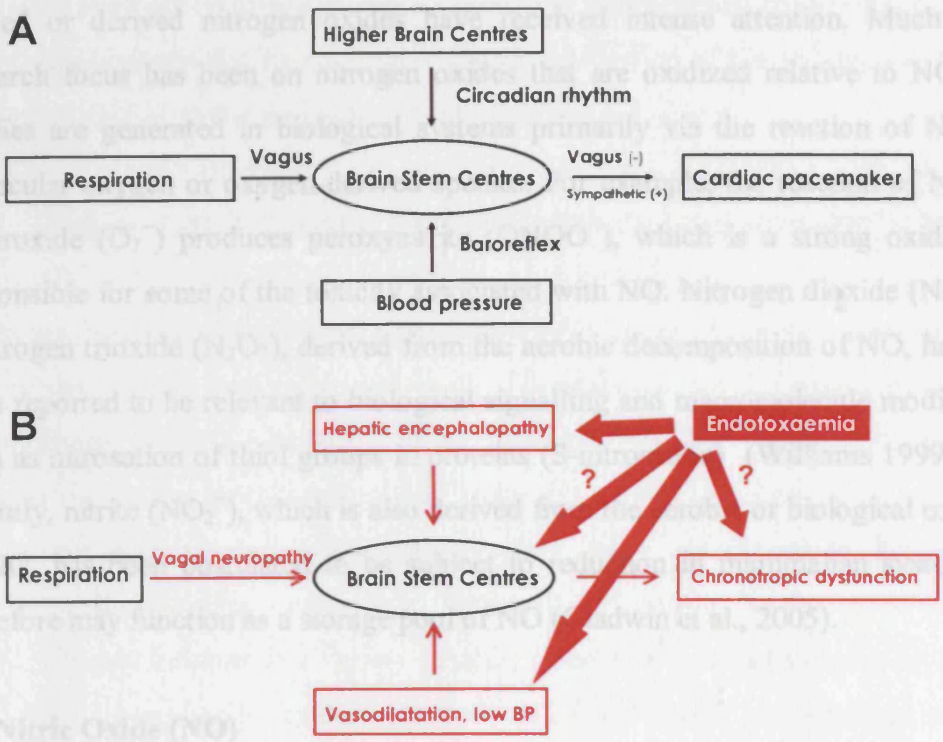

Figure 1.3. Basal heart rate shows fluctuations in healthy subjects due to a complex non-linear interaction between different physiological mechanisms which modulate cardiac cycle (A). Many of these mechanisms can potentially be affected in cirrhosis directly or indirectly through endotoxaemia (B). Cirrhosis is associated with a significant decrease in heart rate variability. However it is unclear which component is responsible for loss of heart rate variability in cirrhosis.

1.4. Reactive nitrogen species

Since the first reports of endogenous generation of nitric oxide (NO) in mammalian systems almost 20 years ago (Ignarro et al., 1987, Palmer et al., 1987 and Furchgott, 1988), the physiology, pathophysiology, biochemistry and pharmacology of NO and related or derived nitrogen oxides have received intense attention. Much of the research focus has been on nitrogen oxides that are oxidized relative to NO. Such species are generated in biological systems primarily via the reaction of NO with molecular oxygen or oxygen-derived species. For example, the reaction of NO with superoxide (O_2^-) produces peroxynitrite ($ONOO^-$), which is a strong oxidant and responsible for some of the toxicity associated with NO. Nitrogen dioxide (NO_2) and dinitrogen trioxide (N_2O_3), derived from the aerobic decomposition of NO, have also been reported to be relevant to biological signalling and macromolecule modification such as nitrosation of thiol groups in proteins (S-nitrosation) (Williams 1999). More recently, nitrite (NO_2^-), which is also derived from the aerobic or biological oxidation of NO, has been postulated to be subject to reduction in mammalian systems and therefore may function as a storage pool of NO (Gladwin et al., 2005).

1.5 Nitric Oxide (NO)

Nitric oxide is the first gaseous species unequivocally identified as an endogenously generated cell signalling agent (Ignarro et al., 1987, Palmer et al., 1987 and Furchgott, 1988). The first established physiological role for NO was vasorelaxation. The ability of NO to elicit vasorelaxation is due to its ability to increase intracellular levels of cGMP secondary to activation of soluble guanylate cyclase (sGC) in smooth muscle cells. However, it appears that the effects of NO go beyond its ability to activate sGC and other mechanisms such as modification of functional proteins by NO (or its reactive derivatives) can explain some physiological or pathological effects of NO. For example *S-nitrosation* of proteins (addition of –NO to the protein's sulfhydryl group) might have a significant role in cell signalling (Hess et al. 2005) and *nitration* of tyrosine residues (addition of $-NO_2$) of critical proteins has been shown to be implicated in the pathophysiology of various diseases such as sepsis and allograft rejection (MacMillan-Crow et al. 1996; Fukuyama et al. 1997).

1.6. Nitric Oxide synthesis in mammals

Nitric oxide is synthesized by the family of enzymes known as nitric oxide synthase (NOS) (see Alderton at al. 2001 for review). NOS enzymes are usually referred as dimeric in their active form and contain relatively tightly bound cofactors FAD, FMN, tertrahydrobiopterin and haem. They catalyse the reaction of L-arginine, NADPH and molecular oxygen to the free radical 'NO, citrulline and NADP:

$$\text{L-Arginine} + 2O_2 + 2\text{NADPH} + 2H^+ \longrightarrow {}^{\cdot}\text{NO} + \text{Citrulline} + 2\text{NADP}^+ + 2H_2O$$

There are three primary isoforms of NOS that originate from separate genes and differ in their sub-cellular localization and mode of regulation. They are typically designated as endothelial (eNOS), neuronal (nNOS), and inducible NOS (iNOS), although these designations do not strictly reflect their tissue expression or utility. eNOS and nNOS are constitutively expressed; nevertheless, their levels can change in response to a variety of physiological events (e.g., hormonal influences). As the name indicates, iNOS is highly induced in a variety of cells, often as a result of immune stimulation (e.g., lipopolysaccharide, cytokines). Both eNOS and nNOS are regulated primarily by Ca^{2+} via the actions of calmodulin. In contrast, iNOS is not regulated by Ca^{2+} (see Alderton at al. 2001 for review).

1.7. NOS regulation

NO is now known to be synthesized in a large number of different tissues playing a wide variety of physiological roles. The regulation of NOS activity in order for NO to perform this variety of roles is complex. Cellular and tissue specific localization of the NOS isoforms can be regulated by transcriptional regulation. Furthermore NOS activity can be regulated by covalent modification (e.g. phosphorylation,), protein–protein interactions (interaction with Heat-shock protein 90) and modulation of its cellular localization (e.g. localization in caveolea).

Calcium-Calmodulin (CaM): CaM was the first protein shown to interact with NOS (Bredt and Snyder 1990) and is necessary for the enzymatic activity of all three isoforms. The Ca^{2+}-dependence of NO synthesis distinguishes the NOS isoforms, with

nNOS and eNOS having a much higher Ca^{2+} requirement than iNOS. CaM binding increases the rate of electron transfer from NADPH to the reductase domain flavins (Gachhui et al. 1996; Gachhui et al. 1998).

Phosphorylation: Phosphorylation of the nNOS and eNOS isoforms can decrease or increase NOS activity. Thus, fluid shear stress elicits phosphorylation of Ser^{1179} residue of eNOS through protein kinase Akt activation and increases NOS activity (Corson et al. 1996; Dimmeler et al. 1999; McCabe et al. 2000). In contrast, the phosphorylation of nNOS at Ser^{847} by CaM-dependent kinases leads to a decrease in NOS activity (Hayashi et al. 1999; Komeima et al. 2000).

Heat-shock protein 90 (Hsp90): The molecular chaperone Hsp90 has been identified as a regulator of eNOS activity, possibly as an allosteric modulator (Garcia-Cardena 1998). Activation by vascular endothelial growth factor (VEGF), histamine or fluid shear stress in human endothelial cells increases the interaction between eNOS and Hsp90 and increases eNOS activity by approximately three folds (Mata-Greenwood et al. 2006). The activity of purified eNOS was also increased by purified Hsp90, suggesting a direct interaction, the details of which are not yet clear.

Caveolin: eNOS is localized to the caveolae (Garcia-Cardena 1996) which are micro-domains of the plasma membrane that are implicated in a variety of cellular functions including endocytosis of plasma proteins and signal transduction events. The caveolin proteins are the major coat proteins of caveolae and in endothelial cells eNOS binds to caveolin-1, while in cardiac myocytes eNOS is associated with caveolin-3 (Feron et al. 1996). Caveolin-1 directly inhibits eNOS activity and this interaction is regulated by CaM (Ju et al. 1997; Michel et al. 1997). Mice lacking the gene for caveolin-1 (cav-1 knockout mice), exhibit a significant increase in eNOS activity (Drab et al. 2001). Caveolin-3 also binds to nNOS in skeletal muscle, inhibiting NO synthesis, and this inhibition is reversed by CaM (Venema et al. 1997).

Protein inhibitor of NOS (PIN): The N-terminal extension of nNOS contains a binding site for the 89-amino-acid protein PIN (Jaffrey and Snyder 1996). However, the literature is contradictory on the ability of PIN to inhibit NOS activity. The identification of PIN as a light chain of myosin and dynein (King et al. 1996) has led to the suggestion of an alternative role for PIN as an axonal transport protein for

nNOS rather than a regulator of nNOS (Hemmens et al., 1998)

1.8. Nitric Oxide reactions and modification of proteins by NO

Nitric oxide-mediated modifications of proteins is rooted in its chemical structure as a free radical (see Eiserich et al. 1998 for review). These modifications include: (1) binding to *metal centres* (e.g. haem proteins) a process which is called nitrosylation; (2) *Nitrosation* of thiol and amine groups to form S-nitrosothiols and N-nitrosamines; (3) *Nitration* of tyrosine, tyrptophan and lipids. However, two particular modifications have recently received much attention, S-nitrosation of thiols to form *S*-nitrosothiols and nitration of tyrosine residues to produce nitrotyrosine (Fig. 1.4).

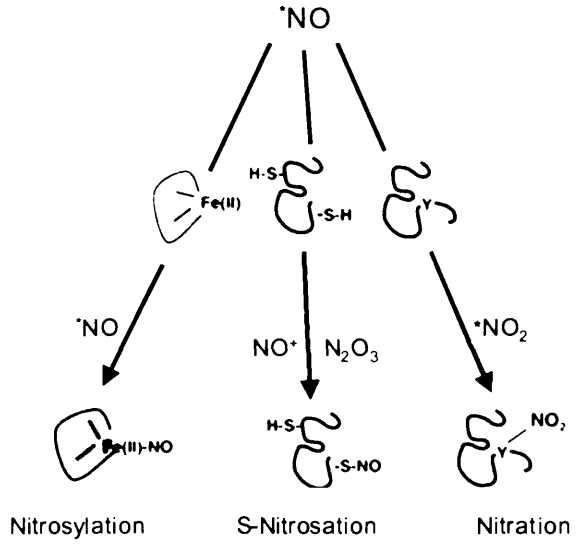

Figure 1.4. Reactive nitrogen species can react with haem proteins to form iron-nitrosyl (*nitrosylation*) and with cysteine or tyrosine residues in proteins to form an S-nitrosothiol (*nitrosation*) or nitrotyrosine (*nitration*) respectively.

1.8.1 Metal centres:

The mechanism by which NO elicits vasorelaxation is known to occur via activation of the enzyme *soluble guanylate cyclase* (sGC) through nitrosylation of haem group (see Cooper 1999 for review). sGC is a haem-containing protein, which exists in the cytosolic fraction of virtually all mammalian cells and acts as a principal intracellular target for NO. Activation of sGC by NO results in an increased conversion of GTP to the second messenger, cGMP, which governs many aspects of cellular function via interaction with cGMP-dependent protein kinases, cyclic nucleotide gated ion channels, or cyclic nucleotide phosphodiesterases (Hobbs 1997). As a consequence, sGC has become accepted as the primary NO receptor, and the NO-sGC-cGMP signal transduction pathway has been established as an important signal transduction system. In addition to sGC, it has been suggested that NO binding to ferrous haem in mitochondrial *cytochrome oxidase* occurs under physiological conditions which might have important implications in the regulation of mitochondrial respiration, cell apoptosis and survival (Moncada and Erusalimsky 2002; Mason et al. 2006).

1.8.2 S-Nitrosation:

The modification of thiol residues by NO to form S-nitrosothiols has been proposed to have a role in physiology of NO signalling since this modification is reversible and might act as a on/off switch of certain proteins. A wide variety of proteins have been found to be susceptible to S-nitrosation. These proteins cover a wide range of functions, including housekeeping enzymes (e.g. GAPDH), G-proteins (e.g. *ras*), transcription factors (e.g. NF-κB) and proteases such as caspases (Mohr et al. 1996; Jaffrey et al. 2001; Marshall and Stamler 2001; Mannick et al. 1999). Based on *in vitro* studies about one hundred proteins have been shown to undergo regulation by S-nitrosation but only a handful of proteins have been identified as targets for S-nitrosation *in vivo* (Jaffrey et al. 2001). As a signalling mechanism, S-nitrosation should show reversibility. Here we briefly discuss about *formation* and *decomposition* of S-nitrosothiols:

A. S-nitrosothiol formation: The modification of thiol proteins by NO typically occurs *indirectly* after the reaction of NO with oxygen (or oxygen-derived species), or oxidized metal (M^{n+1}) to form more oxidized nitrogen oxides like N_2O_3 or the equivalent of nitrosonium ion (NO^+) in the case of a metal-mediated process (see Gow et al. 2004 for review).

(Formation of S-nitrosothiol via NO auto-oxidation)

$$^{\cdot}NO + O_2 \rightarrow 2NO_2$$

$$NO_2 + NO \rightarrow N_2O_3$$

$$N_2O_3 + RSH \rightarrow \mathbf{RSNO} + NO_2^- + H^+$$

(Metal-mediated formation of S-nitrosothiols)

$$^{\cdot}NO + M^{n+1} \rightarrow M^{n+1}\text{-}NO$$

$$M^{n+1}\text{-}NO + RSH \rightarrow M^{n} + \mathbf{RSNO} + H^+$$

Classically, the formation of S-nitrosothiols has been considered to occur via the formation of a nitrosating intermediate such as N_2O_3 following the auto-oxidation of NO (Wink et al. 1994; Kharitonov et al. 1995). Critically important to such a reaction pathway is the requirement for two NO molecules to generate the nitrosating intermediate. This requirement makes such a reaction highly dependent on the local concentration of NO within a system. As such it will occur more readily under inflammatory conditions where the flux of NO is drastically increased and also under hydrophobic conditions where NO's lipophilicity causes it to accumulate in cell membranes (Gow et al. 1997). This is in contrast to metal-catalyzed synthesis of S-nitrosothiols which is first order with respect to NO and hence could potentially occur under physiological concentrations of NO seen in hydrophilic areas.

B. Decomposition of S-nitrosothiols: Loss of NO from S-nitrosothiols can occur photochemically (UV range) or by a Cu^+-dependent reaction where Cu^+ comes from reduction of Cu^{2+} in presence of ascorbate or a thiolate anion (RS^-)(Williams 1999). Moreover a number of enzyme systems catabolize S-nitrosothiols *in vitro*. These include xanthine oxidase (Trujillo et al. 1998), thioredoxin reductase (Nikitovic et al.

1996), glutathione peroxidise (Hou et al. 1996), copper zinc superoxide dismutase (Cu/Zn SOD) (Jourd'heuil et al. 1998) and glutathione-dependent formaldehyde dehydrogenase (which has been referred to as GSNO reductase) (Liu et al. 2001). It is not clear if these enzymes actually have role in S-nitrosothiol decomposition *in vivo*; however S-nitrosothiols can undergo trans-nitrosation reactions both *in vitro* and *in vivo* (Williams 1999; Orie 2005). Trans-nitrosation is the process by which an NO equivalent is transferred from one thiol molecule to another thiol.

(Trans-nitrosation reaction)

$$RSNO + R'SH \leftrightarrow RSH + R'SNO$$

This is particularly important as low molecular weight thiols (such as cysteine and glutathione), will readily undergo trans-nitrosation reactions with high molecular weight S-nitrosothiols to form less stable intermediates such as S-nitrosocysteine (CysNO) or S-nitrosogluathione (GSNO), which readily decompose and release NO (Orie et al. 2005). Mechanistically this may lead to *compartmentalization* of S-nitrosated proteins. For example, the cytosol is perhaps the least conducive cellular environment for *protein-S-NO* stability because protein S-nitrosothiols can be readily reduced by glutathione (~ 5mM in cytosol) or thioredoxin, each of which, once S-nitrosated through trans-nitrosation, can be enzymatically de-nitrosated (Liu et al. 2001). To protect *S*-nitrosothiols from reductive or trans-nitrosative degradation, they may be stored or protected in membranes, in lipophilic protein folds, in vesicles, and in interstitial spaces (Mannick et al. 2001). Caspase activation during apoptosis provides an example of how this type of sequestration is used in the process of cell signalling. These enzymes are ordinarily sequestered in an S-nitrosated (inactive) state in the mitochondrial inter-membrane space. When a cell receives an apoptotic signal, these caspases are released into the cytosol where they rapidly become de-nitrosated. De-nitrosation leads to caspase activation and initiation of apoptosis (Mannick et al. 1999).

1.8.3 Nitration:

Nitrated biological molecules, such as nitrated proteins and nitrolipids, are widely distributed in many organisms, and nitrogen dioxide radical ($^{\cdot}NO_2$) is the most likely nitrogen species to cause their formation (O'Donnell and Freeman 2001; Lim et al. 2002; Radi 2004). $^{\cdot}NO_2$ is formed from the decomposition of peroxynitrite (or reaction with CO_2, see below). In addition, peroxidases such as myeloperoxidase can generate $^{\cdot}NO_2$ or nitryl chloride from the reaction of nitrite with hypochlorous acid (Baldus et al. 2001). The discovery in 1995–1996 that CO_2 reacts rapidly with peroxynitrite and alters its reactivity was vital in understanding its reactions (Lymar and Hurst 1995; Denicola et al. 1996, Uppu et al. 1996). The modulation of peroxynitrite reactivity by CO_2 described above is shown below:

$$\text{(In absence of } CO_2\text{)} \quad H^+ + {}^-OONO \rightarrow HOONO \rightarrow HO^{\cdot} + {}^{\cdot}NO_2$$

$$\text{(In presence of } CO_2\text{)} \quad CO_2 + {}^-OONO \rightarrow ONOOCO_2^- \rightarrow CO^{\cdot}{}_3^- + {}^{\cdot}NO_2$$

In the absence of CO_2, peroxynitrite decomposes slowly to form the free radicals $HO^{\cdot}$ and $^{\cdot}NO_2$. However in mammals, biological fluids and tissues contain 1–2 mM CO_2, and the reaction of peroxynitrite with CO_2 is 50 to 100 times faster than its rate of decomposition to form $HO^{\cdot}$ and $^{\cdot}NO_2$. Furthermore, other biological molecules, such as haem proteins, also react with peroxynitrite at considerable rates. Thus, *in vivo*, it seems unlikely that peroxynitrite decomposes to form $HO^{\cdot}$ and $^{\cdot}NO_2$, because this reaction is too slow. In the presence of CO_2, peroxynitrite generates $CO_3^{\cdot}$ and $^{\cdot}NO_2$ radicals in a fast reaction.

$HO^{\cdot}$ is extremely reactive and reacts with virtually all biomolecules as fast as they collide and consequently live only microseconds. For this reason, biological damage by the $HO^{\cdot}$ radical is random, inefficient, and widespread, and generally does not

affect critical cellular targets. In contrast, other radicals, such as $CO_3^{\cdot-}$ and $^{\cdot}NO_2$, display various degrees of selectivity for biological molecules (Augusto et al. 2002). The $HO^{\cdot}$ radical reacts at or near the rate limit for diffusion with most biomolecules, whereas the $CO_3^{\cdot-}$ and $^{\cdot}NO_2$ radicals react more slowly and consequently have longer diffusion distances. The order of reactivity is $HO^{\cdot} > CO_3^{\cdot-} > {}^{\cdot}NO_2$, and unlike the $HO^{\cdot}$ radical, $CO_3^{\cdot-}$ and $^{\cdot}NO_2$ can be quite selective for certain biomolecules. For example, the $CO_3^{\cdot-}$ radical reacts at least 100,000 times faster with tyrosine, tryptophan, or cysteine than it does with alanine or glycine, effectively targeting only some of the amino acids in a protein. $^{\cdot}NO_2$, also has been found to react selectively with the amino acid residues tyrosine, tryptophan, and cysteine in proteins (see Pryor et al. for review).

Tyrosine nitration is becoming increasingly recognised as a prevalent, functionally significant post-translational protein modification that serves as an indicator of RNS-mediated oxidative inflammatory reactions. It is widely accepted that formation of nitrotyrosine residues in proteins takes place in a two-step reaction in which free radical, such a $CO_3^{\cdot-}$ (carbonyl radical), abstracts a H atom form tyrosine residue, generating a tyrosyl radical which then reacts with a $^{\cdot}NO_2$ in a radical-radical recombination reaction (Fig. 1.5).

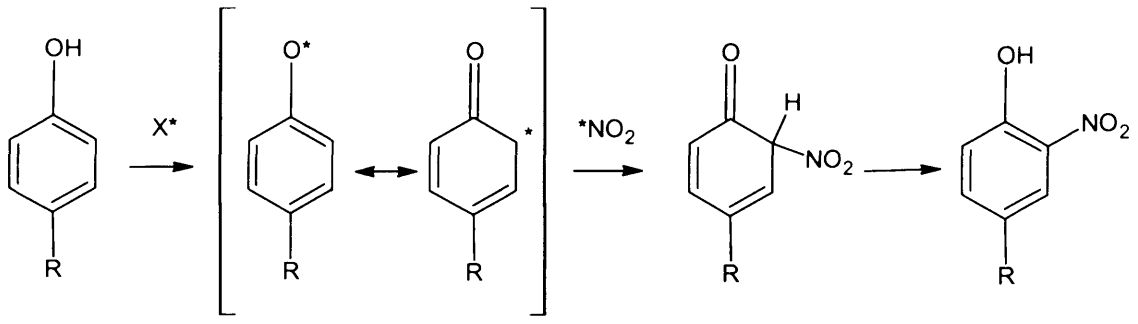

Figure 1.5. Nitration of tyrosine residues in proteins. X* represent any free radical (e.g. carbonyl radical) with ability to convert tyrosine to tyrosyl radical.

The formation of nitrotyrosine not only provides a footprint of oxidative injury by reactive nitrogen species but is critically linked to altered protein structure and function during inflammation. Thus nitration of the *o*-position of tyrosine decreases the pK_a of the tyrosine hydroxyl group from 10.1 to 7.2 (Schopfer et al. 2003). This introduces a net negative charge to approximately half of nitrated tyrosine residues at physiological pH. This bulky, anionic substituent can induce changes in protein conformation, resulting in altered enzyme catalytic activity. Some enzymes contain tyrosyl radicals in their active sites, and these radical centres are targets for reaction with $^{\cdot}NO_2$ since the reaction of these two radicals occurs near the diffusion limit. Thus, preferential nitration of active-site tyrosyl radicals in prostaglandin H_2 synthase-1 (PGSH-1) has been suggested, since the degree of nitration is found to correlate with the loss of enzyme activity (Goodwin et al. 1998). Other important proteins are affected by nitrotyrosine formation. For example, the selective cellular incorporation of nitrotyrosine into the extreme carboxyl terminus of the cytoskeletal protein α-tubulin impaires tubulin function (Eiserich et al. 1999). Also, nitration of a critical tyrosine residue (Tyr 67) in cytochrome c profoundly affects its redox-related properties (Cassina et al. 2000); nitration of sarcoplasmic reticulum calcium pump at Tyr 294 and Tyr 295 inhibits the enzyme (Viner et al. 1999) and finally nitration of Tyr 34 accounts for inactivation of human Mn superoxide dismutase in rejecting transplanted kidneys (MacMillan-Crow et al. 1996). If protein nitration is to be considered a cell signalling mechanism, four basic criteria should be met. First, the precursors for protein nitration should have controlled rates of formation. Second, protein nitration should be specific (i.e. nitration should occur on specific tyrosine residues of particular proteins). Third, nitration should modify target protein activity and cell function. Fourth, nitration must be reversible. Partial fulfilment of these criteria has been convincingly demonstrated for several proteins, but no single protein has successfully met all four of these crucial definitions of a cell signalling molecule (Schopfer et al. 2003).

Degradation of nitrated proteins. Little is known about the fate of nitrated proteins *in vivo*. It has been postulated that there is increased proteolytic degradation of nitrated proteins. For example, Souza et al. (2000) have shown that nitration of tyrosine residue(s) in proteins is sufficient to induce an accelerated degradation of the modified proteins by the proteasome to release free amino acids as well as free

nitrotyrosine. The urinary elimination of free nitrotyrosine is minimal, and it rapidly undergoes metabolism to form 3-nitro-4-hydroxyphenylacetic acid (NHPA) which is excreted as the major urinary metabolite of nitrotyrosine (Fig. 1.6) (Ohshima et al. 1990).

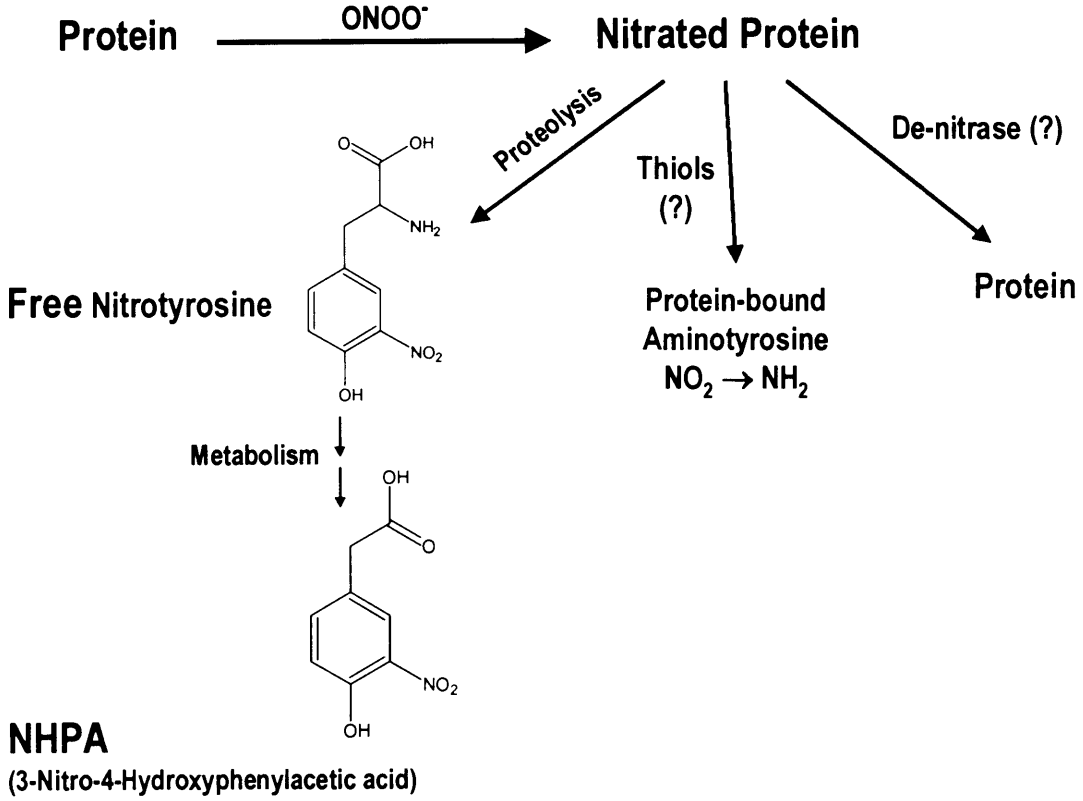

Figure 1.6. Degradation of nitrated proteins: Three distinct pathways have been postulated for degradation of nitrated proteins. *i.* Proteolysis of nitrated proteins releases free nitrotyrosine which undergoes metabolism to form a de-aminated and de-carboxylated product, NHPA (3-nitro-4-hydroxyphenylacetic acid). *ii.* Non-enzymatic reduction of nitrotyrosine to aminotyrosine has been shown *in vitro* (Balabanli et al. 1999). This reaction depends on the presence of haem and thiols and occurs within the physiological pH. Protein-bound nitrotyrosine can potentially undergo reduction to form aminotyrosine *in vitro*. *iii.* A putative *de-nitrase* activity has been reported in rats which removes nitro group form protein-bound nitrotyrosine (nitrotyrosine denitrase).

Apart from proteolytic degradation of protein-bound nitrotyrosine, two other pathways have been postulated which potentially affect nitrated proteins. Murad and colleague reported a putative *"de-nitrase"* activity in tissues obtained from endotoxaemic rats (Kamisaki et al. 1998; Irie et al. 2003). This activity was monitored by the decreased intensity of nitrotyrosine immunoreactive bands in Western blots and increased nitrate levels in reaction mixtures (Kamisaki et al. 1998). However, neither an enzyme catalyzing this reaction nor a product of this reaction was identified. A thiol-dependent *non-enzymatic* pathway which reduces nitrotyrosine to aminotyrosine ($-NO_2 \rightarrow -NH_2$) has also been demonstrated recently (Balabanli et al. 1999). However it is not clear whether or not this reaction occurs *in vivo*. Figure 1.6 summarises different suggested mechanism involved in degradation of nitrated proteins.

1.9. Measurement of S-nitrosothiol formation and protein nitration and

1.9.1 Measurement of S-nitrosothiols:

S-nitrosothiols are unstable under certain conditions. In buffer solution they can be broken down by ultraviolet (UV) light or by trace amounts of copper ions. Therefore solutions should be kept in the dark, and trace metal ions chelated by diethylenetriaminepentaacetic acid (DTPA). They are most stable under acidic conditions. The second important thing to understand is that thiols in biological samples, particularly low molecular weight thiols, will readily undergo trans-nitrosation reactions with S-nitrosothiols to form less stable intermediates such as S-nitrosocysteine (CysNO) or S-nitrosogluathione (GSNO), which readily decompose. This can be prevented by adding N-ethylmaleimide (NEM) to samples during collection. For example, previous studies in our lab showed that whereas 40% of added S-nitrosoalbumin (1 μM) decomposes within 2 hours, it was stable for up to 24 hours at room temperature when NEM was present (Marley et al. 2000). NEM alkylates thiol groups rapidly, and prevents thiol-dependent decomposition of S-nitrosothiols.

Many methods have been described for the measurement of S-nitrosothiols in the literature, but only a few have been validated and successfully applied to their quantitative measurement in biological samples. To validate a method one should be

able to add the analyte to the biological fluid in question, and demonstrate that the assay quantitatively measures an increment of the analyte concentration equal to the amount added. This validation still does not exclude the possibility that other compounds endogenously present in biological samples may cause overestimation. This is a significant problem in the measurement of S-nitrosothiols, since nitrite, present in all biological samples is usually detected by the methods used to measure S-nitrosothiols. Since background nitrite concentrations are ~200 nM in plasma, it is necessary to remove nitrite. Some groups have used a gel filtration methods (Gladwin et al. 2000), but these are time consuming and do not remove nitrite completely. Moore and colleagues have shown that nitrite ions can effectively be removed by reaction with acidified sulfanilamide, and this has no impact on the nitric oxide (NO) signal released by authentic S-nitrosothiols added to plasma (Marley et al. 2000).

The method that has been developed in our laboratory was based on the release of NO by reaction by a mixture of copper sulphate, iodide in acid and release of free iodine, and quantification of released NO by ozone-dependent chemiluminescence (Marley et al. 2000).

$$2Cu^{2+} + 4I^- \rightarrow 2CuI_2 \rightarrow 2\ Cu^{(I)}I + I_2$$

$$I_2 + I^- \rightarrow I_3^-$$

$$I_3^- + 2RS\text{-}NO \rightarrow 3I^- + 2RS^{\bullet} + 2NO^+$$

$$2RS^{\bullet} \rightarrow RSSR$$

$$2NO^+ + 2I^- \rightarrow 2NO + I_2$$

Chemiluminescence-based assays can detect plasma concentrations of S-nitrosothiols as low as ~5 nM (Marley et al. 2000, 2001). This method is similar to, and gives identical results to that developed by Gladwin *et al.* (2000) With this method the concentration of S-nitrosothiols in venous plasma of healthy human volunteers was estimated as ~ 10 nM which is considerably lower than previous reports (0.2-7 μM) (Goldman et al. 1998; Stamler et al. 1992). Many investigators were initially confused by their own findings, since it was originally reported by Stamler et al. (1992) that plasma S-nitrosothiols (predominantly S-nitrosoalbumin) was present at a

concentration of 7 μM. This measurement was based on photolytic cleavage of the S-NO bond. These levels are now widely acknowledged to be too high, with most recent estimates of plasma S-nitrosothiol concentrations as being in the low nano-molar range (Marley et al. 2000 and 2001; Akaike 2000; Rosso et al. 2001). The specificity of chemiluminescence-based analysis of NO-related compounds is high because the majority of other molecules potentially able to give chemiluminescence with ozone are not volatile, or do not occur in biological systems. We have also recently developed a method to stabilise and measure total S-nitrosothiol content in solid tissue homogenates which is discussed in chapter 3.

To detect specific S-nitrosothiols such as GSNO or S-nitrosoalbumin requires a separation system such as high performance liquid chromatography (HPLC). Akaike et al. (1997) developed a sophisticated HPLC method to separate nitrite, and S-nitrosothiols with post-column copper based decomposition of S-nitrosothiols and derivatization by the Griess reaction. However, this method was not sensitive enough to detect basal concentrations of S-nitrosothiols in plasma.

1.9.2 Measurement of protein nitration:

The measurement of protein nitration presents several problems. Most investigators have used immunoassays. Whilst immunoassays imply specificity by using specific antibodies it should be realized that it is easy to generate non-specific staining. The ideal method should be sensitive, specific and quantitative. Therefore mass-spectrometric assays are the most reliable methods for assessment of nitration reaction. A second approach is to measure the urinary excretion of 3-nitro-4-hydroxyphenylacetic, the major urinary metabolite of nitrotyrosine and this method is discussed in chapter 2.

The main problem with measuring nitrotyrosine again is nitrite, which causes artifactual nitration of tyrosine if acidic conditions (pH<3) are employed during sample preparation (Knowles et al. 1974, Frost et al. 2000). To measure protein-bound nitrotyrosine by gas chromatography mass spectrometry (GC/MS) or HPLC, investigators have usually employed acid hydrolysis, which causes artifactual nitration of tyrosine or enzymatic hydrolysis, which may be incomplete or release nitrotyrosine from auto-hydrolysis of the enzymes employed. To circumvent these

problems Moore and colleagues have developed a method in which alkaline hydrolysis of proteins is used to release nitrotyrosine and tyrosine followed by GC/MS analysis (Frost et al. 2000). By using deuterated tyrosine ([$^2H_4$] tyrosine) as an internal standard, one can assess artifactual nitration by measuring the formation of [$^2H_3$] nitrotyrosine (Frost et al. 2000).

1.9.3 Identification of protein targets to nitration or nitrosation:

Based on in vitro studies about one hundred proteins have been shown to undergo regulation by S-nitrosation but only a handful of proteins have been identified as targets for S-nitrosation *in vivo* (Jaffrey et al. 2001). Loss or rearrangement of S-NO group during sample preparation has been the most important technical limitation but recent advances, using thiol blocking agents to stabilize S-nitrosothiols, and the use of the biotin switch method, have provided new tools for identifying S-NO-modified proteins formed *in vivo* (Jaffrey et al. 2001). With the exception of S-nitrosoalbumin, which represents < 0.01% of total albumin (Marley et al. 2001), we do not know what proportion of proteins regulated in this way are S-nitrosated at any one time, and this is similar to that observed for nitrotyrosine which is also present at <0.01% of total tyrosine residues in tissue proteins. The nitrosation and nitration of proteins is a relatively selective process since specific cysteine or tyrosine residues in proteins undergo modification by reactive nitrogen species. Site directed mutagenesis methods have been used to determine the specific residue responsible for altered protein function nitration or nitrosation (Shimokawa et al. 1990; Perez-Mato et al. Sun et al. 2001). Liquid chromatography linked to tandem mass spectrometry (LC/MS/MS) is a commonly used method for identification of selective site(s) of nitration or nitrosation in relatively pure proteins (Ducrocq et al. 1998; Petersson et al. 2001). More recently the combination of 2 dimensional gel electrophoresis and matrix-assisted laser desorption ionization/time-of-flight (MALDI-TOF) mass spectrometric analysis has identified several liver proteins nitrated during endotoxaemia (Aulak et al 2001).

1.10. Aims and hypothesis

Cirrhosis is associated with increased production of reactive oxygen species (e.g. super oxide O_2^-) which react with NO to form reactive nitrogen species. Reactive nitrogen species (e.g. peroxynitrite) readily react with amino acid residues of proteins to form nitrosated or nitrated adducts. Although cirrhosis is well recognized as being associated with increased NO synthesis, the role of nitration or nitrosation of proteins in the genesis of cardiac dysfunction in cirrhosis has not previously been investigated. Here we hypothesised that increased formation of reactive nitrogen species in cirrhosis causes nitration/nitrosation of cardiac proteins and leads to impaired cardiac chronotropic function.

The aims of the work described in this thesis were:

1. To develop a method for dynamic assessment of nitration reactions *in vivo*.
2. To develop a method for stabilization and measurement of S-nitrosothiols in tissues
3. To test the hypothesis that increased formation of reactive nitrogen species in cirrhosis causes nitration/nitrosation of cardiac proteins and leads to impaired cardiac chronographic function.
4. To investigate the underlying mechanism of decreased heart rate variability in cirrhosis.

1.11 Overview of this thesis

Chapter 2 discusses the biochemical pathway in which circulating *para*-hydroxyphenylacetic acid (PHPA) undergoes nitration to form 3-nitro-4-hydroxyphenylacetic acid (NHPA). The chapter proposes that measurement of urinary NHPA can be used to assess the formation of reactive nitrogen species *in vivo*.

Chapter 3 deals with our investigations on the stability of S-nitrosothiols in tissue homogenates and our studies on the nature of the tissue factor which accelerates the decomposition of S-nitrosothiols.

Chapter 4 describes the main experimental work presented to assess the role of nitration/nitrosation reactions in the genesis of impaired heart rate variability and cardiac chronotropic function in rats with biliary cirrhosis.

Chapter 5 provides the background information and experimental set up to study the mechanism of decreased heart rate variability in in 75 patients with cirrhosis.

Chapter 2: Dynamic assessment of nitration reaction *in vivo*

2.1 Introduction

Assessment of protein nitration is commonly used as a footprint for the formation of reactive nitrogen species *in vivo*. However, one of the major disadvantages of measuring nitrotyrosine in proteins is that nitrated proteins are broken down at variable rates, and the resulting free nitrotyrosine is taken up by cells, metabolized, and excreted. For example, Souza et al. (2000) have shown that nitration of tyrosine residue(s) in proteins is sufficient to induce an accelerated degradation of the modified proteins to release free amino acids as well as free nitrotyrosine (Souza et al. 2000). The urinary elimination of free nitrotyrosine is minimal, but its secondary metabolites can potentially serve as biomarkers of overall nitrotyrosine formation *in vivo*. Since the pioneering work of Ohshima et al. (1990), it is known that nitrotyrosine is metabolized to 3-nitro-4-hydroxyphenylacetic acid (NHPA), which is excreted in the urine as the major urinary metabolite. This suggests that measurement of urinary NHPA could be used as a marker of systemic nitrotyrosine formation *in vivo*. It is not known, however, whether urinary NHPA is derived solely from metabolism of nitrotyrosine or whether it can also be formed by nitration of endogenous *para*-hydroxyphenylacetic acid (PHPA), a metabolite of tyrosine (Fell et al. 1978). PHPA readily undergoes nitration *in vitro* (Takahama et al. 2002), and has been used as a chemical probe to monitor nitration reactions *in vitro* (van der Vliet et al. 1997; Eiserich et al. 1998). However, it is not known whether or not this reaction occurs endogenously, and whether or not measurement of the formation of NHPA can be used as an index of nitration reactions *in vivo*. The aims of the present study were thus to determine whether or not NHPA can be formed endogenously from nitration of circulating PHPA, and whether or not measurement of urinary NHPA can be used to monitor systemic nitration reactions *in vivo*.

2.2 Materials and Methods I

Chemicals

All chemicals were purchased from Sigma Aldrich (Poole, Dorset, U.K.) unless stated otherwise. [$^{13}C_9$] Tyrosine, [$^{2}H_4$] acetic acid, $^{2}H_2O$ and ^{2}HCl were purchased from Cambridge Isotope Laboratories (Andover, MA, U.S.A.).

Synthesis of internal standards, [$^{13}C_8$]PHPA and [$^{13}C_8$]NHPA

[$^{13}C_8$]PHPA was synthesized following the de-amination and de-carboxylation of [$^{13}C_9$] tyrosine using Taiwan cobra (*Naja naja atra*) venom as a catalysing enzyme (Nucaro et al. 1998). In brief, [$^{13}C_9$] tyrosine was added to 50 mM ammonium formate buffer (pH 7.4) at a concentration of 0.2 mg/ml, and venom was added at a concentration of 1 mg/ml, before incubation at 37 °C for approx. 2 h. [$^{13}C_8$]PHPA was extracted into ethyl acetate, dried under nitrogen, and was then further purified by HPLC on a Techsphere C_{18} column (25 mM×4.6 mM). This employs a gradient of water containing 0.1% (v/v) TFA (trifluoroacetic acid) (solution A) and 0.1% (v/v) TFA/acetonitrile (solution B). Initial conditions were 100% solution A, changing to 9:1 solution A/solution B over 15 min, then to 1:1 solution A/solution B from 15 to 30 min. The fractions containing [$^{13}C_8$]PHPA were identified by their retention times and characteristic UV spectra with a photodiode array system. Fractions containing [$^{13}C_8$]PHPA were pooled and freeze-dried under vacuum. [$^{13}C_8$]NHPA was synthesized after exposure of [$^{13}C_8$]PHPA to acidified nitrite (1 M hydrochloric acid and sodium nitrite, 200 mM) followed by ethyl acetate extraction, and drying under nitrogen.

Synthesis of deuterium-labelled PHPA

[$^{2}H_6$]PHPA was synthesized by deuterium exchange (Shimamura et al. 1986). In brief, 50 mg of PHPA was dissolved in a mixture of [$^{2}H_4$]acetic acid (0.4 ml) and $^{2}H_2O$ (0.5 ml) and the solvent was evaporated in a stream of nitrogen at 90 °C. This procedure was repeated twice to remove active protons as completely as possible. The resulting residue was dissolved in a mixture of [$^{2}H_4$]acetic acid (0.3 ml), $^{2}H_2O$ (0.3 ml) and

^{2}HCl (37% in ^2H_2O, 0.8 ml). The solution was sealed in an acid-digestion bomb and heated in an autoclave at 190 °C for 8 h. The product was extracted with ethyl acetate and washed with water. After drying of the organic phase, the resulting materials were dissolved in 0.1% (v/v) TFA/water (adjusted to pH 5.0 with ammonia solution) and were then applied to an LC_{18} reverse-phase columns (Supelclean SPE tubes; Sigma) that had been pre-washed with 2 ml of methanol and 5 ml of 0.1% (v/v) TFA/water (pH 5.0). The column was washed with 2 ml of water and [$^2H_6$]PHPA was eluted with 4 ml of 25% (v/v) methanol in water.

The concentrations of ^{13}C-labelled and deuterated standards were determined against known amounts of unlabelled standards using the method described below.

Sample purification and derivatization for urinary NHPA and PHPA

[$^{13}C_8$]NHPA (10 ng) or [$^{13}C_8$]PHPA (100 ng) was added to 100 μl of human urine, or 20 μl of rat urine, and was diluted to 1 ml with de-ionized water. Following the addition of 1 ml of ethyl acetate and vortex mixing, the organic phase was removed, and the sample was evaporated under a stream of nitrogen. The residue was reconstituted in 30 μl of acetonitrile, applied to a silica TLC plate (LK6 60 Å, 250 μm layer thickness, 5 cm×20 cm; Whatman, Clifton, NJ, U.S.A.), and was run to the top of the plate in chloroform/methanol (80:20, v/v). Compounds migrating in the region of R_F~0.22 for NHPA and at 0.20 for PHPA, and 1 cm above and below, were scraped from the plate and extracted in 1 ml of ethyl acetate/ethanol (50:50, v/v), dried under nitrogen, and derivatized to the pentafluorobenzyl ester, by the addition of 20 μl of 10% (v/v) di-isopropyl ethylamine in acetonitrile and 40 μl of 10% (v/v) pentafluorobenzyl bromide in acetonitrile for 1 h at room temperature (21–23 °C), dried under nitrogen and re-dissolved in 20 μl of *n*-undecane for analysis of NHPA or 50 μl of *n*-undecane for analysis of PHPA.

Measurement of plasma concentrations of NHPA and PHPA

To measure plasma levels of NHPA and PHPA, blood was taken from three male Sprague–Dawley rats into tubes containing EDTA, which were centrifuged at 2300 ***g*** for 30 min at 4 °C. The internal standards (10 ng of [$^{13}C_8$]NHPA or 100 ng of [$^{13}C_8$]PHPA) were added to 1 ml of plasma, which was immediately filtered by

centrifugation at 9000 *g* in a microfuge through a 30 kDa molecular-mass cut-off centrifugal membrane (Ultrafree; Millipore, Bedford, MA, U.S.A.) to remove high-molecular-mass proteins. The filtrate was applied to an LC_{18} reverse-phase column that had been pre-washed with 2 ml of methanol and 5 ml of 0.1% (v/v) TFA/water (pH 5.0). The column was washed with 2 ml of water. Then NHPA and PHPA were eluted with 4 ml of 25% (v/v) methanol in water and dried under vacuum before TLC extraction as described above. The samples were derivatized to the pentafluorobenzyl ester by the addition of 20 μl of 10% (v/v) di-isopropyl ethylamine in acetonitrile and 40 μl of 10% (v/v) pentafluorobenzyl bromide in acetonitrile for 1 h at room temperature, dried under nitrogen and re-dissolved in 20 μl of *n*-undecane before GC (gas chromatography)/MS analysis.

GC/MS analysis of derivatized samples

Samples were analysed on a GC equipped with a 15 m DB-1701 (J&W Scientific, Folsom, CA, U.S.A.) capillary column (0.25 mm internal diameter, 0.25 μm film thickness) interfaced with a mass spectrometer (Trio 1000; Fisons Instruments, Beverly, MA, U.S.A.). The ion source and interface temperature were set at 200 °C and 300 °C respectively. Samples were analysed in negative-ion chemical ionization (NICI) mode with ammonia as the reagent gas, using 1 μl of each sample for injection. The initial column temperature was maintained at 150 °C for 1 min increasing to 300 °C at 20 °C/min. Samples were quantified by isotope-dilution GC/MS and ions were monitored at 376 and 384 mass units for NHPA and at 311 and 319 mass units for PHPA with single-ion monitoring. The concentrations were calculated from the known $^{13}C_8$-labelled internal standards, which are 8 mass units heavier than the authentic NHPA and PHPA.

Exclusion of artifactual nitration of PHPA during analysis

Initial studies using buffers at pH 4.0 showed that there was significant artifactual nitration of PHPA during the preparation of samples (results not shown). Therefore, to ensure that there was no artifactual nitration of PHPA during the preparation of urine samples, the formation of $[^2H_5]$NHPA from 100 ng of $[^2H_6]$PHPA added to 100 μl of human urine was monitored in a separate series of experiments.

Standard curves for evaluation of the assays

To determine the accuracy of the assay, known amounts (0–20 ng of NHPA or 0–10 μg of PHPA) were added to 100 μl of human urine and the samples were analysed as unknowns. For measurement of intra-assay variability, six aliquots from a urine sample of one volunteer were analysed as described above and the intra-assay variability was calculated as percentage coefficients of variation (100×S.D./mean).

Nitrotyrosine measurement in biological samples

Nitrotyrosine in biological samples was measured by GC/MS. 10 ng [$^{13}C_9$] labelled nitrotyrosine was used as stable isotopic internal standards. [$^{13}C_9$] Nitrotyrosine was synthesized by nitration of [$^{13}C_9$] tyrosine as described (Frost et al. 2000). Following two steps solid phase extraction using LC_{18} and ENV+ (Isolute, UK) columns, nitrotyrosine was converted into the respective amides by the addition of 100 μl of anhydrous dimethylformamide and 20 μl of di-isopropyl ethylamine. Samples were left for at least 5 min on ice, after which 40 μl of ethyl heptafluorobutyrate was added. After being left for a further 30 min, samples were sonicated for 2 h. Un-reacted and excess reagents were evaporated under nitrogen. The amino acid amides were converted into the *t*-butyl(dimethyl)silyl ester or ether by the addition of 30 μl of TBDMS containing 1% (v/v) N-(*t*-butyldimethylsilyl)-N-methyltrifluoroacetamide chlorosilane at room temperature for 30 min. Derivatized samples were dried under nitrogen and re-dissolved in 20 μl of undecane. Samples were analysed on a GC equipped with a 15 m capillary column (0.25 mm internal diam., 0.2 μm film thickness) interfaced with a Trio 1000 mass spectrometer. The ion source and interface were set at 200 and 300 °C respectively. Samples were analysed in NICI mode with ammonia as the reagent gas. All samples were injected with the on-column injection technique. On-column injection is the method by which a sample is directly injected manually into the analytical column from a fine-bore microlitre syringe. This technique avoids problems that can arise from the interactions between the analyte and the glass injection liner. The initial column temperature was maintained at 150 °C for 1 min and then increased to 300 °C at 20 °C/min for nitrotyrosine analysis.

Animal studies

Male Sprague Dawley rats (body mass 270–300 g) were obtained from the Comparative Biology Unit at the Royal Free and University College Medical School (Hampstead Campus, UCL, London, U.K.). All animal procedures were in accordance with Home Office recommendations. The animals were anaesthetized with an intraperitoneal injection of sodium pentobarbital (60 mg/kg). The jugular vein and the urinary bladder were cannulated with polyethylene cannulae. Physiological saline solution was infused into the animals at 25 ml/kg per h through the jugular vein and urine samples were collected every 30 min as described below.

Metabolism of nitrotyrosine to NHPA

To determine the metabolism of nitrotyrosine to NHPA, 250 nmol of nitrotyrosine was dissolved in 1 ml of sterile PBS and was injected intravenously into three rats as a bolus. Urine samples were collected every 30 min for 5 h, with a single 30 min collection (basal) immediately before injection of nitrotyrosine. The urinary concentration of NHPA and PHPA was determined as described above. Urinary content of un-metabolized nitrotyrosine was also measured in each sample using GC with NICI MS, as previously described above (Frost et al. 2000).

Nitration of PHPA in vivo

[$^2H_6$]PHPA was injected intravenously as a bolus (250 nmol, dissolved in 1 ml of PBS) after the initial basal urine collection (t=30 min) into three rats, and urine samples were collected every 30 min for 4.5 h. Nitration of [$^2H_6$]PHPA produces [$^2H_5$]NHPA as a result of replacement of a single deuterium of the aromatic ring by the NO_2 group.

Effect of endotoxaemia on the formation of NHPA

LPS (lipopolysaccharide) from *Salmonella typhimurium* was injected intravenously into three rats as a bolus (5 mg/kg in 1 ml of PBS). Urine samples were collected every 30 min for 4.5 h, with a single 30 min collection (basal) immediately before the injection of LPS. The urinary content of NHPA, PHPA and nitrotyrosine was determined as above. In a further study, 250 nmol of [$^2H_6$]PHPA was injected

intravenously into three rats 2 h after administration of LPS (5 mg/kg). The urinary content of NHPA, PHPA, [$^{2}H_5$]NHPA and [$^{2}H_6$]PHPA were then quantified by GC/MS using $^{13}C_8$-labelled internal standards. For measurement of the deuterium-labelled compounds, ion masses (*m/z*) of 381 and 337 were selected in selective-ion monitoring, which are 5 and 6 mass units heavier respectively than the authentic NHPA and PHPA.

Statistical analysis

All data are presented as means ± SEM. Statistical evaluation of the data was carried out with the analysis of variance (ANOVA) followed by the Newman–Keuls test for multiple comparisons, and $P<0.05$ was considered statistically significant.

2.3. Results I

To investigate the formation of NHPA *in vivo*, it was necessary to develop a method that can accurately measure this metabolite, and avoid the problems that are encountered during the assay of other nitrated products, such as nitrotyrosine [3,17]. Thus the method needs to be reproducible with biological samples and free of artifactual nitration of its precursor (PHPA).

Characterization of the derivatives of NHPA and PHPA

The structures of the pentafluorobenzyl ester derivatives of NHPA and PHPA are shown in Fig 2.1. The molecular mass of derivatized NHPA is 557 Da, which is 45 mass units heavier than derivatized PHPA (512 Da). The de-protonated molecular ion for the NHPA derivative is evident at *m/z* 556 $[M\text{-H}]^-$ and for PHPA at 511 $[M\text{-H}]^-$, which are visible on the NICI spectra shown in Fig 2.1. Analysis of the pentafluorobenzyl ester derivatives of NHPA and PHPA by full-scan mode (Fig 2.1) showed that NHPA has a dominant ion at *m/z* 376 ([M-181], loss of one pentafluorobenzyl ester group). PHPA has a dominant ion at *m/z* 331 [M-181], which is also compatible with the loss of a pentafluorobenzyl ester group. On the basis of these results, all further work was focused on developing the analytical method for NHPA and PHPA as the pentafluorobenzyl ester derivative with selective-ion monitoring at 376 and 331 mass units for NHPA and PHPA respectively. The detection limit was approx. 1 pg on column injection (for both NHPA and PHPA). After GC/MS analysis of urine samples, a single peak was eluted with the respective ^{13}C-labelled internal standards, which were 8 mass units heavier than the authentic NHPA and PHPA (Fig. 2.2). As shown in Fig. 2.3, full scan analysis of derivatized deuterium-labelled PHPA showed that the synthesized compound had a dominant ion at m/z 337 which is 6 mass units heavier than the authentic PHPA and corresponds to $[^2H_6]$PHPA (Fig. 2.3).

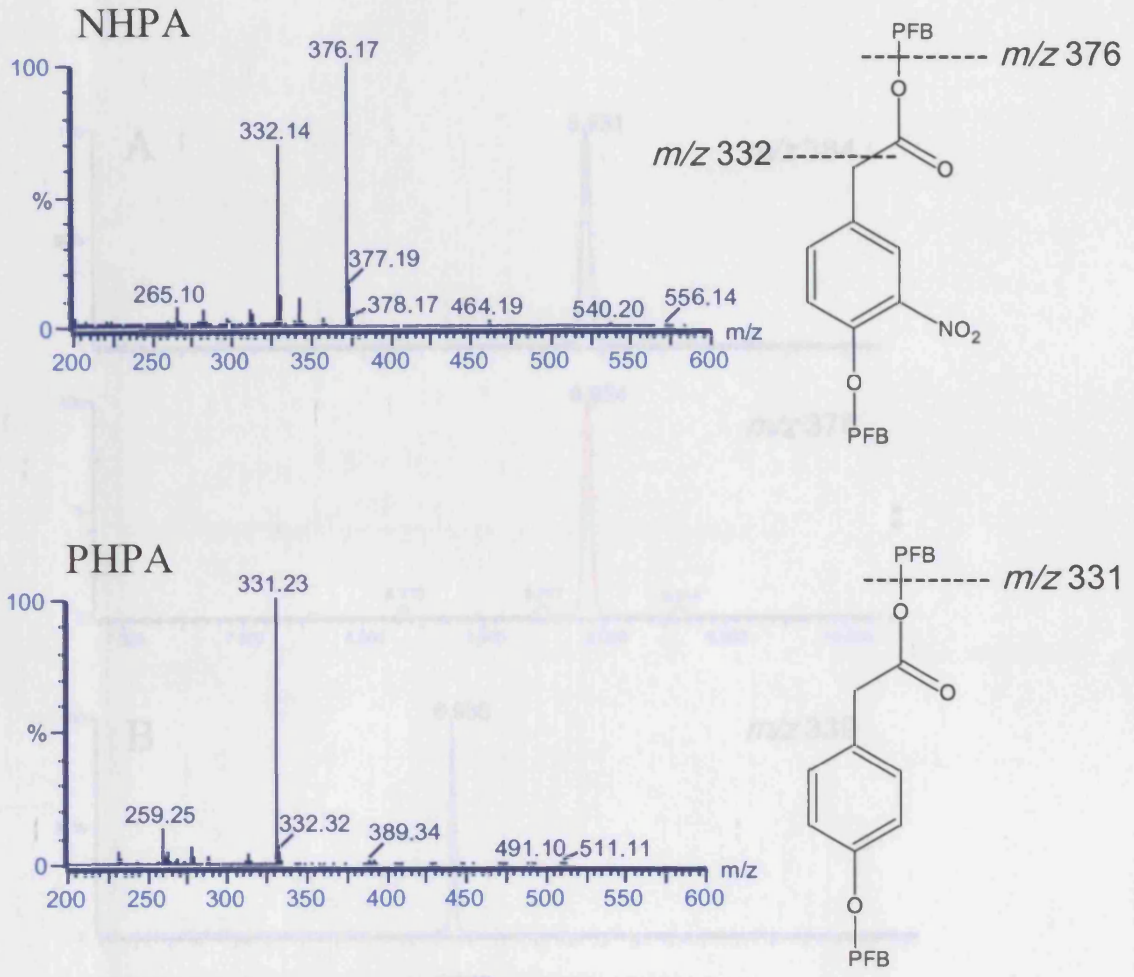

Figure 2.1. Structures and spectra from NICI scans of the pentafluorobenzyl derivative of NHPA (upper panel) and PHPA (lower panel). The molecular mass of derivatized NHPA is 557 Da, which is 45 mass units heavier than derivatized PHPA (512 Da). The de-protonated molecular ion for the NHPA derivative is evident at m/z 556 [M-H]- and for PHPA at 511 [M-H]-. NHPA has a dominant ion at m/z 376 ([M-181], loss of one pentafluorobenzyl ester group). PHPA has a dominant ion at m/z 331 [M-181], which is also compatible with the loss of a pentafluorobenzyl ester group.

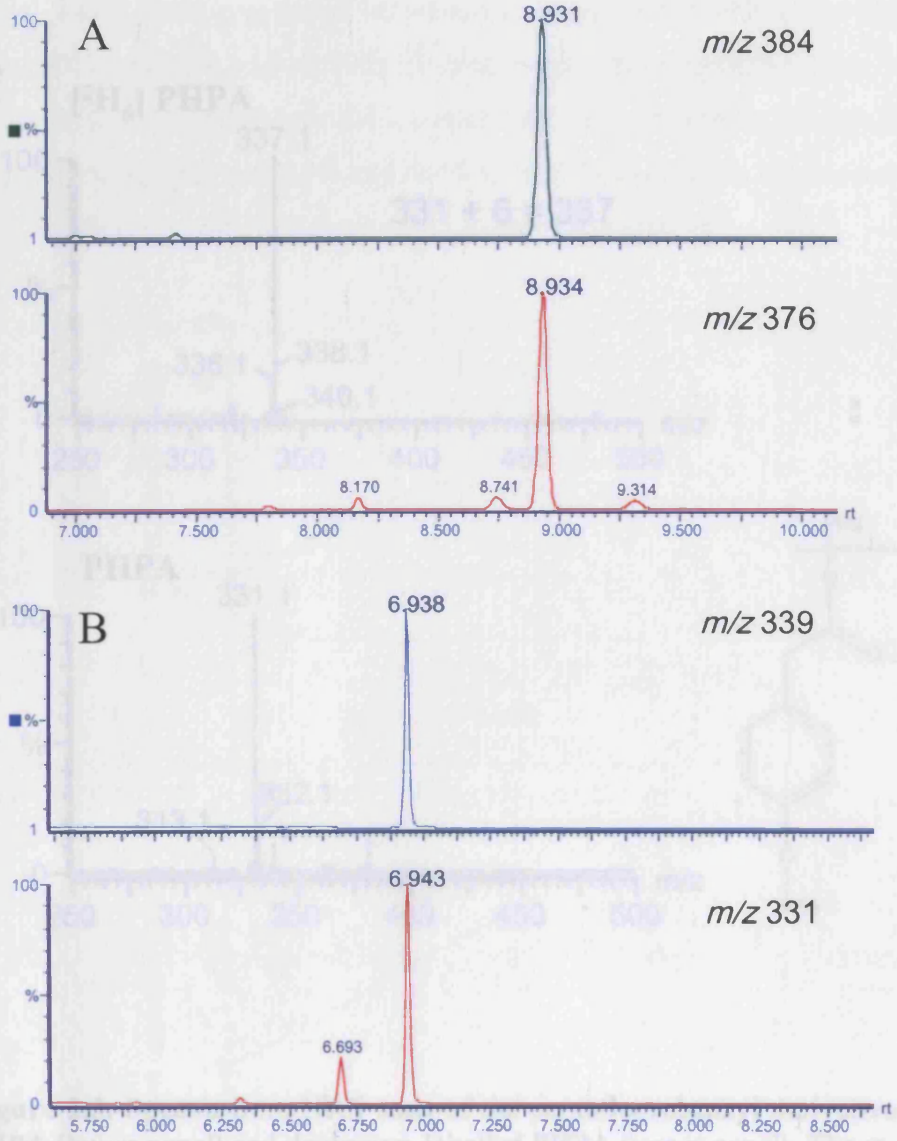

Figure 2.2. Typical chromatogram showing peak shape and resolution for both NHPA (A) and PHPA (B) in a urine sample. The $^{13}C_8$-labelled NHPA and PHPA resulted in derivatives that were 8 mass units heavier than the parent compound. NHPA (A) was quantified by monitoring ions of m/z 376 and 384, and PHPA (B) by monitoring ions of m/z 331 and 339. The x-axis represents the retention time (rt).

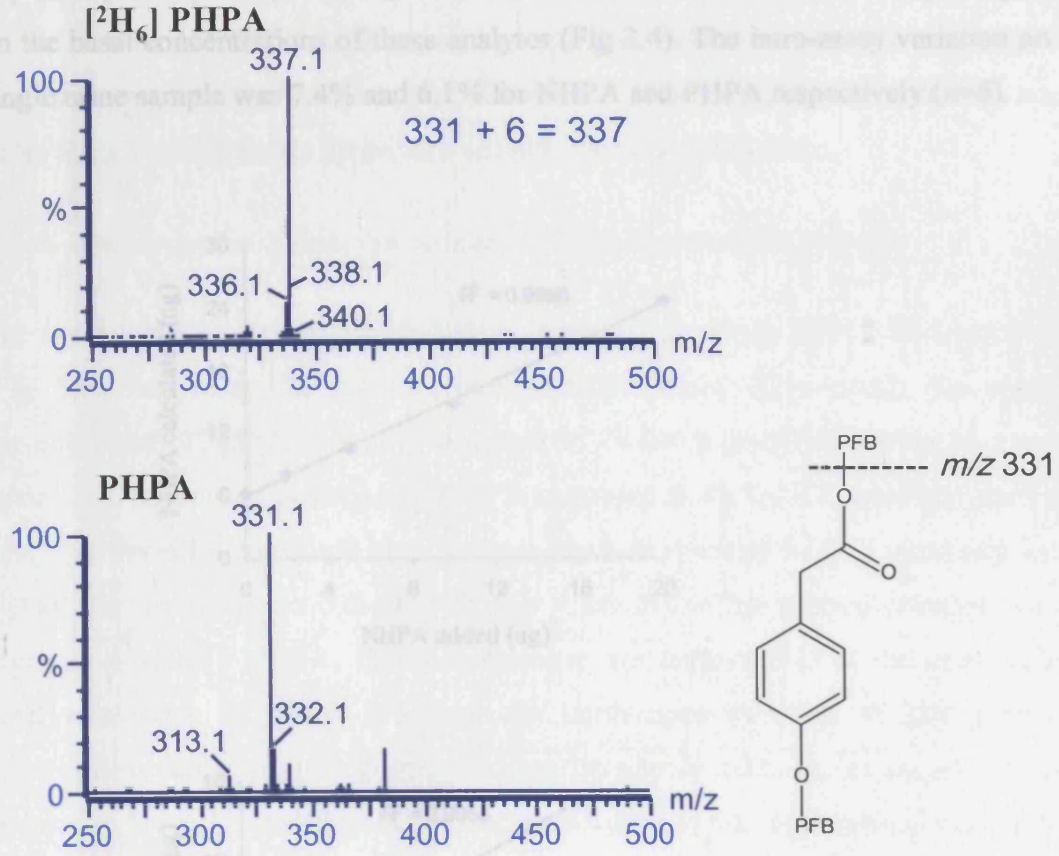

Figure 2.3. Spectra from NICI scan of the pentafluorobenzyl derivative of authentic PHPA (lower panel) and deuterium-labelled PHPA (upper panel). The molecular mass of deuterium lablled PHPA is 6 mass unit heavier than authentic PHPA, showing a successful synthesis of [$^2H_6$]PHPA using deuterium exchange.

Standard curves of NHPA and PHPA

There was a good correlation between the added and measured amounts of NHPA (r^2=0.998) and PHPA (r^2=0.995) in urine, with a linear standard curve superimposed on the basal concentrations of these analytes (Fig 2.4). The intra-assay variation on a single urine sample was 7.4% and 6.1% for NHPA and PHPA respectively (n=6).

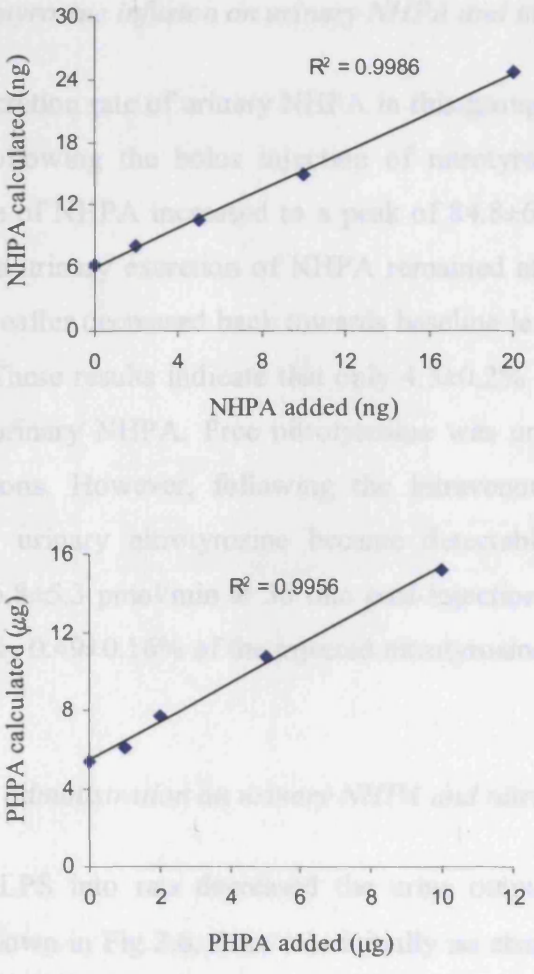

Figure 2.4. Standard curves for NHPA (upper panel) and PHPA (lower panel) in human urine. Known amounts of NHPA and PHPA were added to urine. Following analysis as unknowns, the expected amount of added NHPA or PHPA was recovered with a good correlation when analysed by GC/MS.

Nitration of PHPA as an artifact

Artifactual nitration of PHPA during sample preparation was investigated after the addition of [$^2H_6$]PHPA to 100 µl of urine. Based on the evaluation of *m/z* 381 and retention time, no [$^2H_5$]NHPA was detected after extraction and derivatization of samples using the method described. However, if buffers of pH 4.0 or below were used, there was significant artifactual nitration (results not shown).

Effect of nitrotyrosine infusion on urinary NHPA and nitrotyrosine levels

The basal excretion rate of urinary NHPA in this group of rats was 8.1±0.5 pmol/min (Fig 2.5). Following the bolus injection of nitrotyrosine (250 nmol), the urinary excretion rate of NHPA increased to a peak of 84.8±6.6 pmol/min within 30 min of injection. The urinary excretion of NHPA remained at 81.7±12.2 pmol/min until 60 min, and thereafter decreased back towards baseline levels of 9.1±1.5 pmol/min by 5 h (Fig 2.5). These results indicate that only 4.3±0.2% of the injected nitrotyrosine is excreted as urinary NHPA. Free nitrotyrosine was undetectable in the urine under basal conditions. However, following the intravenous injection of 250 nmol of nitrotyrosine, urinary nitrotyrosine became detectable with an excretion rate of peaking at 16.8±5.3 pmol/min at 30 min post-injection, but was undetectable by 4 h (Fig 2.5). Only 0.49±0.16% of the injected nitrotyrosine was excreted unchanged into the urine.

Effect of LPS administration on urinary NHPA and nitrotyrosine levels

Injection of LPS into rats decreased the urine output from 26.5±5.2 to 16.6±7.1 µl/min. As shown in Fig 2.6, there was initially no change in the urinary excretion of NHPA, but 2 h after the injection of LPS, there was a sustained increase in the urinary excretion of NHPA from 7.61±1.3 to 15.7±2.1 pmol/min ($P<0.01$). Urinary nitrotyrosine was undetectable until 90 min after bolus injection of LPS, but, thereafter, small amounts of free nitrotyrosine were detectable ($P<0.01$) (Fig 2.6).

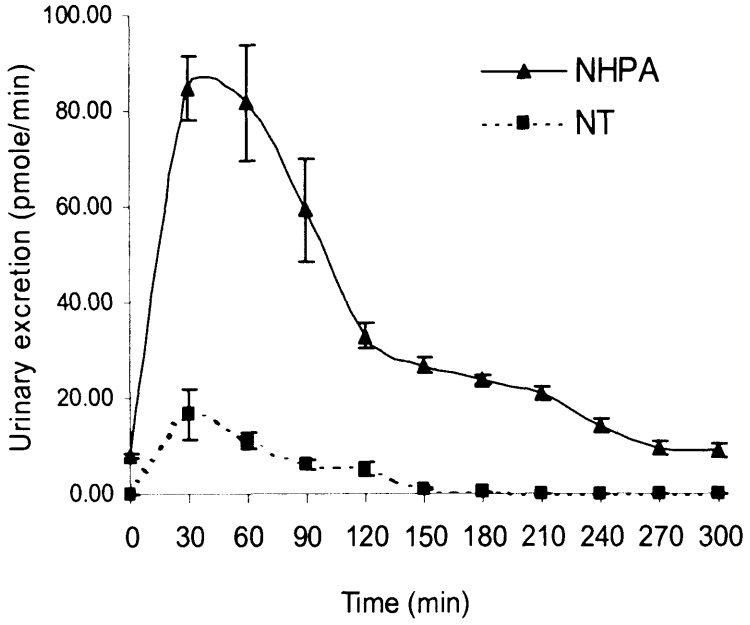

Figure 2.5. Urinary excretion of NHPA and nitrotyrosine (NT) after intravenous injection of nitrotyrosine. Urinary excretion rate of NHPA and free nitrotyrosine increased by 30 min following the intravenous bolus injection of 250 nmol of nitrotyrosine into anaesthetized rats. Results are means ± SEM. (n=3).

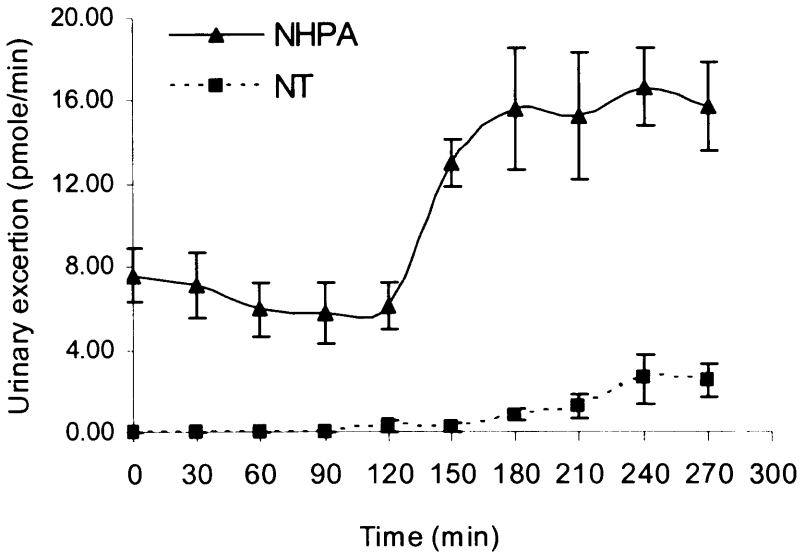

Figure 2.6. Urinary excretion of NHPA and nitrotyrosine (NT) after intravenous injection of LPS. Urinary excretion rate of NHPA and free nitrotyrosine both increased following the injection of LPS (5 mg/kg) into anaesthetized rats at 30 min. Results are means ± SEM. (n=3). ANOVA shows a significant increase in NHPA and PHPA excretion after LPS administration ($P<0.01$).

Nitration of infused [$^2H_6$]PHPA

In order to determine the extent of endogenous nitration of circulating PHPA *in vivo*, the formation of [$^2H_5$]NHPA was investigated in rats injected with [$^2H_6$]PHPA. A GC/MS chromatogram revealed a peak with an *m/z* of 381, consistent with the nitration of [$^2H_6$]PHPA to [$^2H_5$]NHPA (Fig 2.7). The urinary excretion rate of [$^2H_5$]NHPA was 12.6±3.0 and 5.1±1.8 pmol/min at 30 and 60 min after the bolus injection of [$^2H_6$]PHPA respectively (Fig 2.8). The urinary excretion of unmetabolized [$^2H_6$]PHPA peaked within 30 min after the bolus injection, and total recovery of [$^2H_6$]PHPA was 78±2% within the initial 4 h of urine collection. This suggests that there is relatively little metabolism, if any of PHPA *in vivo*. At 60 min after [$^2H_6$]PHPA injection, the urinary excretion rate of [$^2H_6$]PHPA was very close to the normal range of authentic PHPA excretion (2.3±0.7 nmol/min) (Fig 2.8), and this time interval was selected for comparison of the endogenous NHPA/PHPA ratio with the [$^2H_5$]NHPA/[$^2H_6$]PHPA ratio. At 60 min, the ratio of [$^2H_5$]NHPA/[$^2H_6$]PHPA was 6.1±1.0 (pmol/nmol), and the ratio of endogenous NHPA/PHPA was 7.0±0.9 (pmol/nmol). Assuming that endogenous PHPA is handled in the same way as infused PHPA, there is approx. 0.9 pmol/nmol of NHPA unaccounted for, and which is assumed to be derived from metabolism of nitrotyrosine. Injection of LPS resulted in a significant increase ($P<0.05$) in the NHPA/PHPA ratio as well as the [$^2H_5$]NHPA/[$^2H_6$]PHPA ratio (Fig 2.9). Meanwhile, the total recovery of [$^2H_6$]PHPA was significantly decreased after LPS administration (39.2±4% compared with 78±2%; $P<0.05$) during 4 h of urine collection. We attribute this to the marked decrease in urine volume post-LPS.

Plasma concentrations of PHPA and NHPA

The plasma concentration of PHPA was 2.7±1.1 μmol/l (410±171 ng/ml) in rats. In contrast, the plasma concentrations of NHPA were undetectable.

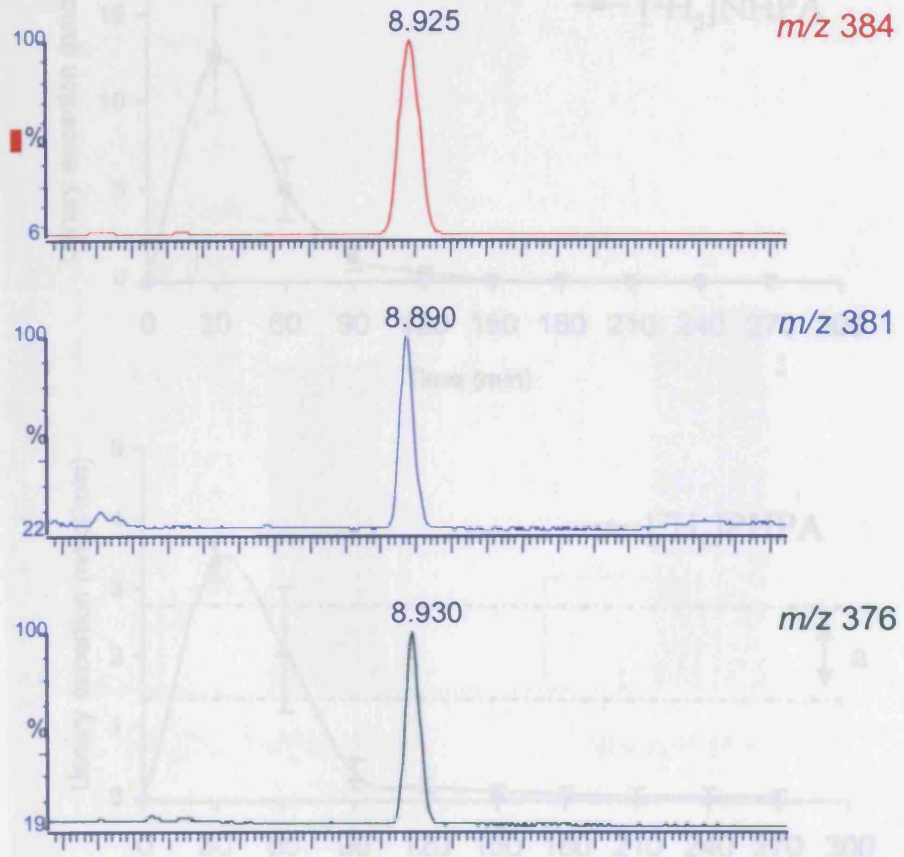

Figure 2.7. Chromatogram of a urine sample obtained from a rat injected with [$^{2}H_{6}$]PHPA. *In vivo* formation of [$^{2}H_{5}$]NHPA, represented as a distinguished peak, was detected with m/z 381. The values of m/z 376 and m/z 384 represent authentic NHPA and $^{13}C_{8}$-labelled internal standard respectively.

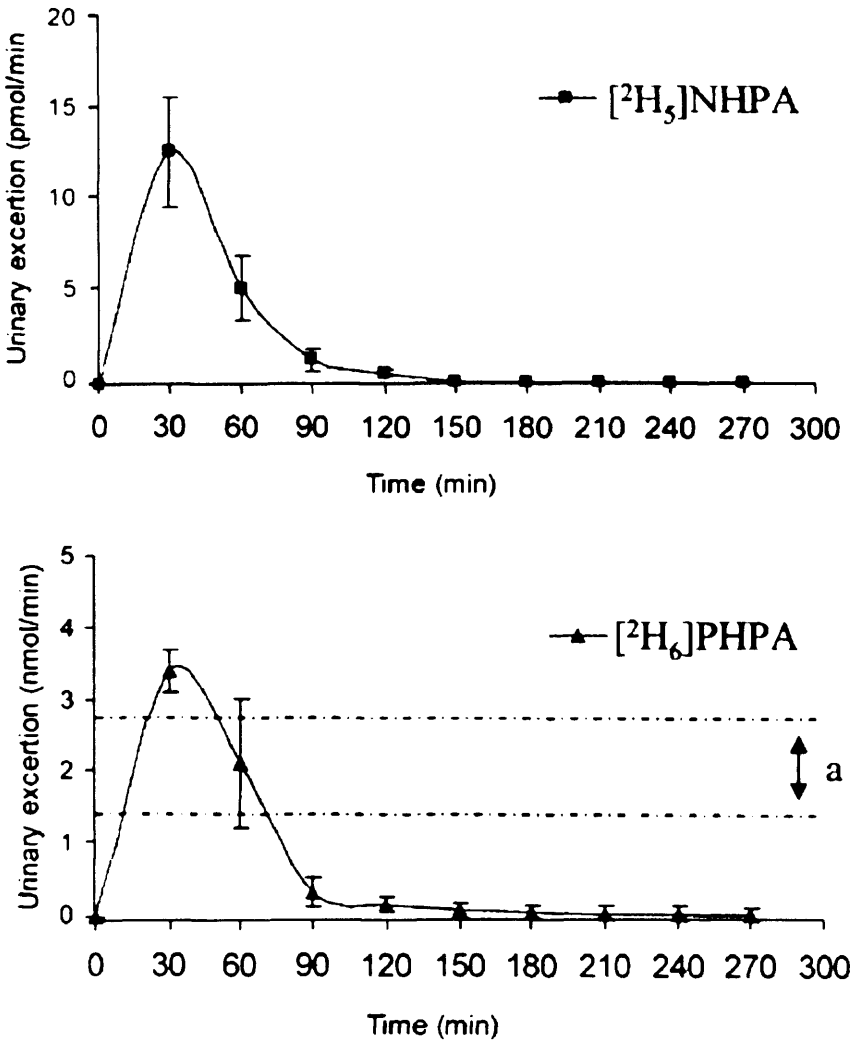

Figure 2.8. Urinary excretion of [$^2H_5$]NHPA and [$^2H_6$]PHPA after intravenous injection of [$^2H_6$]PHPA. The urinary excretion rate of [$^2H_5$]NHPA (upper panel) and [$^2H_6$]PHPA (lower panel) both increased following the intravenous bolus injection of [$^2H_6$]PHPA (250 nmol) into anaesthetized rats. As shown in the upper panel, there was a marked increase in the formation of [$^2H_5$]NHPA, which can only arise from nitration of infused [$^2H_6$]PHPA. The total recovery of injected [$^2H_6$]PHPA was 78±2% during the first 4 h of urine collection. Results are means ± SEM. (n=3). The mean urinary excretion rate of endogenous PHPA was 2.3±0.7 nmol/min, and the range of excretion rate observed in normal rats is shown by the dotted lines (a).

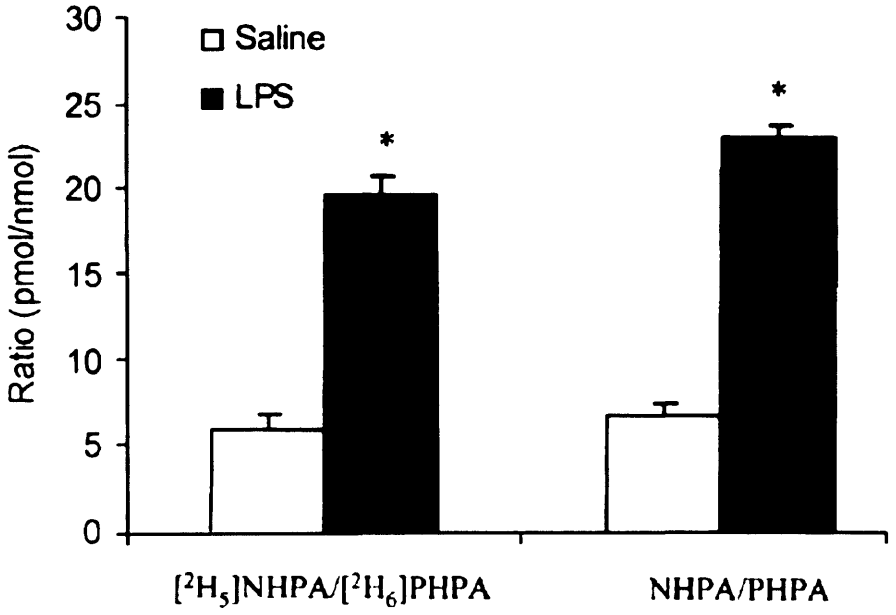

Figure 2.9. NHPA/PHPA ratio as an index of RNS formation. Under basal conditions, the ratio of NHPA/PHPA gives an index of the rate of nitration of PHPA, and the metabolism of nitrotyrosine. [$^2H_6$]PHPA was used as a probe to assess the nitration of PHPA to NHPA *in vivo*. Injection of LPS increases the ratio of endogenous NHPA/PHPA as well as that of [$^2H_5$]NHPA/[$^2H_6$]PHPA, suggesting that much of the NHPA that is excreted in urine during endotoxaemia is derived from the nitration of circulating PHPA. Results are means ± SEM. *P<0.05 compared with the saline-treated group.

2.4. Discussion I

One of the major disadvantages of measuring nitrotyrosine in tissues or biological fluids is that nitrated proteins are broken down at variable rates, and nitrotyrosine is metabolized and excreted (Souza et al. 2000, Tabrizi-Fard et al. 1999). Thus the concept that measurement of NHPA, as the major urinary metabolite of nitrotyrosine, is attractive, since it can provide a time-integrated index of nitrotyrosine formation *in vivo*. However, it is important to know whether this metabolite is formed exclusively from nitrotyrosine, or whether it can be formed via nitration of PHPA, which is present at high concentrations in plasma.

Since the identification of NHPA as the major metabolite of nitrotyrosine, there have been no reliable assays for the measurement of NHPA in biological fluids. For instance, an electrochemical-based HPLC method has been described for the measurement of NHPA (Crow 1999), but the specificity and reproducibility of this method have not been evaluated so far. Beal et al. (1997) have also reported an assay for measurement of NHPA in spinal tissue, but their method has the disadvantage that extractions are performed in extremely acidic conditions in which nitrite, always present in biological samples, can cause artifactual nitration of PHPA. In the present study, we have described a novel assay for the measurement of urinary NHPA, which has the advantage of being highly sensitive, specific and reproducible.

The major finding of this study is that urinary NHPA is not derived solely from nitrotyrosine metabolism and at least one other pathway is responsible for its formation *in vivo* (Fig. 2.10). The nitration of [$^2H_6$]PHPA to [$^2H_5$]NHPA provides unequivocal proof that nitration of circulating PHPA can occur. Indeed, based on our animal studies, we estimate that most of the urinary NHPA (approx. 85%) is formed by nitration of PHPA *in vivo* in the rat, despite the fact that only a relatively small fraction of the infused PHPA is nitrated *in vivo*. This occurs because PHPA is present in plasma at a concentration of approx. 2.7 µmol/l, whereas free nitrotyrosine is only present at approx. 4.2 nmol/l (Moore and Mani 2002).

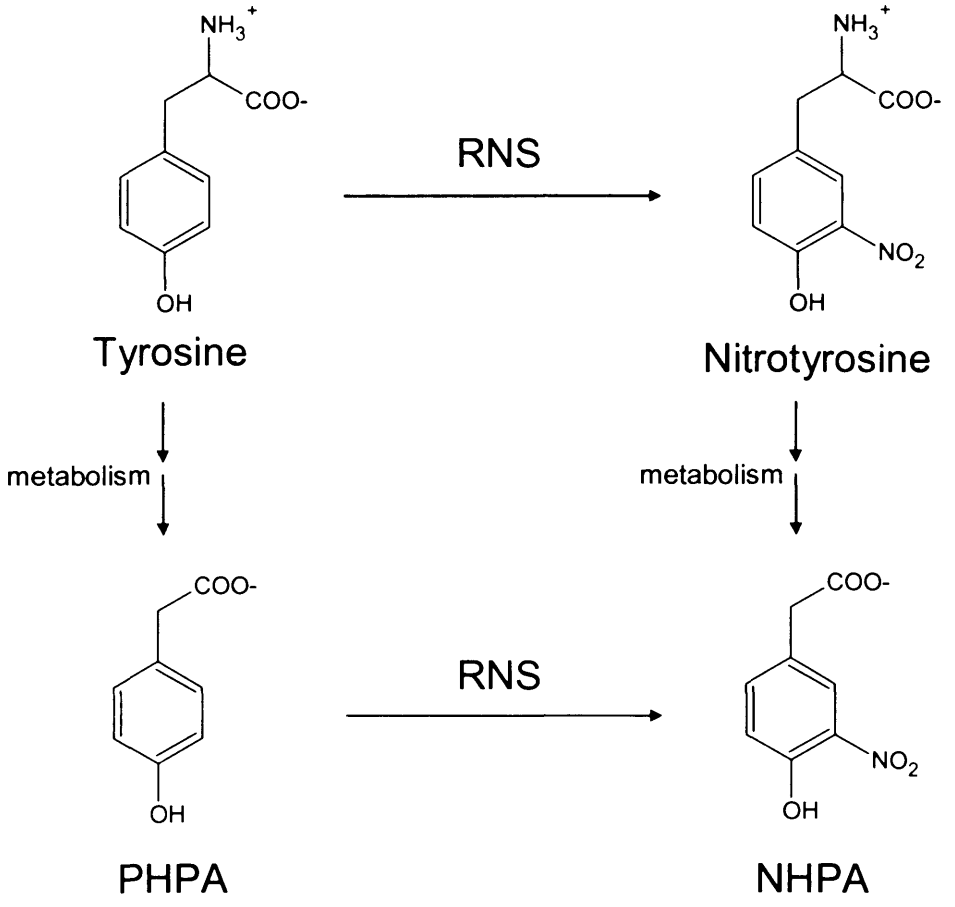

Figure 2.10 Two identified pathways, which can produce NHPA *in vivo*. NHPA can be formed by either nitration of PHPA or catabolism of free nitrotyrosine. Tyrosine decarboxylase and tyramine oxidase are two identified metabolic enzymes that are responsible for conversion of tyrosine and nitrotyrosine into PHPA and NHPA. RNS: Reactive nitrogen species.

Although the major source of urinary NHPA is formed by nitration of endogenous PHPA, we also demonstrate that NHPA excretion increased after intravenous nitrotyrosine injection. Less than 5% of injected nitrotyrosine was excreted in the urine as NHPA over 5 h, which is consistent with the observations of Tabrizi-Fard et al. (1999), who also observed that only 5–6% of infused nitrotyrosine was

metabolized to NHPA. The large volume of distribution of free nitrotyrosine and the absence of detectable nitrotyrosine in normal urine suggest that there is cellular uptake as well as tubular re-absorption of free nitrotyrosine by various amino-acid transporters in the cell membrane. In contrast, 78 ± 2% of injected [$^2H_6$]PHPA was rapidly excreted into the urine unchanged, demonstrating that there is little, if any metabolism of this compound. Based on a plasma concentration of PHPA of 2.7±1.1 μmol/l, and a urinary excretion rate of PHPA at 2.3 ± 0.7 nmol/min in rats, the renal clearance of PHPA is estimated to be approx. 0.85 ml/min. This value is very close to the glomerular filtration rate of our laboratory rats (1.02±0.1 ml/min) (Anand et al. 2002), and suggests that PHPA is simply filtered and not re-absorbed by the kidneys.

We have also shown that measurement of [$^2H_5$]NHPA after infusing [$^2H_6$]PHPA may be used as an index of reactive nitrogen species formation *in vivo*. Our observation that endotoxaemia causes a significant increase in [$^2H_5$]NHPA excretion (Fig 2.9) supports the validity of this novel approach. Moreover our observation that the ratio of nitration of [$^2H_5$]NHPA from infused [$^2H_6$]PHPA was almost identical with that of endogenous NHPA to PHPA suggests that measurement of the NHPA/PHPA ratio may be useful to assess nitration reactions *in vivo* (Fig 2.9).

The present study has shown for the first time that endogenous PHPA can be nitrated to NHPA *in vivo*, which, until the present study, has been regarded as the major metabolite of nitrotyrosine. On a practical level, we have also shown that measurement of urinary NHPA can be used to monitor nitration reactions *in vivo*, although its sensitivity and specificity at this stage of these studies are unknown. We conclude that the measurement of urinary NHPA excretion provides a time-integrated index of reactive nitrogen species formation *in vivo*, although it is not exclusively related to nitrotyrosine metabolism.

Chapter 3: Stabilization and measurement of S-nitrosothiols in tissues

3.1 Introduction

S-Nitrosothiols are formed by the reaction of reactive nitrogen species (e.g., N_2O_3) with a sulfhydryl group, either with a low-molecular-weight species such as glutathione or within a protein such as albumin. The control of protein function by S-nitrosation is counter-regulated by de-nitrosation, a process which may involve low-molecular-weight thiols such as glutathione or cysteine, which can undergo trans-nitrosation reactions to form *S*-nitrosoglutathione (GSNO) and *S*-nitrosocysteine (CysNO), respectively (Williams 1999). Both GSNO and CysNO are inherently unstable in a biological milieu such as plasma or tissues and may release NO or react with other thiols to form thiolated adducts together with the secondary release of NO (Williams 1999). Therefore, methods which measure the tissue concentrations of *S*-nitrosothiols should ensure that all tissue *S*-nitrosothiols, including low-molecular-weight species, are stable under the conditions employed.

Various methods have been developed to measure the tissue levels of *S*-nitrosothiols and, more specifically, identify S-nitrosated proteins. These include chemiluminescence-based assays of total tissue *S*-nitrosothiol concentration, and the biotin-switch assay (Jaffrey et al. 2001). While many advances have been made in the detection of either total cellular S-nitrosation or individual S-nitrosothiols, proteomic methods for the detection of S-nitrosation are in relative infancy due to the rapid decomposition of S-nitrosothiols both *in vivo* and *in vitro*.

The decomposition of *S*-nitrosothiols is accelerated in plasma by free thiols and transition metals (Williams 1999). Thus, both low- and high-molecular-weight *S*-nitrosothiols can be stabilized in plasma by reaction of the free thiol group with *N*-ethylmaleimide (NEM) and chelation of metal ions by DTPA (diethylenetriamine pentaacetic acid) (Moore and Mani 2002). As part of our program to develop assays for tissue *S*-nitrosothiols based on the chemiluminescence method, we initially wished to confirm that tissue *S*-nitrosothiols are stabilized in tissue homogenates by perfusing tissues with buffer containing NEM and DTPA. In our laboratory we had previously shown that both *S*-nitrosoalbumin and GSNO are stable in plasma under these conditions (Marley et al 2001), which enable sampling and subsequent measurement

by reductive chemiluminescence assays. However, it rapidly became apparent to us that, low-molecular-weight *S*-nitrosothiols decompose in liver and kidney tissue homogenates, even in the presence of NEM and DTPA. Studies in cell culture by Zhang and Hogg (2004) have also indicated that spiking cells with GSNO or *S*-nitrosoalbumin before homogenization with NEM/DTPA results in incomplete recovery of GSNO, whereas *S*-nitrosoalbumin is fully recovered. The present study reports our investigations on the stability of *S*-nitrosothiols in tissue homogenates and our studies on the nature of the tissue factor which accelerates the decomposition of *S*-nitrosothiols.

3.1 Materials and methods II

Chemicals

All *S*-nitrosothiols used in this study were synthesized in our laboratory and stored at −80°C in the presence of NEM (10 mM) and DTPA (2 mM). All chemicals were purchased from Sigma (Poole, UK).

Synthesis of S-nitrosothiols

S-Nitroso-L-cysteine (L-CysNO), *S*-nitroso-D-cysteine (D-CysNO), and *S*-nitrosoglutathione (GSNO) were prepared by reacting equal volumes of sodium nitrite (10 mM) with the corresponding reduced thiols (10 mM) at pH 2 as described previously (Moore and Mani 2002). Stocks of *S*-nitrosoalbumin were prepared by incubation of reduced human serum albumin with L-CysNO (prepared as above) at room temperature for 30 min in the dark. Any remaining un-reacted thiol groups were then alkylated with NEM (1 mM) at room temperature, followed by dialysis at 4°C against 4 × 3 litres of PBS supplemented with DTPA (100 mM) for 72 h (Marley et al. 2000).

Preparation of tissue homogenates

Male Sprague–Dawley rats (280–300 g) were housed in a standard caging system and kept on a reversed 12/12 light/dark cycle. Animals were fed a standard chow diet and

allowed access to food and water *ad libitum*. All animal procedures were in accordance with Home Office (UK) recommendations. On the day of the experiment, animals were anesthetized by intraperitoneal injection of sodium pentobarbital (60 mg/kg). After thoracotomy, organs were flushed free of blood and perfused through the left ventricle with NEM/DTPA (10/2 mM) freshly prepared in PBS, which leads to efficient in situ alkylation of thiols and complexation of free transition metals. Organs (liver, kidney, heart, and brain) were cut into small pieces and homogenized in ice-cold NEM/DTPA phosphate buffer (10/2 mM, pH 7.4; 5/1 vol/wet wt) using a Potter–Elvehjem homogenizer. Homogenates were kept on ice in the dark and used within 30 min of preparation. The protein content of the homogenates was assessed by the Biuret method and the final concentration of tissue homogenates as set at 5 mg protein/ml using NEM/DTPA in PBS. Blood was also collected from the aorta into tubes containing EDTA (final concentration 2 mM) and centrifuged for 10 min at 1300*g*. After addition of NEM (final concentration 10 mM), the plasma samples were kept at 4°C and used on the day of collection.

Measurement of S-nitrosothiols

S-Nitrosothiols were quantified, as previously described (Marley et al. 2000; 2001), by a copper/iodide-mediated cleavage of *S*-nitrosothiols to release NO, which was quantified by its gas phase chemiluminescence reaction with ozone (NO analyzer; Sievers, Boulder, CO, USA). Immediately before analysis of the samples, nitrite was removed by reacting with acidified sulfanilamide as described (Marley et al. 2000). The reaction mixture, consisting of potassium iodide and iodine in glacial acetic acid, was kept at constant temperature in a septum-sealed, water-jacketed reaction vessel, continuously bubbled with nitrogen (Scheme 3.1). The purge vessel we use is approximately eight times as large as the conventional Sievers purge vessel. It contains 8 ml glacial acetic acid and 2 ml potassium iodide (50 mg/ml) and 400 μl copper sulfate (50 mg/ml). Addition of copper sulfate makes the solution brown due to the release of iodine. In this regard this method is similar to the triiodide method described by Gladwin and colleagues (Gladwin et al. 2000). The outlet of the gas stream was passed through a scrubbing bottle containing sodium hydroxide (1 M) in order to trap traces of acid and iodine before transfer into the detector. Standards and sample aliquots (500 μl) were injected into the reaction mixture by gas-tight Hamilton

syringes. Nitric oxide signal output was sampled at 2 Hz. Peak integration was performed after signal smoothing to eliminate high-frequency noise and baseline correction. To confirm that the species is an *S*-nitrosothiol rather than an *N*-nitrosamine or an iron-nitrosyl, samples were run before and after the addition of $HgCl_2$ (final conc 2%) (Feelisch et al. 2002). Calculated NO amounts were validated by injection of freshly prepared nitrite standards into the same reaction chamber (without acid sulfanilamide). We have previously shown that *S*-nitrosothiols give the same signal as nitrite.

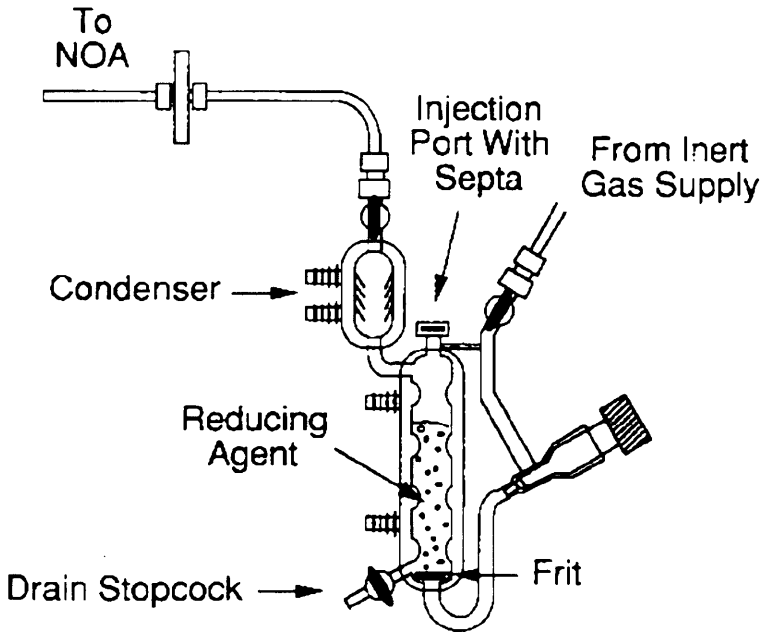

Scheme 3.1. Reaction chamber set up for reduction of nitros(yl)ated compounds. The reaction chamber is attached to a nitric oxide analyse (NOA). This figure is adapted from Siever's NO analyzer catalogue (NOA^{TM} 280, Revision C, 1997).

The decomposition of S-nitrosothiols in homogenates of rat liver

Various *S*-nitrosothiols (L-CysNO, D-CysNO, GSNO, *S*-nitrosoalbumin) were incubated to give a final concentration of 250 nM with aliquots of rat liver homogenates (5 mg/ml protein concentration, volume 500 μl). This low concentration of added *S*-nitrosothiols was used ($\sim$50 pmol/mg protein) because this is most likely to represent what may be observed *in vivo*. The presence of NEM, which alkylates free thiol groups, blocks all *trans*-nitrosation reactions with proteins or other thiols. A vertical rota shaker was employed for continuous stirring during the incubation. The aliquots were incubated with the *S*-nitrosothiol at either 37 or 4°C and kept in the dark. The levels of *S*-nitrosothiols were measured at different time intervals (1, 15, 60, and 120 min) using the chemiluminescence-based assay. In a separate experiment, aliquots of liver homogenate were heated at 80°C for 30 min to denature the proteins. After the samples were cooled to 4°C, L-CysNO was added to give a final concentration of 250 nM and the levels of *S*-nitrosothiol were then measured at different time points as above. The reason for carrying out most measurements at 4°C was to slow decomposition down to a rate that could be easily followed. In a separate experiment, liver tissues were homogenized in PBS and were incubated with 0.1 mg/ml proteinase K at 37°C in the presence of 1 mM $CaCl_2$. Thirty minutes after incubation with proteinase K, NEM and DTPA were added to liver homogenate (final concentration of 10 and 2 mM, respectively). After the samples were cooled to 4°C, L-CysNO was added to give a final concentration of 250 nM and the levels of *S*-nitrosothiol were then measured at different time points as above. Each experiment was repeated at least five times (in tissue homogenates obtained from different rats).

The decomposition of L-CysNO in homogenates of different tissue

Different tissue homogenates (kidney, heart, and brain) were also prepared as above (5 mg/ml protein concentration, aliquots of 500 μl) and incubated with L-CysNO (final concentration of 250 nM) at 4°C in the dark. The levels of *S*-nitrosothiol were then measured at 1, 15, 60, and 120 min by chemiluminescence. Acceleration of CysNO decay was also tested after supplementation of liver and heart homogenates with either NADH or NADPH (1 mM final concentration).

Effects of different enzyme inhibitors on CysNO decomposition

In some experiments, allopurinol (500 μM; xanthine oxidase inhibitor), iodoacetate (1 mM; inhibitor of thioredoxin reductase and glutathione peroxidase, an alkylating agent) (Jourd'Heuil et al. 2000), or oxamic acid/propargylglycine (2 mM; inhibitors of H_2S-producing enzymes cystathionine ß-synthase and cystathionine γ-lyase, respectively) (Stipanuk et al. 1982) were incubated with liver tissue homogenates for 30 min at 4°C before addition of L-CysNO (final concentration 250 nM). Based on published studies one would expect that γ-glutamyl transpeptidase (γ-GT) would decay GSNO to *S*-nitroso-cysteinylglycine, which then may get hydrolyzed to CysNO (Hogg et al. 1997). To test this, liver homogenates were incubated with acivicin (2 mM; a γ-GT inhibitor) for 30 min at 4°C before addition of GSNO or L-CysNO (final concentration 250 nM). The level of *S*-nitrosothiols was then measured at different time points (1, 15, 60, and 120 min).

Effects of specific transition metal chelators on CysNO decomposition

Diethyl dithiocarbamate (1 mM) and histidine (10 mM), which are reported to remove copper from copper-containing proteins (such as Cu/Zn superoxide dismutase) (Misra et al. 1979), were incubated with rat liver homogenates for 30 min (4°C) before addition of L-CysNO (final concentration 250 nM). The levels of CysNO were then measured at different time points (1, 15, 60, and 120 min). The effects of a selective Cu^+ chelator (neocuproine; 1 mM) and a free iron chelator (deferoxamine; 1 mM) on L-CysNO decomposition were also examined as described above.

Effects of oxygen depletion on the decomposition of L-CysNO in liver

Liver homogenates were deoxygenated by sparging with helium for 10 min and kept in a gas-tight chamber filled with argon (4°C). L-CysNO was added with a gas-tight syringe and the levels of *S*-nitrosothiols were measured 30 min after addition of CysNO.

Stabilization of L-CysNO in liver homogenate by potassium ferricyanide

S–NO bonds can be reduced by ferrous proteins such as ferrous deoxyhemoglobin and deoxymyoglobin (Gladwin et al. 2000). Gladwin and colleagues has previously

reported that potassium ferricyanide [$K_3Fe^{III}(CN)_6$] can stabilize *S*-nitrosohemoglobin in red blood cells (Gladwin et al. 2000). Thus, in a separate set of experiments potassium ferricyanide was used to oxidize ferrous proteins ($Fe^{2+} \rightarrow Fe^{3+}$) in rat liver homogenates containing NEM and DTPA. In brief, liver homogenates were incubated in potassium ferricyanide (4 mM final concentration) 10 min before the addition of CysNO (final concentration 250 nM) at 4°C. The levels of CysNO were then measured at different time points (1, 15, 60, and 120 min).

Preparation of cellular fractions and ultra-filtration of cytoplasmic proteins

Mitochondrial, microsomal, and cytoplasmic fractions of rat liver homogenates were isolated using differential centrifugation as described (Evans 1992). The mitochondrial and microsomal fractions were re-suspended in NEM/DTPA buffer (2 mg protein/ml). In some experiments the cytoplasmic fraction was subjected to centrifugal filtration to remove high-molecular-weight proteins (Microcon YC-10 centrifugal filter units, cut-off 10, 50, and 100 kDa; Millipore, Bedford, MA, USA). The effects of cellular fractions on CysNO decomposition were then examined as above.

Measurement of nitrite + nitrate after incubation of CysNO with liver homogenate

Important elements of *S*-nitrosothiol decomposition are reductive pathways that form NO. The released NO might undergo oxidation to form nitrite and nitrate in the presence of molecular oxygen. To address the role of such reactions in contributing to the metabolism of CysNO in liver homogenate, nitrite + nitrate levels were measured after incubation of liver homogenates with CysNO. Liver tissue homogenate was prepared as described above in NEM/DTPA PBS buffer (5 mg/ml protein concentration, 0.5 ml aliquots) and incubated with L-CysNO (4°C, final concentration of 2.5 μM) for 2 h. A higher concentration of CysNO was employed in these experiments because at low concentrations (250 nM) changes in nitrite + nitrate could not be detected due to high level of background nitrite + nitrate in tissue homogenates (4.13 ± 0.53 μM). Nitrite + nitrate levels were determined by chemiluminescence as described (Harry et al. 1999). In brief, samples were centrifuged for 10 min (10,000*g*) and 100 μl of supernatant was incubated with nitrate reductase, FAD, and NADPH to convert nitrate to nitrite (1 h, room temperature). Nitrite then was reduced to NO by

refluxing with acetic acid and potassium iodide and measured by chemiluminescence. Standard curves of sodium nitrite and nitrate were used for calibration. Preliminary data showed that NEM (which is present in liver homogenate; 10 mM) did not interfere with nitrate conversion to nitrite under the conditions employed.

Is there inducibility of the protein causing decomposition of S-nitrosothiols?

During preliminary experiments it became apparent that liver tissue homogenates from rats with biliary cirrhosis caused an accelerated decomposition of *S*-nitrosothiols, compared to normal liver tissue. Because biliary cirrhosis is associated with endotoxaemia (Harry et al. 1999), we tested whether injection of lipopolysaccharide (LPS) could induce up-regulation of the tissue factor responsible for the decomposition of L-CysNO *in vitro* and formally measured its activity in cirrhotic liver tissue. Thus two models were employed:

(A) *Endotoxaemia*: Endotoxaemia was induced by intraperitoneal injection of LPS (5 mg/kg from *Salmonella typhimurium*) to male Sprague–Dawley rats (280–300 g, $n = 4$). Animals were killed under pentobarbital anaesthesia 6 h after LPS injection and organs were perfused with NEM/DTPA PBS buffer as described above. Liver tissue homogenate was homogenized (5 mg/ml protein concentration, 0.5-ml aliquots) and incubated with CysNO (4°C, final concentration 2.5 μM) for different time intervals (0, 15, 60, and 120 min). A higher concentration of CysNO was employed in this experiment because at low concentrations, changes in *S*-nitrosothiols could not be detected due to the high concentration of background *S*-nitrosothiols in liver homogenates.

(B) *Biliary cirrhosis*: Biliary cirrhosis is associated with chronic endotoxemia and a systemic inflammatory response (Harry et al. 1999). Biliary cirrhosis was induced in male rats by ligation of the bile duct under general anaesthesia as described elsewhere (Harry et al. 1999). Cirrhotic animals ($n = 6$) were killed under pentobarbital anaesthesia 4 weeks after the operation. The liver was perfused in NEM/DTPA PBS buffer. Liver tissue homogenates (5 mg/ml protein concentration, 0.5 ml aliquots) were incubated with L-CysNO (4°C, final concentration 250 nM) for different time intervals (0, 15, 60, and 120 min) and assessed using chemiluminescence.

Time-dependent decay of endogenously formed S-nitrosothiols in endotoxemic liver

Liver tissues from endotoxemic rats (see above, $n = 4$) were perfused and homogenized in ice-cold NEM/DTPA PBS buffer (~500 mg tissue in 5 ml buffer). Some liver tissues were homogenized separately in NEM/DTPA PBS buffer supplemented with potassium ferricyanide (4 mM; ~500 mg tissue in 5 ml buffer). Homogenates were kept on ice in the dark and were analyzed 1, 5, and 15 min after tissue homogenization. In order to measure low-molecular-weight *S*-nitrosothiols the liver homogenates were subjected to centrifugal filtration to remove high-molecular-weight proteins using Millipore YC-10 centrifugal filters (cut-off 30 kDa). All samples were run before and after the addition of $HgCl_2$ (final concentration 2%).

3.2 Results II

Incubation of CysNO with rat liver homogenates resulted in a time-dependent decrease in CysNO concentration in the presence of NEM and DTPA at 37°C, which was slowed on cooling, with a half-life of 3 and 31 min at 37 and 4°C, respectively (Fig. 3.1). In contrast, CysNO was stable in PBS containing NEM/DTPA at both 4 and 37°C as shown in Fig. 3.1. Because of the very rapid decomposition at 37°C, all subsequent experiments were carried out at 4°C. To determine whether this rapid decomposition of L-CysNO was a generalized phenomenon of low-molecular-weight *S*-nitrosothiols, the effects of liver homogenate on the decomposition of D-CysNO, GSNO, and S-nitrosoalbumin were also assessed. The rate of decomposition of D-CysNO was identical with that of L-CysNO as shown in Fig. 3.2. GSNO also undergoes rapid decomposition in liver homogenates, with a half-life of 16 min at 4°C. By contrast, the high-molecular-weight *S*-nitrosothiol *S*-nitrosoalbumin was stable under these conditions, with no significant loss over 2 h.

To determine whether the decomposition of low-molecular-weight *S*-nitrosothiols by tissue was liver-specific we next incubated CysNO with kidney, heart, and brain homogenates as well as plasma. As shown in Fig. 3.3, there was a time-dependent decomposition of CysNO in kidney homogenates and, to a lesser extent, in heart homogenates in the presence of NEM/DTPA. This activity was minimal in brain tissue homogenates as well as plasma. The order of L-CysNO degradation activity was liver > kidney > heart > brain > plasma. The data in Fig. 3.3 seem to indicate that although an activity is present in other organs, the activity is lost very rapidly (except for liver and kidney). This raised the question of whether the factor is unstable in these tissues or whether an important cofactor is being consumed. As the mechanism is likely to be reductive, we examined if the addition of NADH or NADPH could accelerate CysNO decay in these and other tissues. The results showed that supplementation with NAD(P)H had no significant effect on CysNO decomposition in liver or heart homogenates (data not shown).

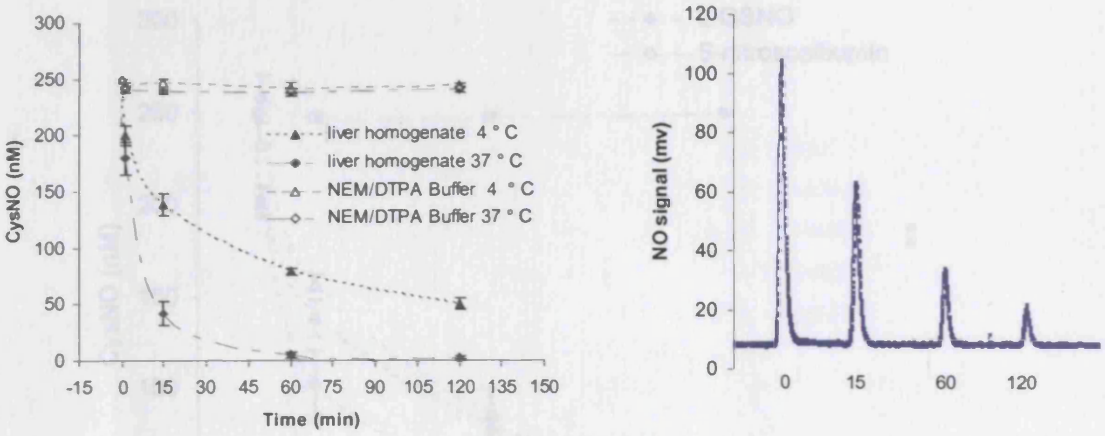

Figure 3.1. CysNO decomposition by liver homogenate incubated with *N*-ethylmaleimide/DTPA PBS at different temperatures (37°C vs 4°C). Liver tissue was perfused with *N*-ethylmaleimide/DTPA (10/2 mM) containing PBS and homogenized. CysNO was then added (final concentration 250 nM) to the liver homogenates (5 mg/ml) or buffer and measured at the different time points shown. Data are expressed as means ± SEM. The right side represents a typical detector response after addition of CysNO to rat liver homogenates at 4°C and its measurement at the different time points by chemiluminescence.

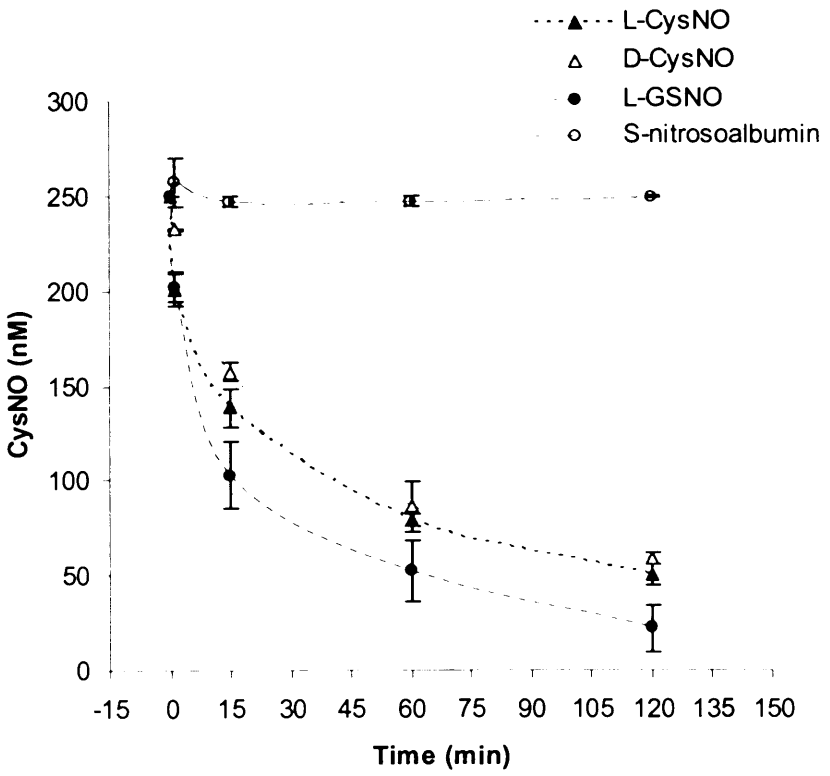

Figure 3.2. *S*-Nitrosothiol decomposition in presence of liver homogenate at 4°C. Liver tissue was perfused with *N*-ethylmaleimide/DTPA (10/2 mM) in PBS and homogenized. L-CysNO, D-CysNO, GSNO, or *S*-nitrosoalbumin was added (final concentration 250 nM) to the liver homogenates (5 mg/ml) and measured at different time points. Each experiment was repeated at least five times and data are expressed as means ± SEM.

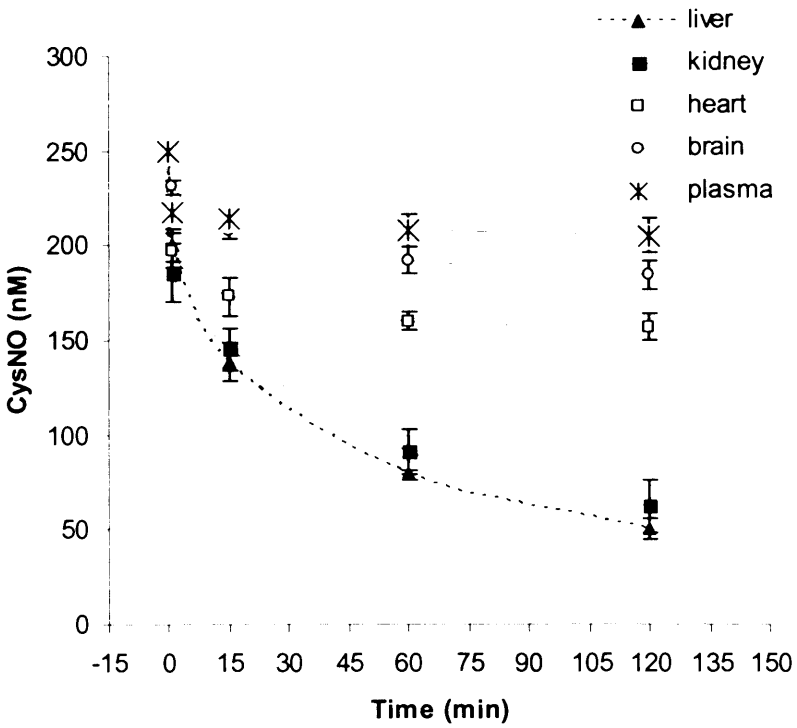

Figure 3.3. CysNO decomposition in presence of plasma, liver, kidney, heart, and brain homogenates (4°C). All organs were perfused with *N*-ethylmaleimide and DTPA (10 and 2 mM ,respectively) in phosphate buffer and homogenized. L-CysNO was added (final concentration 250 nM) to the homogenates (5 mg/ml) and measured at different time points. Each experiment was repeated at least five times and data are expressed as means ± SEM.

The marked temperature dependency of L-CysNO decomposition, as well the tissue heterogeneity, suggested to us that a protein/enzyme might be responsible for the rapid decomposition of CysNO. Therefore, we initially tried heating the liver homogenate (80°C for 30 min), and secondly we added proteinase K, a proteolytic enzyme, to the liver homogenate for 30 min before adding CysNO. Either proteolysis of proteins or their denaturation by heating inhibited the ability to catalyse CysNO decomposition by ~90% in liver tissue (Fig. 3.4).

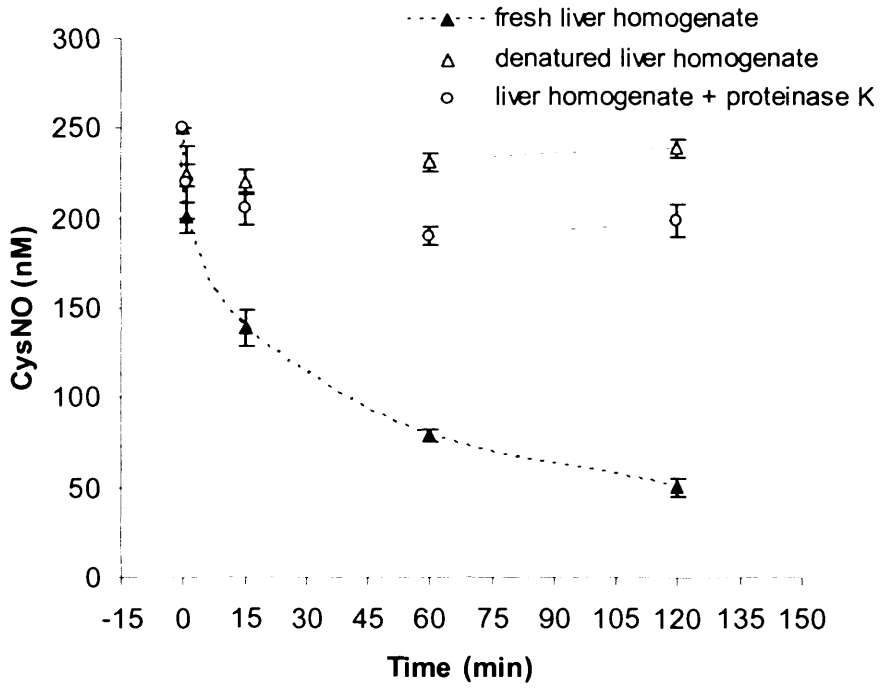

Figure 3.4. CysNO decomposition by fresh, heat-denatured liver homogenates or after proteolysis by proteinase K. After the samples were cooled down (4°C), L-CysNO was added to give a final concentration of 250 nM in either freshly prepared, proteolyzed, or denatured liver homogenates followed by measurement of CysNO at different time points. Data are expressed as means ± SEM.

To determine which cellular fraction was responsible for the decomposition of CysNO, mitochondrial, cytoplasmic, and microsomal preparations were prepared from liver homogenates. CysNO was stable in both the microsomal and the mitochondrial fractions, and the decomposition of CysNO was observed only in the cytoplasmic fraction of rat liver homogenates (Fig. 3.5).

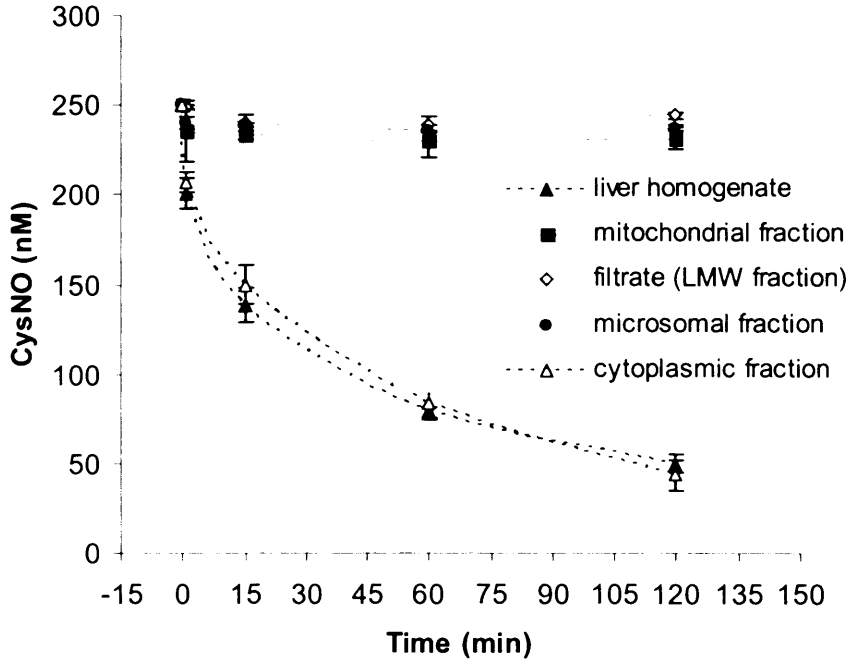

Figure 3.5. CysNO decomposition in the presence of whole liver homogenate and mitochondrial, microsomal, cytoplasmic, and low-molecular-weight (LMW) fractions of rat liver at 4°C. Each fraction was resuspended in *N*-ethylmaleimide/DTPA (10/2 mM) containing PBS. Each experiment was repeated at least five times and data are expressed as means ± SEM.

To determine whether the factor causing CysNO degradation activity resided in a high- or low-molecular-weight species, the cytoplasmic fraction was subjected to centrifugal filtration at different molecular weight cut-offs. Ultrafiltration of the

cytoplasmic fraction resulted in no detectable CysNO decomposition activity in filtrates obtained through 10-, 50-, and 100-kDa cut off filters, suggesting that activity resides in a high-molecular-weight fraction. Re-suspension of the retained cytoplasmic fraction (e.g., in the sludge that remains above the filter) in buffer showed >90% of CysNO degradation activity compared with liver homogenates. Thus, in liver homogenates, there is a factor which is (a) heat labile, (b) resides in the cytoplasm, and (c) has a high molecular weight (i.e., cannot be filtered through the Millipore centrifuged filters).

These data suggested that a protein might be responsible for catalyzing the decomposition of CysNO. Many proteins have been described as affecting the stability of *S*-nitrosothiols. Fig. 3.6 shows that neither selective metal chelators (neocuproine and deferoxamine) nor iodoacetate (an inhibitor of thioredoxin reductase and glutathione peroxidase), acivicin (γ-glutamyl transpeptidase inhibitor), allopurinol (xanthine oxidase inhibitor), or oxamic acid/propargylglycine (inhibitors of H_2S-producing enzymes) had any effect on the decomposition of CysNO. We also tested the effect of acivicin on GSNO decay in liver homogenate; however, we were unable to show any significant effect (data not shown). Diethyl dithiocarbamate, which removes copper from copper-containing proteins, did not block the CysNO decomposition activity of liver homogenates (Fig. 3.6). One possible candidate to cause decomposition of L-CysNO and other low-molecular-weight *S*-nitrosothiols is a redox-sensitive metalloprotein. To test this we initially tested the effect of potassium ferricyanide, which can oxidize ferrous iron proteins to ferric iron proteins. Incubation of normal liver homogenate with potassium ferricyanide significantly inhibited L-CysNO decay as shown in Fig. 3.6 ($P<0.001$, ANOVA). The effect of hypoxia on the stability of L-CysNO in liver tissue was also assessed. Sparging of liver homogenates with helium to cause oxygen depletion led to a significant stabilization of L-CysNO, with the decomposition decreasing from 46 ± 4 to 24 ± 7% ($P<0.025$, $n = 4$, *t*-test) 30 min after addition of CysNO in control and hypoxic homogenates, respectively.

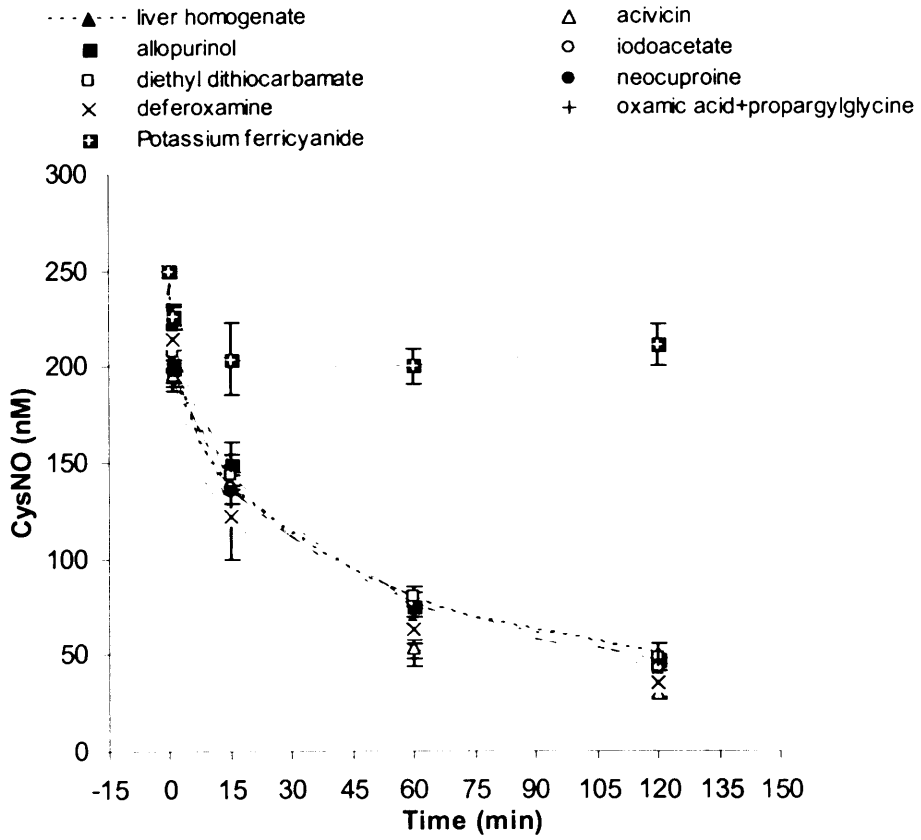

Figure 3.6. CysNO decomposition by liver homogenate after 30 min incubation with acivicin (2 mM), allopurinol (500 μM), iodoacetate (1 mM), oxamic acid/propargylglycine (2 mM), diethyl dithiocarbamate (1 mM), neocuproine (1 mM), deferoxamine (1 mM), and potassium ferricyanide [$K_3Fe^{III}(CN)_6$; 4 mM]. Liver was homogenized in *N*-ethylmaleimide/DTPA containing PBS (4°C). Each experiment was repeated at least five times and data are expressed as means ± SEM.

Because iron proteins can reduce reactive nitrogen species to nitrate, we determined whether the major product of CysNO decomposition was either nitrite or nitrate. We observed a significant increase in both nitrite and nitrate concentrations in liver homogenate ($P < 0.05$, paired *t*-test), with nitrate contributing more than 95% of detected nitrite + nitrate (Fig. 3.7). Thus, incubation with CysNO (2.5 μM final concentration) led to an increase in nitrite + nitrate concentration by 2.2 ± 0.3 μM in liver homogenates.

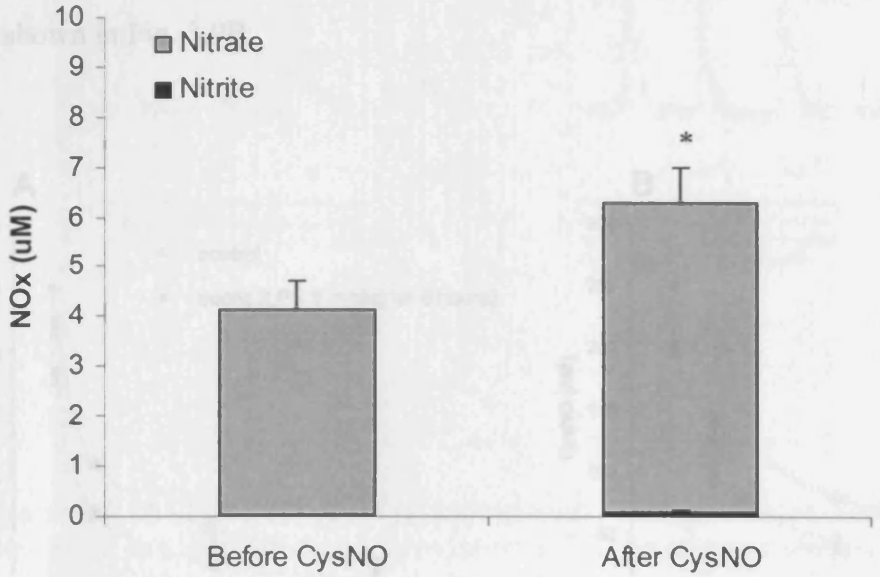

Figure 3.7. Formation of nitrite + nitrate (NOx) in liver homogenate after 2 h incubation with CysNO in *N*-ethylmaleimide/DTPA buffer. Incubation with CysNO (2.5 μM final concentration) led to a 2.17 ± 0.25 μM increase in NOx levels. * $P < 0.05$ in comparison with nitrite + nitrate levels before addition of CysNO (paired *t*- test).

To determine whether liver disease or endotoxaemia could induce an increase in the level or activity of the putative iron protein, the decomposition of L-CysNO was measured in liver homogenates from rats with endotoxaemia or cirrhosis (Fig. 3.8). Both endotoxaemia and biliary cirrhosis significantly increased the rate of decomposition of L-CysNO, even in the presence of NEM and DTPA ($P<0.02$, ANOVA). We also looked at the basal level of hepatic nitroso compounds in septic rats. Homogenization of septic liver in NEM/DTPA phosphate-buffered saline was associated with a time-dependent decay of the signal as shown in Fig. 3.9A. Under these experimental conditions, the mercury-resistant signal was stable over a 30-min period. Homogenization of the endotoxaemic livers in ferricyanide-containing buffer stabilized the hepatic levels of nitrosated compounds and gave a series of stable peaks as shown in Fig. 3.9B.

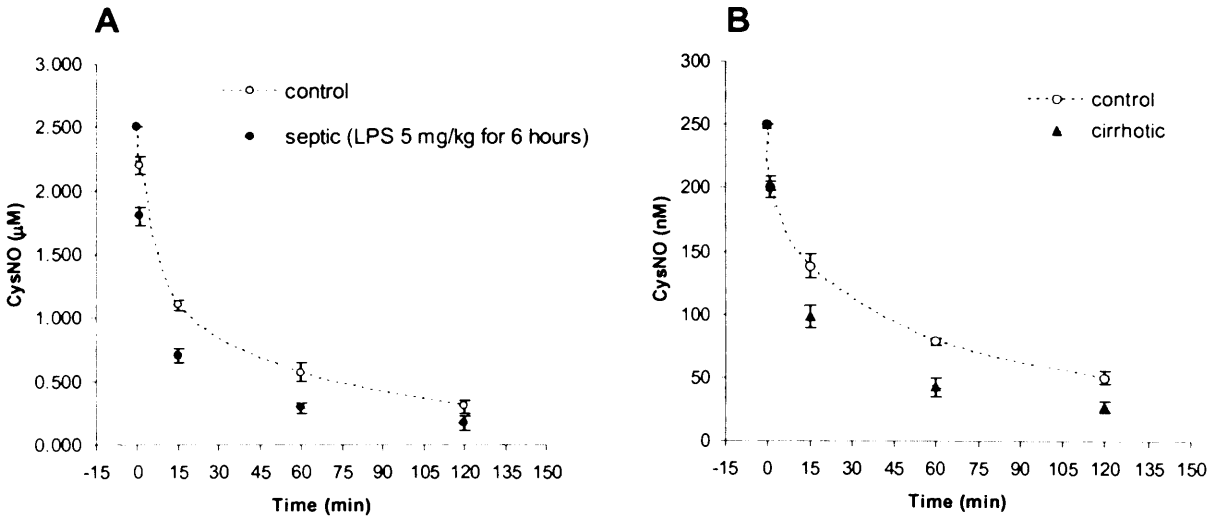

Figure 3.8. CysNO decomposition in the presence of liver homogenates of rats with (A) acute sepsis or (B) biliary cirrhosis. Each experiment was repeated at least four times and data are expressed as means ± SEM.

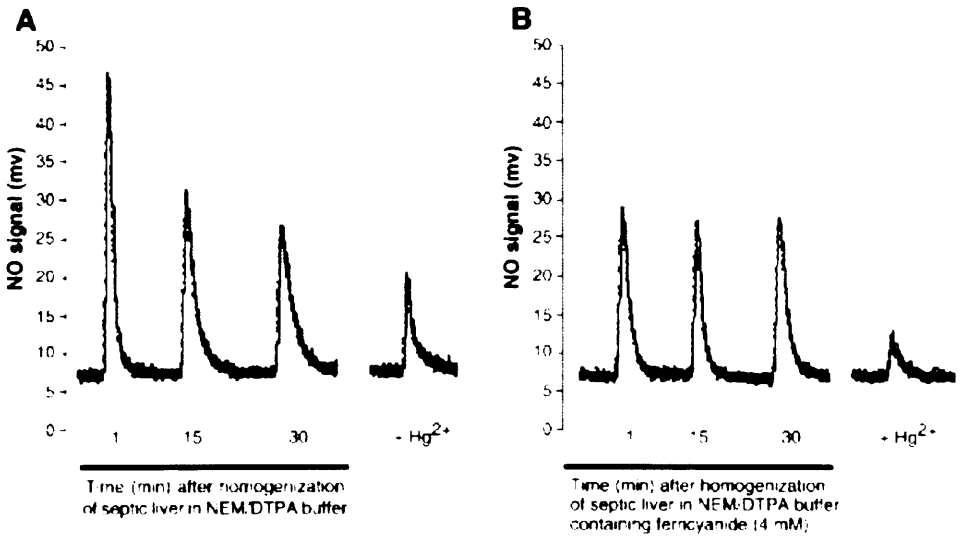

Figure 3.9. (A) Decomposition of endogenously formed nitroso compounds in liver obtained from a rat with acute endotoxaemia. Liver was homogenized in NEM/DTPA phosphate-buffered saline and kept on ice before analysis at different time intervals (1, 15, 30 min). Addition of mercury (Hg^{2+}) selectively cleaves S–NO bonds and the mercury-resistant nitroso compounds contain both *N*-nitrosamines and iron–nitrosyl. (B) Ferricyanide stabilizes *S*-nitrosothiols and selectively cleaves iron–nitrosyl complexes. Homogenization of septic liver in ferricyanide containing buffer stabilizes the hepatic levels of *S*-nitrosothiols over 30-min periods.

3.3 Discussion II

This study shows that low-molecular-weight *S*-nitrosothiols are inherently unstable in tissue homogenates and that assays which measure tissue *S*-nitrosothiol concentration probably simply measure the levels of relatively stable *S*-nitroso proteins. More importantly we have shown that the decomposition of CysNO is catalyzed by a factor(s) which has the characteristics of a cytoplasmic ferrous protein, based on its sensitivity to proteolysis, thermal instability, high molecular weight, and sensitivity to potassium ferricyanide.

It has been shown that degradation of CysNO in the presence of vascular tissue homogenate can be completely eliminated by the alkylation of thiol groups with NEM (Kostka et al. 1999). Here we have shown that unlike vascular tissue, liver and kidney homogenates decompose CysNO in a thiol-independent manner. This CysNO degradation activity was negligible in brain and heart homogenates and was almost absent from plasma. We used a high concentration of a potent thiol-blocking agent (NEM; 10 mM) to ensure that the maximum yield of alkylation was achieved (i.e., 2 μmol/mg protein, which is $\sim$20 times more than the expected amount of cysteine residues in proteins). In a separate set of experiments NEM concentration was increased to 50 mM and almost identical results were achieved (data not shown). Apart from non-enzymatic degradation, several enzymatic mechanisms, including glutathione peroxidise (Hou et al. 1996), thioredoxin reductase (Nikitovic et al. 1996), xanthine oxidase (Trujillo et al. 1998), Cu/Zn superoxide dismutase (Jourd'heuil et al. 1998), glutathione-dependent formaldehyde dehydrogenase (Liu et al. 2001), and H_2S-producing enzymes (Giles et al. 2004), are able to decompose *S*-nitrosothiols *in vitro*, but their physiological relevance is not well understood. In our study pharmacological tests were negative for several candidate enzymes, namely glutathione peroxidase, thioredoxin reductase, xanthine oxidase, superoxide dismutase, γ-GT, cystathionine β-synthase, and cystathionine γ-lyase. Recently Liu et al. have shown that glutathione-dependent formaldehyde dehydrogenase (GSNO reductase) reduces GSNO to disulfide and ammonia (Liu et al. 2001). However, this 44-kDa GSNO reductase is highly specific for GSNO and no activity has been observed for CysNO and *S*-nitrosohomocysteine (Liu et al. 2001). Although we have not directly investigated whether the protein responsible for CysNO decomposition is

the same as the recently identified enzyme, GSNO reductase, the GSNO selectivity of GSNO reductase over other low-molecular-weight *S*-nitrosothiols makes this unlikely.

To determine whether the observed activity was stereoselective, we carried out studies comparing D-CysNO and L-CysNO decomposition and observed that liver homogenates are equally active at decomposing both isomers (Fig. 3.2). This observation is not in favour of a direct enzymatic pathway by which CysNO is being consumed as a substrate. Furthermore the ability of potassium ferricyanide to stabilize CysNO decay in tissue homogenates shows that a cytoplasmic ferrous protein (or a group of ferrous proteins) might be involved in this process. NEM cannot prevent the formation of *N*-nitrosation and iron–nitrosyl products. According to studies by Feelisch and colleagues, the formation of N-nitrosation and iron–nitrosyl products is as ubiquitous as that of S-nitrosation products (Feelisch et al. 2002). Spencer et al. (2000) have already shown that GSNO can be reduced by ferrous deoxyhaeme proteins such as haemoglobin and myoglobin. Gladwin et al. (2000) have also used ferricyanide/cyanide to selectively cleave NO from nitrosyl haemoglobin before analysis by a methodology similar to the one presented here. This approach relies on the classical Evelyn and Malloy technique of haemoglobin quantification in blood based on the oxidation of oxyhaemoglobin to methaemoglobin (Evelyn and Malloy 1938). Here we have shown that incubation with potassium ferricyanide inhibits the decomposition of both added CysNO (Fig. 3.6) and endogenously formed *S*-nitrosothiols in rat liver homogenates (Fig. 3.9). As shown in Fig. 3.9, the signal detected from endogenously formed nitroso compounds in an endotoxaemic rat was subjected to a time-dependent decay in liver tissue homogenates in the presence of NEM and DTPA. Under these experimental conditions, the mercury-resistant signal was stable over a 30-min period. Addition of mercury selectively cleaves S–NO bonds and the mercury-resistant peak which remain, contains both *N*-nitrosamines and iron–nitrosyl complexes. On the other hand, homogenization of the endotoxaemic liver in ferricyanide-containing buffer was associated with detection of a series of stable peaks (Fig. 3.9B). Ferricyanide oxidizes the ferrous proteins, which leads to decomposition of iron–nitrosyls and stabilization of *S*-nitrosothiols. Thus the mercury-resistant fraction under this condition contains just *N*-nitrosamines because the iron–nitrosyl complexes are unstable in the presence of ferricyanide. Based on this chemistry a method for stabilization and measurement of tissue *S*-nitrosothiols, *N*-

nitrosothiols, and iron–nitrosyl complexes is proposed in Fig. 3.10. This method has the advantage that it can potentially measure both high-molecular-weight and low-molecular-weight nitroso species using centrifugal filtration (Fig. 3.10). The currently most used method for separation of low- and high-molecular-weight nitroso compounds is based on trichloroacetic acid (TCA) precipitation of tissue proteins. However, TCA precipitation may be associated with artifactual formation of nitroso compounds due to acidification of nitrite and formation of reactive nitrogen species. Our unpublished data have also shown that homogenization of tissues in TCA-containing medium is subject to a time-dependent decomposition of *S*-nitrosothiol levels, which might be due to formation of hydrogen sulfide from sulfide in acidified tissue homogenates (unpublished observation). Incubation with CysNO led to an increase in nitrite + nitrate concentration in liver homogenates in which nitrate contributed more than 95% of detected nitrite + nitrate. This mechanism is oxygen dependent and ferricyanide sensitive. It has been theorized that iron–nitrosyl complexes (such as $HbFe^{II}NO$) react with oxygen; forming a haem–peroxynitrite adduct and finally liberating nitrate (Cooper 1999). However, the elucidation of the nature of the tissue factor involved in the catabolism of CysNO requires further study. Most importantly, we have described the decomposition of low-molecular-weight *S*-nitrosothiols by a metalloprotein and described a simple method to stabilize these compounds until analysis. Thus, homogenization of tissues in ferricyanide-containing buffers in the presence of NEM and DTPA can stabilize *S*-nitrosothiols in tissues before the measurement of their levels.

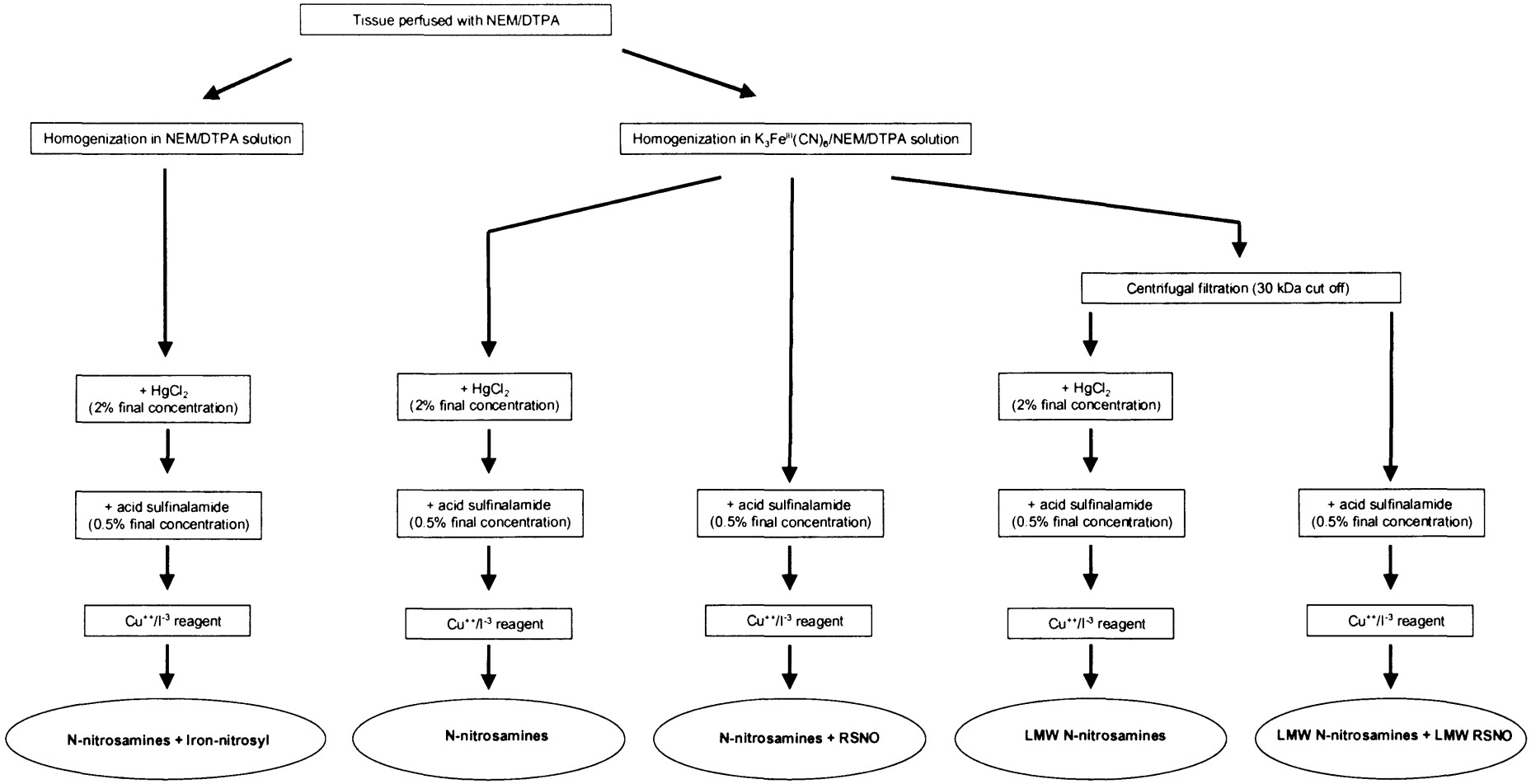

Figure 3.10. Flow diagram for the measurement of S-nitrosothiols, N-nitrosamines and iron-nitrosyl complexes in tissues. The method is based on detection of NO released form nitos(yl)ated compounds in presence of Cu^{2+}/I^{-3}, Hg^{2+} (which selectively cleaves S-NO) and ferricyanide (which stabilizes S-nitrosothiols and cleaves iron-nitrosyl complexes).

Chapter 4: Role of nitration and/or S-nitrosation of cardiac proteins in the pathogenesis of cardiac chronotropic dysfunction in rats with biliary cirrhosis

4.1 Introduction

The cardiac cycle undergoes a natural variation due to respiratory cycle, baroreflex activation, the intrinsic variability of cardiac pacemaker activity, circadian rhythms and other physiological mechanisms (see for Altimiras 1999 for review). Loss of heart rate variability (HRV) and increased heart rate regularity is a common feature of systemic inflammatory conditions such as endotoxaemia and liver failure (Mani et al. 2006a; Fleisher et al. 2000). Previous studies have shown that indices of depressed heart rate variability in patients with liver failure correlate not only with the extent of disease progression, but also predict survival in these patients (Fleisher et al. 2000). Thus, Fleisher et al. (2000), have shown that heart rate variability was significantly lower in the non-survivor patients awaiting liver transplantation compared with survivors.

The mechanism of decreased heart rate variability in cirrhosis remains unclear however it shares some basic characteristics with other systemic illnesses such as congestive heart failure and sepsis. Malave et al., (2003) have shown that circulating levels of tumour necrosis factor-alpha (TNF-α) correlate with indices of depressed heart rate variability in patients with congestive heart failure. TNF-α has a crucial role in pathogenesis of inflammatory conditions such as endotoxaemia as well as the progression of heart failure. Since TNF-α can blunt ß-adrenergic signalling (Chung et al., 1990), Malave et al. (2003) suggested that TNF-α is a major circulating mediator which decreases ß-adrenergic responsiveness and leads to a decrease in heart rate variability observed in heart failure and systemic inflammatory conditions.

Abnormalities in both cardiac muscle physiology and cardiac neural autonomic regulation have been documented in patients with cirrhosis (Hendrickse et al. 1992; Lee et al. 2007). Cardiac function is abnormal in cirrhosis, with subnormal cardiac responses to pharmacological and physiological stimuli. Manoeuvres leading to sympathetic nervous system activation by different means, such as tilting, physical exercise and pharmacological stimulation, do not evoke an adequate acceleration of heart rate in cirrhotic patients compared with normal subjects (Bernardi et al. 1987;

Bernardi et al 1991, Wong 2001). Despite the fact that down regulation of ß-adrenergic signalling is well documented in cirrhosis, its role in the loss of heart rate variability in cirrhosis is unknown.

Recent studies proposed a pathophysiologic role for increased cardiac nitric oxide (NO) and endocannabinoid formation in the development of cardiac abnormalities in experimental cirrhosis (Liu et al. 2000; Gaskari et al. 2005). Inhibition of either NO synthase (NOS) or endocannabinoid receptors improves the blunted responsiveness of isolated papillary muscle to adrenergic stimulation *in vitro* (Liu et al. 2000; Gaskari et al. 2005). The reason for increased cardiac NO and endocannabinoid formation is not precisely understood, however it is proposed that endotoxaemia, possibly from gut-derived bacterial translocation, causes induction of NO as well as endocannabinoid formation leading to cardiovascular dysfunction in cirrhosis (Rasaratnam et al. 2004). Endotoxaemia is a common feature of cirrhosis and high concentrations of circulating endotoxins are found in cirrhotic patients with no clinical evidence of infection due to impaired clearance of gut bacterial endotoxin in diseased liver (Wiest and Garcia-Tsao 2005). Since endotoxin can induce the synthesis of both NO (Petros et al. 1991) and anandamide (Varga et al. 1998), here we have hypothesised that this may have two consequences. Firstly there may be increased NO and endocannabinoid formation leading to altered cardiac responsiveness to ß-adrenergic stimulation and secondly the subsequent loss of cardiac responsiveness to autonomic modulation contributes to the decrease in heart rate variability (Fig. 4.1).

The contribution of nitric oxide (NO) to the pathophysiology of cardiac dysfunction in cirrhosis is well documented (Van Obbergh et al. 1996; Liu et al. 2000; Mani et al. 2002). Nitric oxide is involved in the modulation of cardiac function in the normal heart, as well as in various cardiac diseases via mechanisms involving NO that are both dependent on and independent of guanylate cyclase (Balligand et al. 1997; Paolocci et al. 2000). For example, evidence suggests NO attenuates cardiac pacemaker activity, mediated by cGMP (Herring et al. 2002), However, NO may also modify cardiac function through nitration or S-nitrosation of cardiac proteins (Paolocci et al. 2000; Gow et al. 2004). Tyrosine residues in proteins are targets for nitration by reactive nitrogen species such as peroxynitrite and may lead to loss of

function. One example of this is actin, which when nitrated loses its ability to contract effectively (Aslan et al. 2003). Likewise, cell signalling via phosphorylation of tyrosine residues also may become impaired after nitration of critical regulatory proteins (Gow et al. 2004). Moreover, the concept that protein function may be controlled by S-nitrosation of a critical cysteine residue has emerged in biology as a potentially important mechanism or pathway to control cellular function (Hare and Stamler 2005). Although cirrhosis is well recognized as being associated with increased NO synthesis, the role of nitration or nitrosation of cardiac proteins in cardiac function in cirrhosis has not previously been investigated.

The aims of the work described in this chapter were:

1. Evaluate the relationship between heart rate variability and the degree of atrial chronotropic responsiveness to adrenergic stimulation.

2. To test the hypothesis that increased formation of reactive nitrogen species in cirrhosis causes nitration/nitrosation of cardiac proteins and leads to impaired cardiac chronographic function. Therefore, we have investigated the effects of two independent treatments (a low-molecular-weight thiol and an NO synthase inhibitor), both of which can decrease nitration/nitrosation of proteins, on cardiac chronotropic responses in a rat model of biliary cirrhosis.

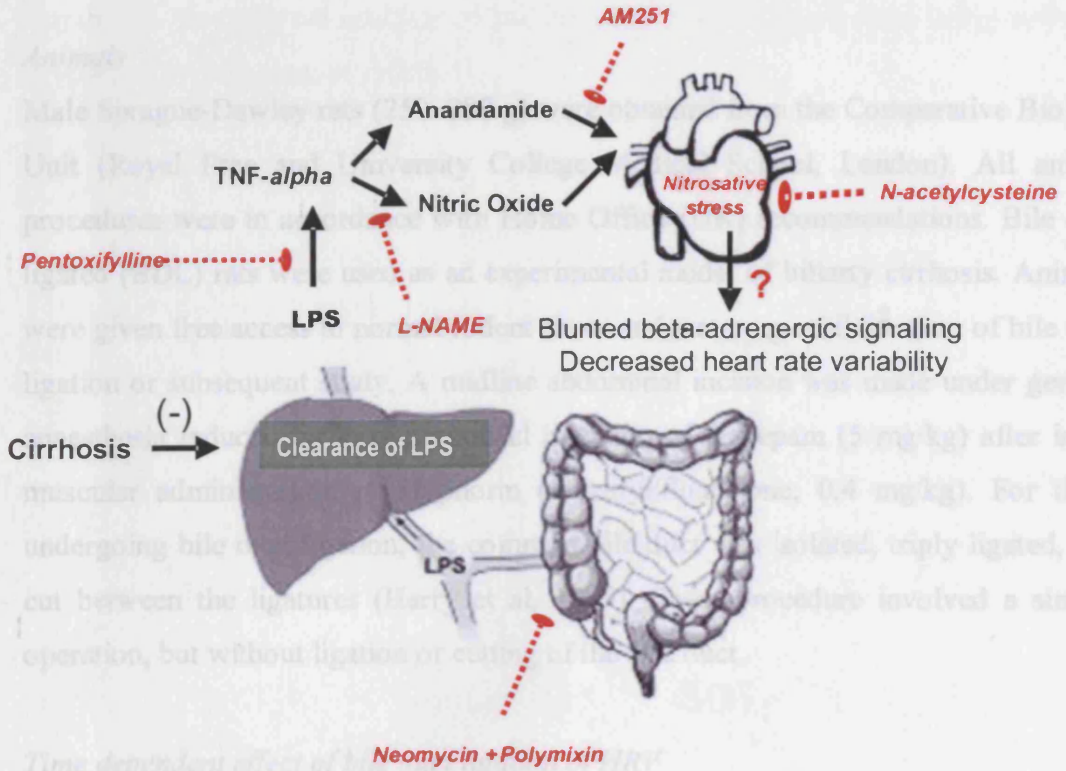

Fig. 4.1. A schematic representation of the working hypothesis on the mechanism of decreased heart rate variability in cirrhosis. Cirrhosis leads to impaired clearance of endotoxins derived from gut bacterial flora. Since endotoxaemia enhances the formation of both NO and anandamide, it is hypothesised that this may lead to cardiac dysfunction through induction of nitrative/nitrosative stress and a subsequent decrease in heart rate variability. These hypothetical pathways can be inhibited by various pharmacological interventions (red arrows).

4.2 Material and Methods

Chemicals

All materials were purchased from Sigma (Pool, UK), otherwise specified in the text.

Animals

Male Sprague-Dawley rats (250–280 g) were obtained from the Comparative Biology Unit (Royal Free and University College Medical School, London). All animal procedures were in accordance with Home Office (UK) recommendations. Bile duct ligated (BDL) rats were used as an experimental model of biliarty cirrhosis. Animals were given free access to normal rodent chow and water up until the time of bile duct ligation or subsequent study. A midline abdominal incision was made under general anaesthesia induced by intra-peritoneal injection of diazepam (5 mg/kg) after intra-muscular administration of Hypnorm (fentanyl/fluanisone; 0.4 mg/kg). For those undergoing bile duct ligation, the common bile duct was isolated, triply ligated, and cut between the ligatures (Harry et al. 1999). Sham procedure involved a similar operation, but without ligation or cutting of the bile duct.

Time dependent effect of bile duct ligation of HRV

Bile duct ligation was induced as described above. Bile duct ligated and sham operated rats were anaesthetized 1,2,3,4 and 5 weeks post operation using isoflurane (n=8-12 each group). A 20-min single channel (lead II) electrocardiogram (ECG) was recorded. We used low concentration of isoflurane (1.5 %) for smooth recording of ECG as isoflurane has the minimal systemic homodynamic effects in rats compared with other volatile or non-volatile anaesthetics (Janssen et al. 2004). The ECG signal was amplified using a Powerlab system (ADInstrument, Australia) and was digitized at a sampling rate of 1 kHz. The R-R interval time series was first generated using the automatic scheme in order to detect the R peak in the ECG. To exclude the influence of diurnal variations, the ECG recordings were begun between 2 p.m. and 5 p.m.

Heart rate variability analysis using Poincaré plot

The Poincaré plot was used for HRV analysis. The Poincaré plot is a graphical presentation of the correlation between the consecutive R-R intervals (Fig. 4.2). If the heart rate rhythm is regular then the points in Poincaré plot are located closely around

the line of identity (axis of the first quadrant). The standard deviation of the points perpendicular to the line-of-identity denoted by SD1 describes short-term variability, which is mainly caused by the respiratory sinus arrhythmia (vagal modulation). The standard deviation along the line-of-identity denoted by SD2 describes long-term variability. Quantitative analysis of the Poincaré plot was performed using software developed by Niskanen et al (2004).

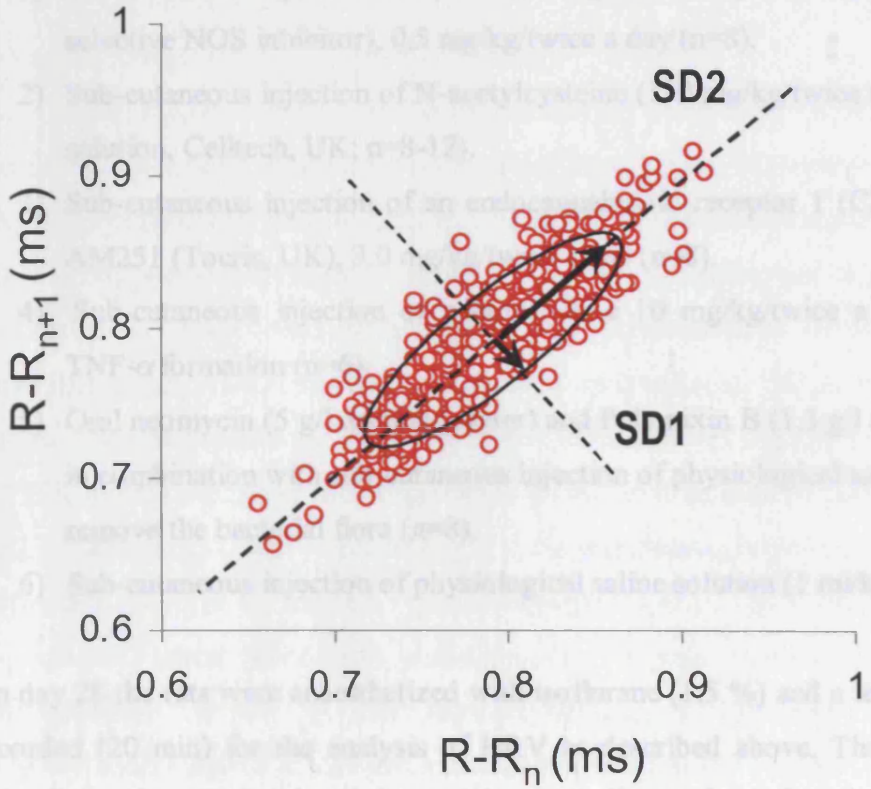

Figure 4.2. The Poincaré plot is a graphical presentation of the correlation between the consecutive R-R intervals. A common way to analyse heart rate dynamics using the Poincaré plot is to fit an ellipse to the graph. The ellipse is fitted onto the line-of-identity at 45° to the normal axis. The standard deviation of the points perpendicular to the line-of-identity denoted by SD1 describes short-term variability, which is mainly caused by the effect of respiration on vagal drive. The standard deviation along the line-of-identity denoted by SD2 describes long-term variability.

Pharmacological manipulation

All subsequent studies were performed at day 28 post-bile duct ligation or sham operation, when biliary cirrhosis had developed. Histological examination was performed on formalin-fixed liver stained with haematoxylin and eosin to confirm the development of biliary cirrhosis. At 24 days after the operation, the animals (BDL and control) were divided into six experimental groups, which received one of the following treatments for 4 days:

1) Sub-cutaneous injection of N^G-L-nitro-arginine methyl ester (L-NAME, a non-selective NOS inhibitor), 0.5 mg/kg/twice a day (n=8).
2) Sub-cutaneous injection of N-acetylcysteine (130 mg/kg/twice a day; infusible solution, Celltech, UK; n=8-12).
3) Sub-cutaneous injection of an endocannabinoid receptor 1 (CB1) antagonist, AM251 (Tocris, UK), 3.0 mg/kg/twice a day (n=8).
4) Sub-cutaneous injection of pentoxifylline 10 mg/kg/twice a day to inhibit TNF-α formation (n=6).
5) Oral neomycin (5 g/l drinking water) and Polymixin B (1.3 g/l drinking water) in combination with sub-cutaneous injection of physiological saline solution to remove the bacterial flora (n=8).
6) Sub-cutaneous injection of physiological saline solution (1 ml/kg; n=12).

On day 28 the rats were anaesthetized with isoflurane (1.5 %) and a lead II ECG was recorded (20 min) for the analysis of HRV as described above. The heart of each animal was then removed and the auricles were dissected out from isolated hearts in cold oxygenated physiological solution. Blood was also collected in nitrate-free ethylendiamine-tetraacetic acid (EDTA) containing tubes for measurement of plasma nitrate + nitrite levels in the experimental groups.

Preparation of isolated atria (in vitro study)

Isolated rat atria were used as a model system in this investigation because it is amenable to direct measurements of cardiac chronotropic response without being encumbered by confounding physiological mechanisms operative in more complex systems. In brief, the left and right atria were isolated in cold oxygenated

physiological solution and suspended under isometric tension of 1,000 mg force in a 25 mL organ bath glass chamber (Mani et al. 2002). The temperature of the bathing solution was 37.0 ± 0.1°C, and pH was 7.4. The composition of physiological solution in mM was as follows: NaCl, 112; KCl, 5; $CaCl_2$, 1.8; $MgCl_2$, 1; NaH_2PO_4, 0.5; KH_2PO_4, 0.5; $NaHCO_3$, 25; glucose, 10; and EDTA, 0.004. The solution was oxygenated with a gas mixture of 95% O_2 and 5% CO_2. The right atrium, which contains the sino-atrial node, was used for recording the spontaneous atrial beating, and was stimulated by increasing concentrations of isoproterenol from 10^{-10} to 10^{-6} mol/L (chronotropic study).

Western blotting

Snap frozen cardiac tissues were homogenized in ice-cold RIPA buffer containing protease inhibitors (protease inhibitor mixture from Roche, Mannheim, Germany), 50 mM Tris (pH 8), 150 mM NaCl, 1% NP-40, 0.5% Sodium Deoxycholate and 0.1% SDS. Homogenates were then sonicated followed by centrifugation at 10,000 ×g for 5 min at 4 °C. After determining the protein concentrations of the supernatants (Bradford assay with bovine serum albumin as standard), 10 μg protein of each sample was fractionated by SDS-PAGE and transferred to a polyvinylidene fluoride (PVDF) membrane. After blocking with Tris buffered saline (10 mM Tris, 100 mM NaCl) containing 0.1% Tween-20 for 1 h, the membranes were incubated overnight with rabbit anti-eNOS, iNOS or CB1 antibody (1:2000, 1:1000 and 1:100 dilutions respectively, rabbit polyclonal antibody from Sigma, Upstate and Santa Cruz Biotechnology respectively). After rigorous washing, the membranes were incubated with anti-rabbit IgG alkaline phosphatase-linked antibody (1:5000 dilution, Perbio Science, UK). Alkaline phosphatase was detected using a BCIP/NBT developing kit (Promega, Madison, USA). Proteins extracted from rat endothelium, stimulated macrophages and rat brain were used as the positive control for eNOS, iNOS and CB1 immunoreactivity respectively. Cardiac myosin (heavy chain) was used as the housekeeping protein. Developed immunoblot membranes were digitized and band optical densities were quantified using a computerized imaging system (Imaging densitometer model GS-670, Bio-Rad, Hercules, CA, USA). Densitometry data are expressed as relative optical densities (ROD) in arbitrary units.

Plasma nitrite+ nitrate concentrations

Plasma nitrite and nitrate was measured by a chemiluminescence-based assay as described chapter 3. In brief, nitrate was converted to nitrite using nitrate reductase. Samples were then injected into a reaction chamber containing acetic acid and potassium iodide (50 mg/mL) at a ratio of 4:1. This reduces nitrite to NO, which is purged from the refluxing solution by nitrogen and reacts with ozone before analysis by chemiluminescence (NOA). Measurements were calibrated against standard curves of sodium nitrate.

Tissue nitrotyrosine levels

Protein-bound nitrotyrosine levels were measured in the cardiac atrium, ventricle, liver and brain obtained from controls and rats with biliary cirrhosis using an isotope-dilution mass spectrometric method developed in our laboratory (Frost et al. 2000, Moore and Mani 2002). The effect of L-NAME and N-acetylcysteine on the levels of free nitrotyrosine was also measured in ventricular tissue, but not in the atria, since insufficient tissue was obtained. In brief, tissue was homogenized in a mixture of ice-cold saline (2 mL) and chloroform/methanol (2:1) containing 10 ng $^{13}C_9$-nitrotyrosine, and the protein precipitate (middle layer) was isolated by centrifugation at 2000 × *g* for 30 minutes at 4°C. The supernatant was used for measuring free nitrotyrosine (in ventricles) and the protein precipitates were lyophilized under vacuum for assessment of protein-bound nitrotyrosine. 1-1.5 mg of lyophilized protein was hydrolyzed for 15 hours at 120°C in 1 mL 4 M sodium hydroxide following the addition of 10 ng [$^{13}C_9$]nitrotyrosine and 10 μg of [$^{2}H_4$]tyrosine as stable isotopic internal standards. These conditions prevent the artifactual nitration of tyrosine that occurs during acidic hydrolysis conditions. Following two steps of solid phase extraction, nitrotyrosine and tyrosine were quantitated by stable isotope dilution gas chromatography/negative ion chemical ionization mass spectrometry (Frost et al. 2000, Moore and Mani 2002). Results of protein bound nitrotyrosine are expressed as a ratio of nitrotyrosine to tyrosine (pg/μg).

Assessment of nitration reactions in vivo using deuterated PHPA as a probe

To determine whether N-acetylcysteine inhibits the formation of reactive nitrogen species *in vivo*, or inhibits the nitration of circulating phenolic compounds, a novel method was employed based on infusion of deuterated *para*-hydroxyphenylacetic acid ([$^2H_6$]PHPA) followed by measurement of the urinary excretion of it's nitrated product using mass spectrometry (see chapter 2). This experimental approach allows us to assess the formation of reactive nitrogen species dynamically, since the formation of nitrated deuterated *para*-hydroxyphenylacetic acid (PHPA) can only occur through direct attack of its phenolic ring by reactive nitrogen species *in vivo*. Therefore, in a separate set of experiments, BDL or sham-operated rats were anesthetized with isoflurane (1.5%) and the external jugular vein and the urinary bladder were cannulated with PE-10 and PE-50 tubes respectively. [$^2H_6$]PHPA (250 nmol) was infused intravenously by bolus injection, and the level of urinary deutrated 3-nitro-*para*-hydroxy-phenylacetic acid ([$^2H_5$]NHPA) was measured sequentially during a 4-hour urine collection (nitration of [$^2H_6$]PHPA produces [$^2H_5$]NHPA as a result of replacement of a single deuterium of the aromatic ring by the -NO_2 group) using mass spectrometry (chapter 2; Mani and Moore 2005). The basis for this method is illustrated in Scheme 4.1.

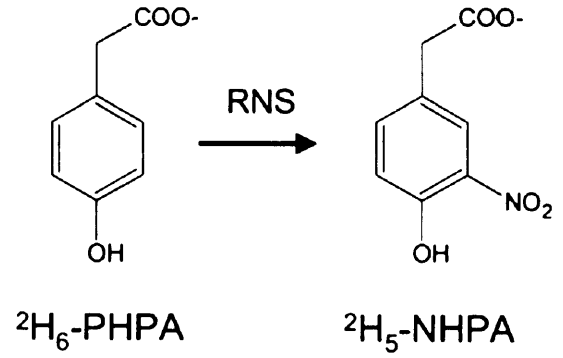

Scheme 4.1. Nitration of deuterium-labelled PHPA by reactive nitrogen species (RNS)

Cardiac concentrations of S-nitrosothiols.

A reductive chemiluminescense-based assay was used for measuring cardiac levels of S-nitrosothiols as described in chapter 3. In a separate set of experiments, the left ventricle was perfused with ice-cold perfusion buffer (phosphate saline buffer, pH 7.4 containing a thiol blocking agent NEM and DTPA of 5 and 1 mmol/L respectively). After homogenization of ≈500 mg of the snapped-frozen tissue in ice-cold perfusion buffer, S-nitrosothiols were determined by a copper (II)/iodine/iodine-mediated cleavage of S-nitrosothiols to NO, which was then quantified by its gas phase chemiluminescent reaction with ozone in a NO analyzer (NOA, Sievers, Boulder, CO) by a method developed in our laboratory (chapter 3)

Measurement of cardiac F_2-isoprostanes and arachidonic acid.

Since many reactive nitrogen species also initiate lipid peroxidation reactions *in vivo* we also measured the concentration of esterified F_2-isoprostanes in cardiac tissue (Moore et al. 1995). In short, ≈250 mg whole cardiac tissue was homogenized in a mixture of saline and chloroform/methanol solution containing butylated hydroxytoluene (5%) (to inhibit *ex vivo* lipid peroxidation), and centrifuged at 3,000g for 10 minutes. This process results in three phases, an upper aqueous phase, separated from the lower lipid containing phase by a ring of protein precipitate. The lower lipid layer was aspirated and, following the addition of 500 pg of [$^2H_4$]iso-PGFα and 50ng of [$^2H_8$]arachidonic acid (Cayman Co., Ann Arbor, MI) as internal standards, was dried down under nitrogen, and hydrolyzed in methanolic 15% potassium hydroxide solution (1 hour, 37°C). To extract the F_2-isoprostanes, the pH was adjusted to 3.0, and the samples were extracted on a C_{18} solid-phase extraction cartridge (Elstree, Hertsfordshire, Waters, UK) as described, (Moore et al. 1995) converted to the pentaflurobenzyl ester, purified by thin-layer chromatography and analyzed as the tri-methysilyl ether. Detection was performed by selected ion monitoring gas chromatography negative ion chemical ionization/mass spectrometry with monitoring of ions at *m/z* 569 and 573 (Moore et al. 1995). To control for the hydrolysis step, the levels of free (*i.e.*, hydrolyzed) arachidonic acid were also measured by a mass spectrometric method developed in our laboratory (Mani and Moore, unpublished). In brief, arachidonic acid was extracted on a C_{18} solid-phase extraction cartridge (Waters), converted to the pentaflurobenzyl ester, purified by

thin-layer chromatography and analyzed by stable isotope dilution negative ion chemical ionization mass spectrometry by monitoring ions at *m/z* 303 and 311. The levels of F_2-isoprostanes were expressed as the ratio of F_2-isoprostanes to arachidonic acid in cardiac tissue homogenates.

Immunogold electron microscopy

In a separate set of experiments freshly-isolated atria from controls and rats with cirrhosis were excised and immersed in isotonic fixative (4% paraformaldhyde, 0.5% glutaraldehyde, in 0.1 mol/L phosphate buffer, pH 7.4, with 0.1 mol/L sucrose) for electron microscopic immunocytochemistry as has previously described (n = 2) (Mihm et al. 2002). Tissues were then infiltrated and embedded in LR white resin. Thin sections (70-90 nm) were cut and mounted on coated nickel grids. The grids were then blocked (0.1% bovine serum antigen, 0.1 mol/L glycine in PBS) for 30 minutes and incubated for 2 hours with rabbit polyclonal antibody raised against nitrotyrosine (anti-nitrotyrosine, 1:500, a kind gift of Dr. Joseph Beckman, University of Alabama at Birmingham, Alabama). Following a series of washes, grids were incubated for 1 hour with 10 nm Immunogold-linked, EM grade, goat anti-rabbit IgG (1:50 dilution). Following another series of washes, grids were successively stained with uranyl acetate and Reynold's lead citrate before visualization with a transmission electron microscope. Electron micrographs (31,000 × original magnification) were scanned using a digital imaging system.

Statistical analysis

The results are presented as mean ± SEM. ANOVA was applied with Newman-Keuls test and P values less than 0.05 were considered statistically significant. In conditions where the parametric test was not permitted (owing to heterogeneity of variances) a non-parametric Kruskal-Wallis test followed by Dunn's multiple comparison test were used for statistical analysis.

4.3. Results III

Time dependent effect of bile duct ligation on basal heart rate and HRV

Time-dependent effect of bile duct ligation on basal heart rate and HRV parameters is shown in Figure 4.3. Four and five weeks after bile duct ligation rats showed a significant bradycardia compared with sham-operated animals (Fig 4.3A). Bile duct ligation did not have any significant effect on short-term HRV (SD1), however long-term HRV (SD2) was significantly affected by the ligation of bile duct, 4 and 5 weeks post operation (Fig 4.3).

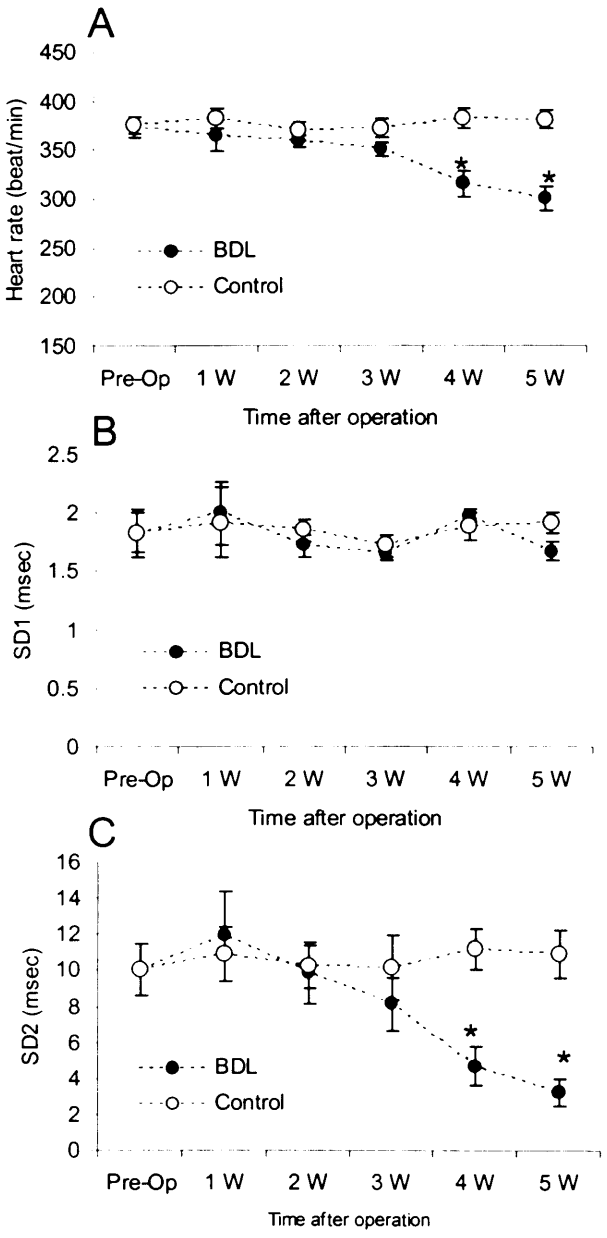

Figure 4.3. Time-dependent effect of bile duct ligation on basal heart rate (A), short-term HRV (B) and long-term HRV (C) in bile duct ligated (BDL) or sham operated (Control) rats. * $P<0.01$ compared with control rats.

In vivo study: heart rate and HRV in cirrhotic rats (4 weeks BDL rats)

The heart rate of cirrhotic rats was significantly ($P<0.01$) lower than control rats. Administration of L-NAME, N-acetylcysteine or AM251 led to normalization of the basal heart rate in BDL rats. Neither pentoxifylline nor oral neomycin/polymixin B administration was able to normalize bradycardia in BDL cirrhotic rats (Fig 4.4).

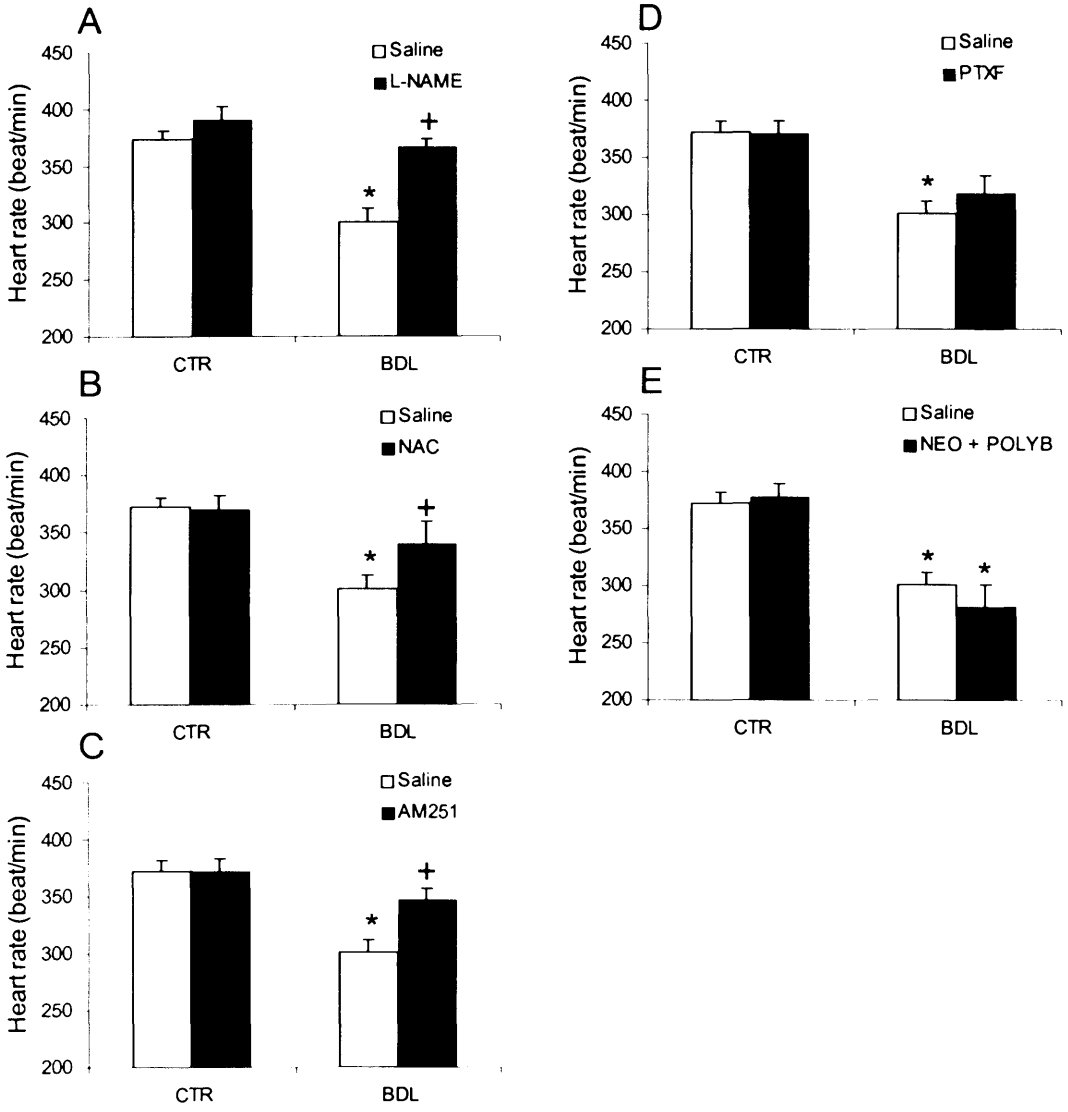

Figure 4.4. Basal heart rate (beat/min) in control or cirrhotic rats given saline, L-NAME (A), N-acetylcystemine (B: NAC), AM251 (C), pentoxifylline (D: PTXF) or neomycin/polymixin B (E: NEO + POLY B). Data are shown as Mean ± SEM. * $P<0.05$ compared controls. + $P<0.05$ compared with Saline treated BDL rats. 6-8 rats were used in each group.

The Poincaré plot in two representative rats is shown in Fig 4.5. In healthy rats the Poincaré plot is scattered along the line of identity while this scattering is significantly less in cirrhotic rats. There was a marked decrease in long-term HRV (SD2) in rats with cirrhosis in comparison with sham-operated animals (4.2 ± 0.4ms vs 11.2 ± 0.9ms to $P<0.01$). No significant difference was found between control and cirrhotic rats in short-term HRV as assessed by measuring SD1 (Fig 4.6). Decontamination of gut bacterial flora using neomycin/polymixin B significantly normalised decreased long-term HRV (SD2) in BDL rats (4.2 ± 0.4 versus 10.9 ± 1.2), whereas none of the pharmacological manipulations (L-NAME, N-acetylcysteine, AM251 or pentoxifylline) had a significant impact on long-term HRV (SD2) in cirrhosis (Fig 4.7).

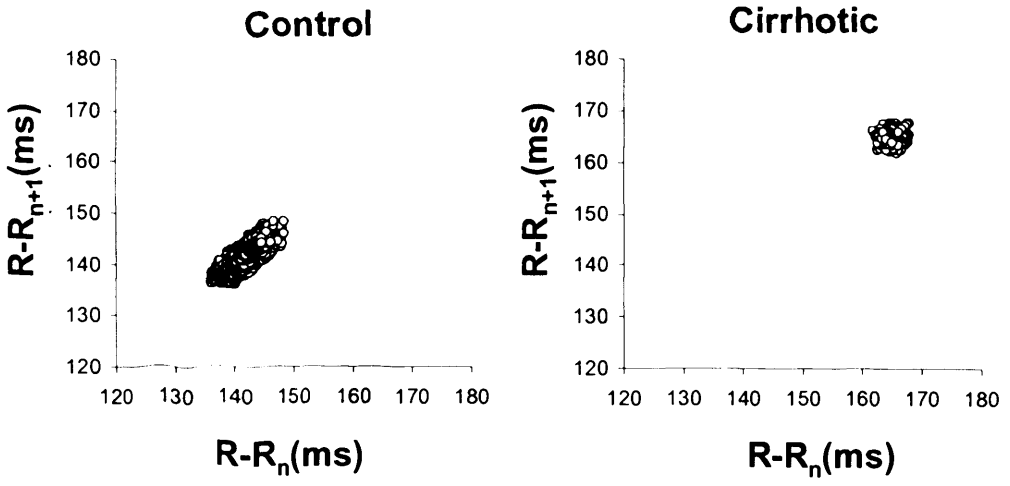

Figure 4.5. Poincaré plots in two representative control and cirrhotic rats.

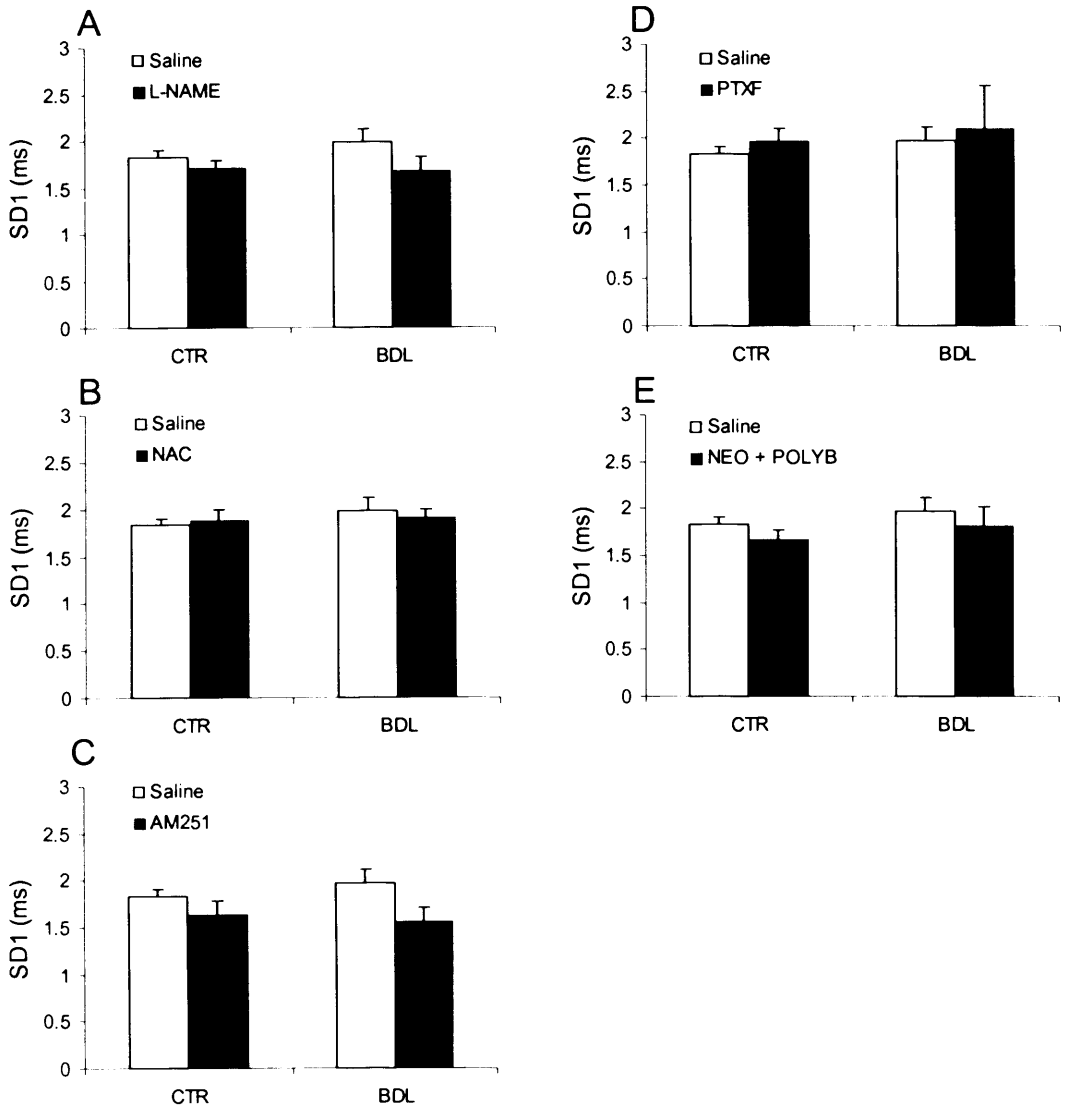

Figure 4.6. Short-term heart rate variability (SD1) in control or cirrhotic rats given saline, L-NAME (A), N-acetylcysteine (B: NAC), AM251 (C), pentoxifylline (D: PTXF) or neomycin/polymixin B (E: NEO + POLY B). Data are shown as Mean ± SEM. No statistically significant difference was found between the groups.

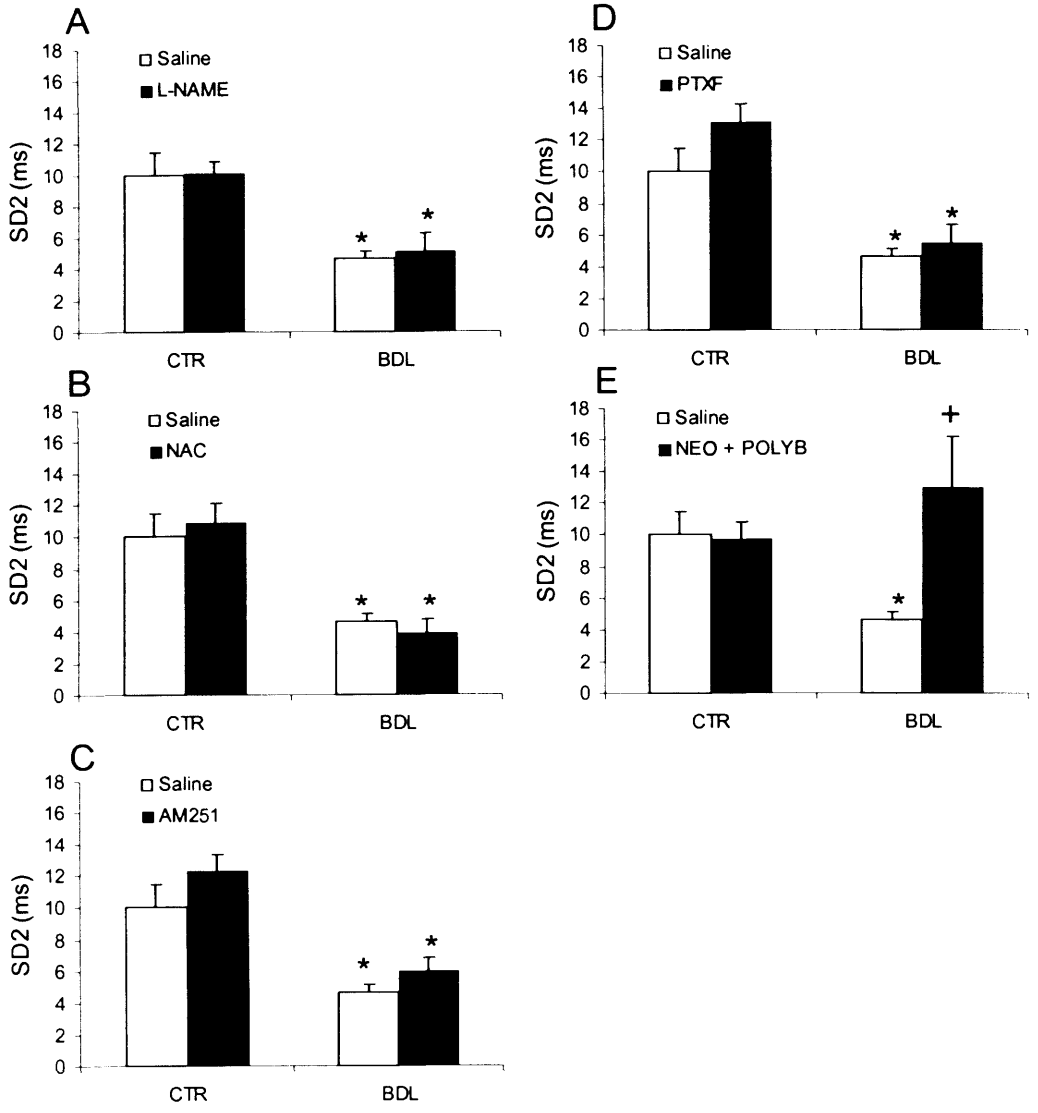

Figure 4.7. Long-term heart rate variability (SD2) in control or cirrhotic rats given Saline, L-NAME (A), N-acetylcysteine (B: NAC), AM251 (C), pentoxifylline (D: PTXF) or neomycin/polymixin B (E: NEO + POLY B). Data are shown as Mean ± SEM. * $P<0.05$ compared with controls.
+ $P<0.05$ compared with Saline treated BDL rats. 6-8 rats were used in each group.

In vitro study

Initial studies confirmed that chronotropic responses to isoproterenol were impaired in isolated atria (Fig 4.8). Thus, there was a 1.8-fold increase in the EC_{50} of isoproterenol necessary to evoke the same response as normal rat atria in the spontaneously beating right atria isolated from cirrhotic rats ($P<0.02$). This confirms the observation that there are impaired cardiac responses to adrenergic stimulation in cirrhotic rats. The maximum response (R_{max}) to isoproterenol was not statistically different between controls and animals with cirrhosis (477 ± 10 beats/minutes vs. 466 ± 3 beats/minutes in control and animals with cirrhosis, respectively). The maximum response (R_{max}) to the chronotropic effect of ß-adrenergic stimulation was similar in all experimental groups. As shown in Fig. 4.8, administration of L-NAME, N-acetylcysteine or AM251 for four days normalized the chronotropic responsiveness of isoproterenol in cirrhotic rats ($P<0.05$). Neither pentoxifylline nor oral neomycin/polymixin B administration could normalize the impaired responsiveness to adrenergic stimulation in isolated atria (Fig. 4.8).

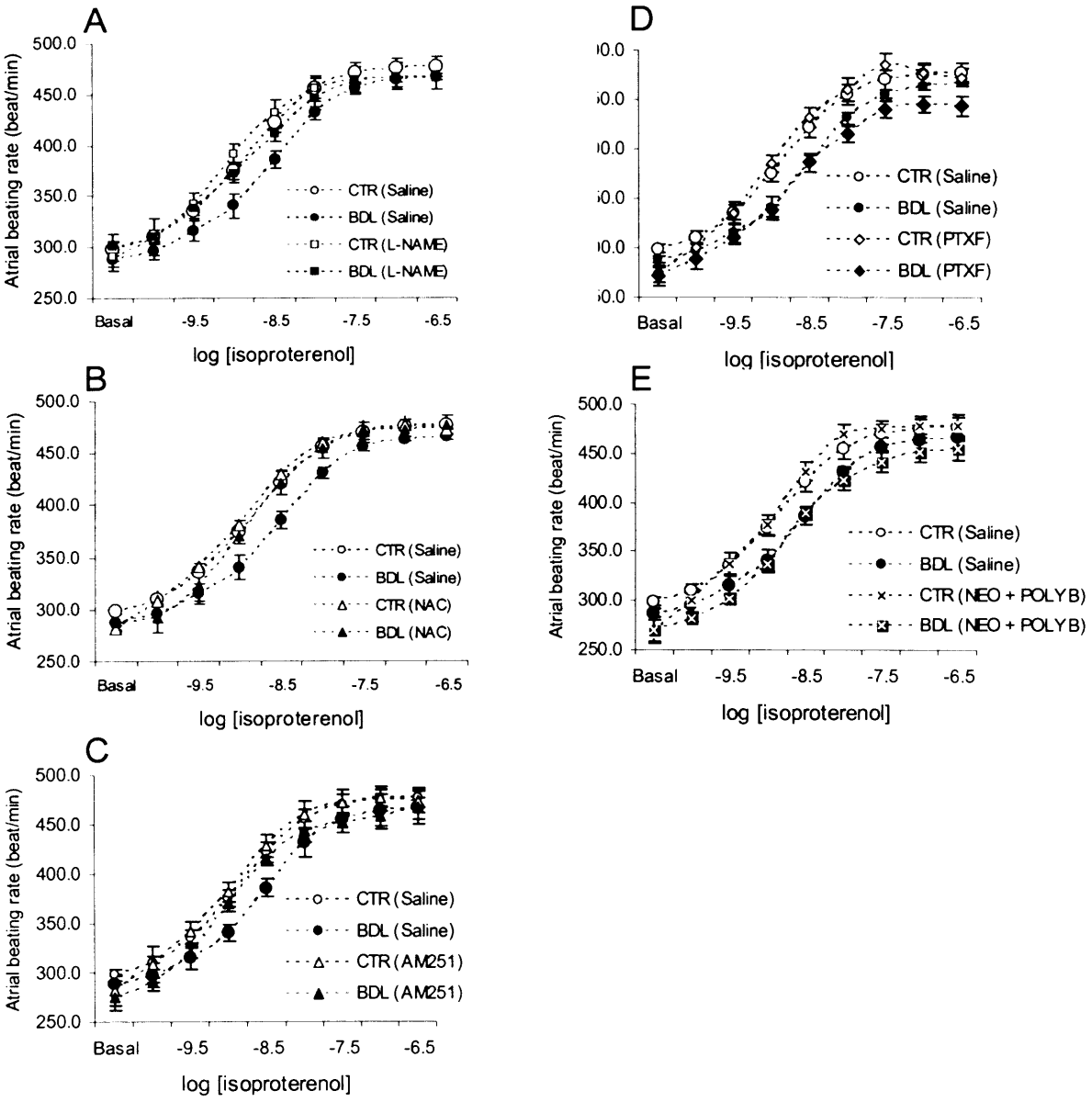

Figure 4.8. Chronotropic response of spontaneous beating isolated atria to cumulative concentrations of isoproterenol (10^{-10}-10^{-7}). Atria are obtained from sham-operate (CTR) and bile duct ligated (BDL) cirrhotic rats given Saline, L-NAME (A), N-acetylcysteine (B: NAC), AM251 (C), pentoxifylline (D: PTXF) or neomycin/polymixin B (E: NEO + POLY B). n=6-8 in each group. Data are expressed as mean ± SEM.

Western blotting

As shown in Fig. 4.9, there was no significant alteration in eNOS band density in cardiac tissues obtained from cirrhotic and control rats (3.1±1.2 versus 2.7±0.9; ROD). We were not able to demonstrate iNOS expression in cardiac tissue obtained from controls or cirrhotic rats. Cirrhosis was associated with a significant ($P<0.05$) increase in the relative density of CB1 receptor compared with sham-operated rats (14.65±2.2 versus 23.2±3.2 ROD in sham-operated and cirrhotic rats respectively).

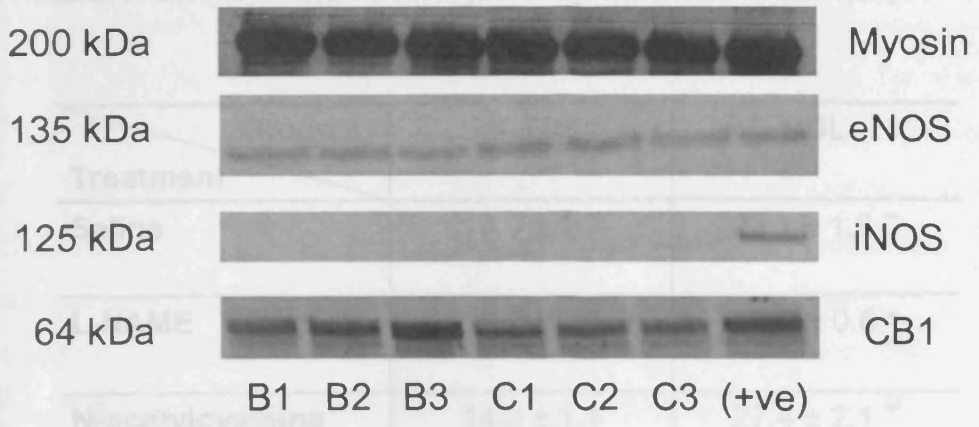

Figure 4.9. Western blot analysis of eNOS and iNOS and cannabinoid CB1 receptor in cardiac tissue obtained from control (C1, C2, C3) and bile-duct ligated (B1, B2, B3) rats. Proteins extracted from endothelial monolayer, activated macrophages and rat cerebrum were used as the positive control (+ve) for eNOS, iNOS and CB1 receptor immunoreactivity respectively. Myosin (heavy chain) was used as the housekeeping protein.

Plasma nitrite + nitrate concentrations

As shown in Table 4.1, there was a significant increase in plasma concentrations of NO end products (nitrite + nitrate) in rats with biliary cirrhosis (13.9 ± 1.7 to 21.7 ± 1.8 μM, $P<0.01$), which decreased following inhibition of NO synthase by L-NAME (13.0 ± 0.6 μM, $P<0.01$ compared with BDL rats given saline). Pre-treatment with N-acetylcysteine, AM251 or pentoxifylline did not affect the plasma concentrations of nitrite + nitrate levels in rats with biliary cirrhosis (Table 4.1). Decontamination of gut bacterial flora using neomycin/polymixin B increased plasma levels of nitrite + nitrate in BDL rats ($P<0.05$ in cirrhotic groups).

Table 4.1. Plasma nitrate + nitrite (μmol/L) in control or cirrhotic rats given Saline, L-NAME, N-acetylcysteine, AM251, pentoxifylline or neomycin + polymixin B.

Group / Treatment	CTR	BDL
Saline	13.9 ± 1.7	22.1 ± 1.8 **
L-NAME	11.7 ± 0.9	13.0 ± 0.6 +
N-acetylcysteine	14.3 ± 1.1	27.4 ± 2.1 **
AM251	14.5 ± 2.0	19.1 ± 1.3 *
Pentoxifylline	11.9 ± 0.6	18.6 ± 3.3 +
Neomycin + Polymixin	19..0 ± 3.2	42.1 ± 5.9 **,++

Data are shown as Mean ± SEM. * $P<0.05$ compared controls. + $P<0.05$ compared with Saline treated BDL rats. 6-8 rats were used in each group.

Nitrotyrosine concentrations in cardiac tissue and nitration of deuterated PHPA

As shown in Table 4.2, protein-bound nitrotyrosine levels increased significantly in atrial tissue, ventricle and liver but not in the brain of rats with biliary cirrhosis compared with controls. The administration of L-NAME or N-acetylcysteine decreased atrial nitrotyrosine concentrations from 23 ± 3 pg/μg of tyrosine to 15 ± 1 and 17 ± 1 pg/μg respectively (Fig. 4.10). The same pattern of changes was observed in the ventricles as shown in Fig. 4.11. L-NAME decreases nitration of cardiac proteins by decreasing synthesis of nitric oxide, and the secondary formation of reactive nitrogen species which cause nitration of cardiac proteins. However, the mechanism by which N-acetylcysteine decreases nitration of proteins is unknown. One potential mechanism could be scavenging of reactive nitrogen species *in vivo*. To determine whether N-acetylcysteine scavenged and reduced the nitration potential of reactive nitrogen species, rats were infused with [$^2H_6$]PHPA, and the formation of [$^2H_5$]NHPA was measured by mass spectrometry. Biliary cirrhosis was associated with increased formation of [$^2H_5$]NHPA following intravenous infusion of [$^2H_6$]PHPA ($P<0.01$; Fig. 4.12) consistent with increased formation of reactive nitrogen species in rats with cirrhosis and nitration of the phenolic ring of PHPA. However, administration of N-acetylcysteine did not decrease the nitration of [$^2H_6$]PHPA *in vivo* (Fig. 4.12). An alternative potential mechanism of N-acetylcystene could involve increased clearance and proteolysis of nitrated proteins *in vivo*, since others have shown that nitration of proteins is associated with increased proteolysis of the "abnormal" protein (Souza 2000). To test this, we hypothesized that increased proteolysis would increase levels of free nitrotyrosine in cardiac tissue. Therefore free nitrotyrosine levels were measured in cardiac ventricular tissue of normal rats as well those with cirrhosis ± treatment with N-acetylcysteine. We measured free nitrotyrosine in ventricular tissue, since the tissue concentration of free nitrotyrosine is very low (<2 pg/mg wet tissue), making it undetectable in small tissues such as rat atrium. However, free nitrotyrosine was easily measured in ventricular tissues and the levels were not significantly different in controls and rats with cirrhosis. However, the administration of N-acetylcysteine led to a marked increase in the concentration of free nitrotyrosine in the ventricular tissue in rats with cirrhosis ($P<0.05$; Fig. 4.11). Thus, whereas these data suggest N-acetylcysteine leads to increased proteolysis of nitrated proteins, the mechanism remains unclear.

Table 4.2. Comparison of protein-bound nitrotyrosine levels between controls

	Protein-Bound Nitrotyrosine (pg/μg tyrosine)		
Tissue	CTR	BDL	P (*t*- test)
Liver	63 ± 10	178 ± 40	<0.02
Atrium	16 ± 1	23 ± 3	<0.05
Ventricle	22 ± 9	57 ± 8	<0.05
Brain	9 ± 1	12 ± 3	ns

NOTE. Proteins were extracted from different tissues (liver, atrium, ventricle and brain) obtained from sham operated (control) or bile duct ligated (BDL) rats and analyzed by mass spectrometry. Levels are corrected for tyrosine. Data are Mean ± SEM. *P < 0.05, compared with control. 6-8 rats were used in each group. ns: non statistically significant.

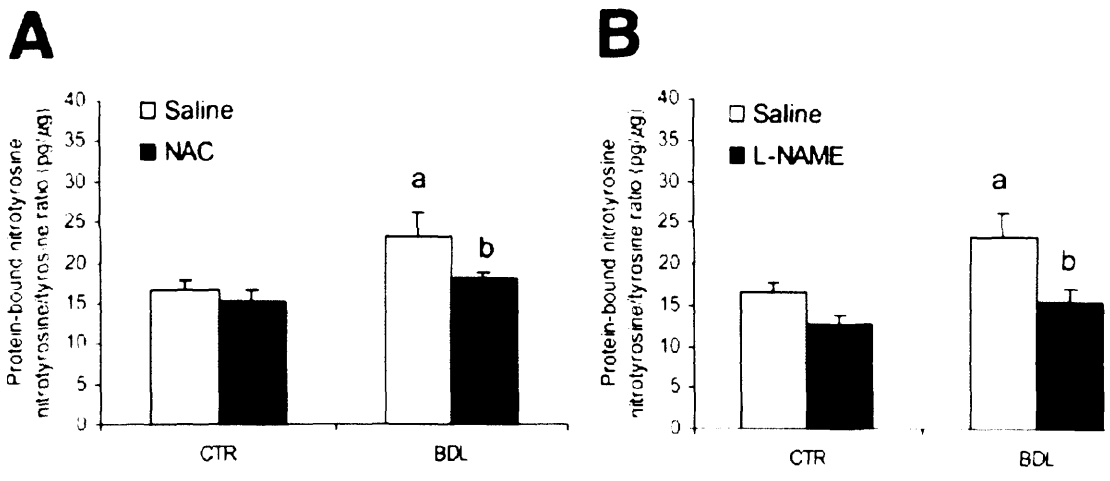

Figure 4.10. Protein-bound nitrotyrosine content of atrial tissue obtained from control and rats with cirrhosis given saline, N-acetylcysteine (NAC; A), or L-NAME (B). (a) P < 0.05 compared with control. (b) P < 0.05 compared with saline-treated BDL rats.

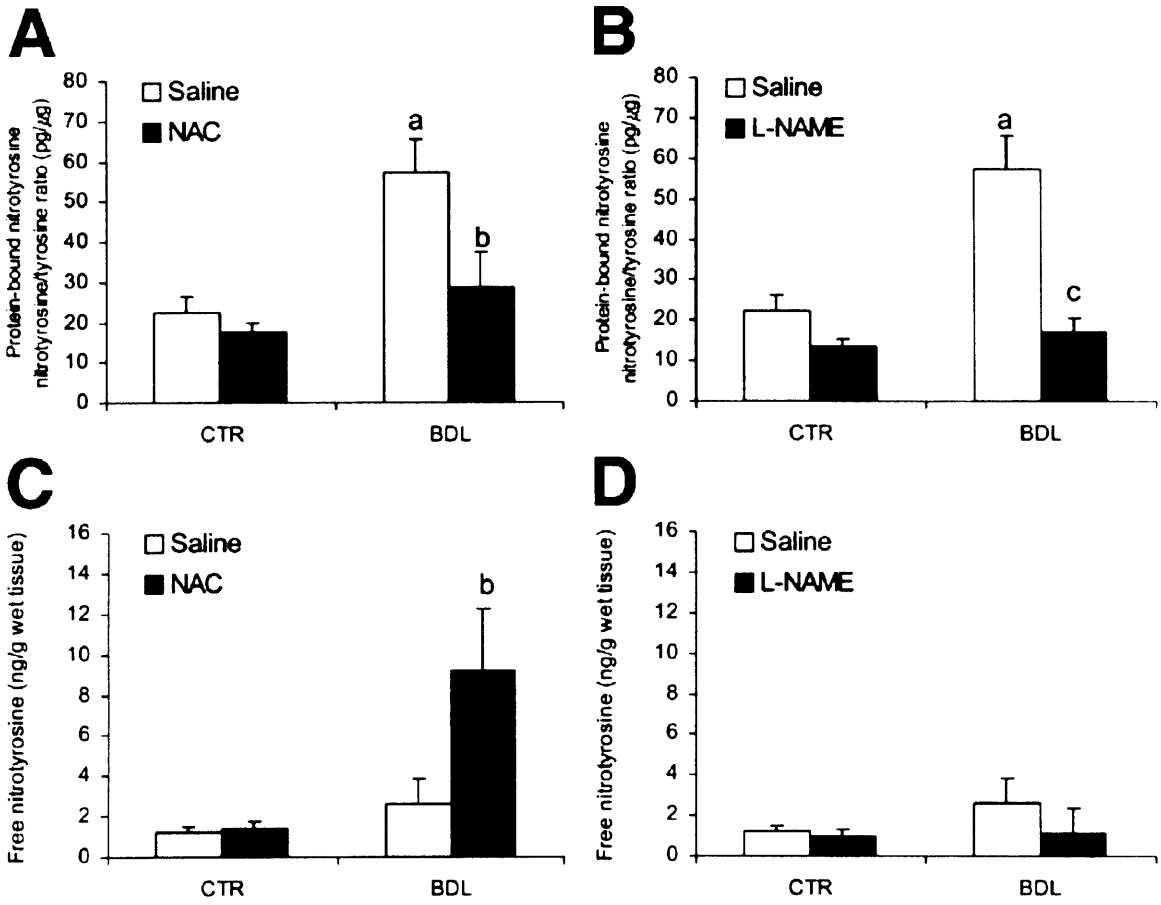

Figure 4.11. Protein-bound (upper panel, A-B) and free (lower panel, C-D) nitrotyrosine content of ventricular tissue obtained from control and rats with cirrhosis treated with saline, N-acetylcysteine (NAC; A,C) or L-NAME (B,D). (a) $P<0.05$ compared with controls. (b) $P<0.05$. (c) $P<0.01$ compared with saline-treated BDL rats. Protein-bound nitrotyrosine levels are expressed as a ratio to tyrosine (pg/µg).

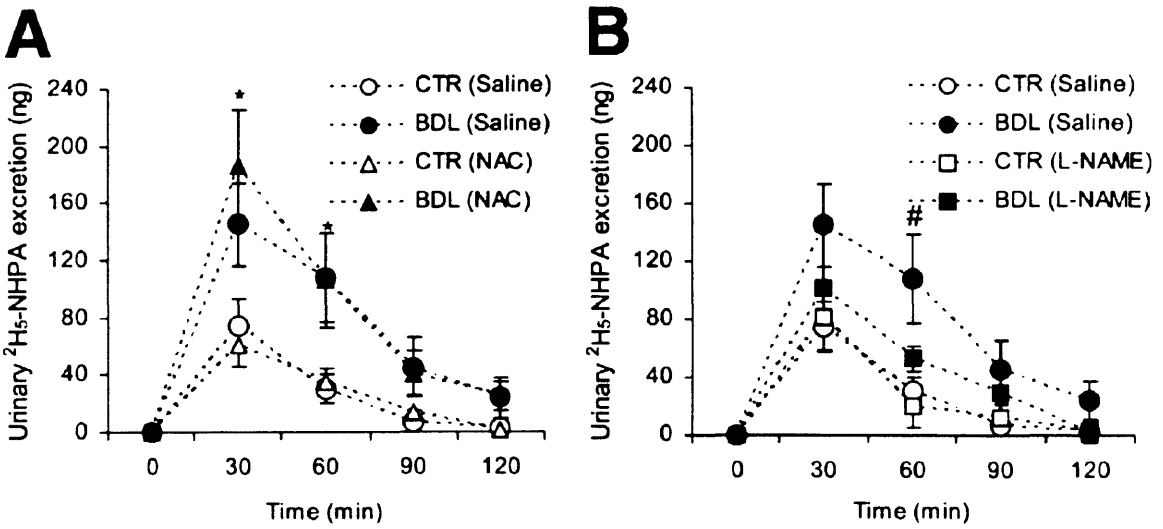

Figure 4.12. Assessment of nitration reactions *in vivo* using deuterated PHPA ([$^2H_6$]PHPA) as probe. Injection of [$^2H_6$]PHPA into rats with biliary cirrhosis leads to increased nitration of PHPA and formation of [$^2H_5$]NHPA, which is excreted in urine. Pre-treatment of animals with cirrhosis with N-acetylcysteine (NAC) did not decrease [$^2H_5$]NHPA formation *in vivo* (A), and indicates that NAC does not work by scavenging reactive nitrogen species. However, L-NAME, which inhibits nitric oxide synthase, significantly reduced [$^2H_5$]NHPA formation in rats with cirrhosis (B). Data are expressed as mean ± SEM. 6-8 rats were used in each group. *$P<0.01$ compared with control groups. #$P<0.05$ in comparison with BDL (L-NAME) and control groups.

Cardiac S-nitrosothiols.

To determine whether there was an increase in S-nitrosation of cardiac proteins we measured the concentration of S-nitrosothiols in cardiac tissue from control rats with cirrhosis with treatment with L-NAME or N-acteylcysteine, and rats with cirrhosis but without treatment. There was no difference in cardiac S-nitrosothiols following induction of cirrhosis, and neither N-acetylcysteine nor L-NAME had any effect on the cardiac levels of S-nitrosothiols (Table 4.3).

Cardiac F_2-isoprostanes.

The ratio of esterified F_2-isoprostanes to arachidonic acid was significantly increased in cardiac tissue from rats with cirrhosis at 2.9 ± 0.5 ng/μg AA (arachidonic acid) compared to controls (1.8 ± 0.2 ng/μg AA, $P<0.05$), consistent with oxidative stress and increased lipid peroxidation in cardiac tissue. Treatment with either N-acetylcysteine or L-NAME had no significant effect on the tissue levels of F_2-isoprostanes (Table 4.3).

Table 4.3. Cardiac S-nitrosothiol and F_2-isoprostanes concentrations in control and cirrhotic rats treated with saline, N-acetylcysteine (NAC) or L-NAME.

	CTR			BDL		
	Saline	NAC	L-NAME	Saline	NAC	L-NAME
S-nitrosothiol (pmol/g)	56 ± 9	50 ± 9	49 ± 11	61 ± 7	53 ± 10	55 ± 9
F_2-isoprostanes (ng/μg AA)	1.8 ± 0.2	1.6 ± 0.2	1.8 ± 0.1	2.9 ± 0.5*	2.4 ± 0.4*	2.2 ± 0.4

NOTE. F_2-isoprostanes are expressed as a ratio of 8-iso-$PGF_{2\alpha}$ to arachidonic acid (AA). S-Nitrosothiols are expressed as pmol/g of wet tissue. Data are Mean ± SEM.

* $P < 0.05$, compared with control (saline) group. 6-8 rats were used in each group.

Immunogold electron microscopy studies

Representative electron micrographs from the atria of controls and rats with cirrhosis are shown in Fig. 4.13. Myofibrillar and mitochondrial organelles are clearly visible. Black electron dense circles (5 nm gold particles) represent positively stained tissue for nitrotyrosine. In control images, relatively sparse immunostaining was observed, with roughly equal staining density between myofibrillar and mitochondrial compartments. However, an increase in staining of myofibrillar and mitochondrial proteins in the atria of rats with biliary cirrhosis was noted (Fig. 4.13).

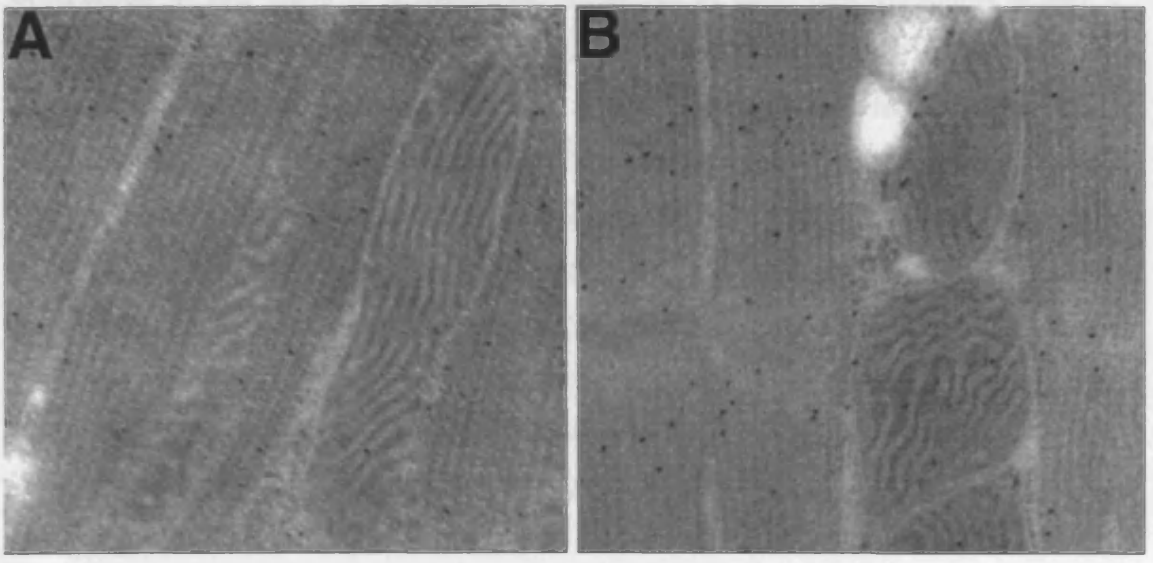

Figure 4.13. Immunogold electron microscopy for nitrotyrosine in atria from control (A) and bile duct ligated (B) rats. Electron-dense circles indicate positive staining for nitrotyrosine.

4.4 Discussion III

Recent studies have shown that indices of depressed heart rate variability appear to predict adverse outcomes in patients with cirrhosis (Fleisher et al. 2000). The mechanisms that have been proposed for decreased heart rate variability include an imbalance in sympatho-vagal activation, abnormal baroreflex function and cirrhotic cardiomyopathy (Fig. 1.3), however the precise mechanism by which liver disease induces "regularisation" of heart rate variability in unclear.

In BDL rats, liver injury and the elevation of serum transaminases peak at day 3 following bile duct ligation. However portal hypertension and cirrhosis does not develop unitil weeks 3-4 (Bomzon et al. 1985). Most investigators use rats 4 to 6 weeks after bile-duct ligation when portal hypertension is well established (Lee et al. 1986). Animals usually die from sepsis or unexplained sudden death 6 weeks after bile dut ligation (unpublished observation). The present study showed that biliary obstruction in rats leads to a significant reduction in heart rate variations 4 and 5 weeks after bile duct ligation. This shows that the decreased HRV and the development of liver cirrhosis are two parallel phenomena. In addition, three independent treatments (NOS inhibition, CB1 blockade and N-acetylcysteine) which lead to normalization of cardiac chronotropic function were unable to restore the loss of heart rate variability in cirrhotic rats. Likewise, decontamination of gut bacterial flora which normalizes heart rate variability in cirrhotic rats did not have a significant effect on impaired acceleration of heart rate in response to ß–adrenergic stimulation. These data demonstrate that decreased end-organ responsiveness to the ß-adrenergic system does not play a role in the alteration of HRV parameters following liver cirrhosis.

Bacterial translocation of gut flora into the portal circulation is well recognized in liver cirrhosis (see Wiest and Garcia-Tsao 2005 for review) and, in the presence of both porto-systemic shunting and impaired clearance by the liver, has been implicated in the delivery of endotoxins to the systemic circulation resulting in high local concentrations of biologically active endotoxins capable of activating the cytokine cascade. Loss of HRV and increased heart rate regularity is a common feature of systemic inflammatory conditions such as endotoxaemia (Mani et al. 2006a). In the present study decontamination of gut bacterial flora normalized loss of HRV in

cirrhotic rats which suggests that bacterial translocation of gut flora might have a role in decreased heart rate variability in biliary cirrhosis. We unexpectedly observed an increase in plasma nitrite + nitrate levels in cirrhotic rats treated with oral neomycin/polymixin B. This is in contrast with the traditional proposal that endotoxins from gut-derived bacterial translocation, causes induction of iNOS leading to increased vascular NO production. In fact, we were unable to show a detectable induction of iNOS in cardiac tissues obtained from BDL rats using conventional western blotting. To have a better picture of the consequences of intestinal decontamination in experimental cirrhosis, further studies are required using real time PCR to detect the expression of NOS isoforms in different tissues as well as bacterial DNA (16S) in plasma and mesenteric lymph nodes.

Pentoxifylline, a xanthine derivative, is a known inhibitor of TNF-α production (Strieter et al. 1988). Circulatory concentration of TNF-α is shown to be elevated in patients with cirrhosis (Yoshioka et al. 1989). Since TNF-α can blunt cardiac ß-adrenergic signalling we used pentoxifylline to test the hypothesis that elevation of TNF-α decreases ß-adrenergic responsiveness and leads to a decrease in heart rate variability in cirrhotic rats. However, five days administration of pentoxifylline to cirrhotic rats did not show any signifincant effect on HRV or impaired cardiac responsiveness to a ß-agonist. This suggests that TNF-α per se is not the ultimate mediator in the pathogenesis of cardiac dysfunction in BDL rats. We did not measure plasma TNF-α levels in control and BDL rats following pentoxifylline administration, thus further studies are required to rule out a role of TNF-α in the genesis of cardiac dysfunction in cirrhosis. Although great strides in the last decade have helped to elucidate the pathways to systemic inflammation, single immunomodulatory therapies (e.g. anti-TNF-α antibodies) have failed to make a significant impact on the treatment of circulatory dysfunction during inflammation (Abraham et al. 1998). Systemic inflammatory repsonse is an example of a self-regulating complex system, with multiple cascading non-linear interactions and feedbacks. Alteration of heart rate dynamics in cirrhosis can be considered to be a reflection of these non-linear interactions in the cardiovascular regulatory system.

Acceleration of the heart rate in response to catecholamines is impaired in cirrhosis. The endogenous ligand for the endocannabinoid CB1 receptor is anandamide which

has a negative chronotropic effect on cardiac pacemaker cells via activation of CB1 receptors (Krylatov et al. 2006). Although recent studies have shown that the endocannabinoid system is involved in the pathogenesis of cardiovascular dysfunction in liver disease (Batkai et al. 2001; Gaskari et al. 2005; Moezi et al. 2006), the possibility that impaired chronotropic response to catecholamines might relate to endocannabinoid signalling does not seem to have been considered in the studies undertaken to date. The present study showed that the impaired responsiveness of isolated atrium was normalized by treatment of cirrhotic animals with AM251 for four days (3 mg/kg). There was a significant up-regulation of CB1 receptors in atria obtained form cirrhotic rats compared with controls as assessed by immuoblotting. The effects of AM251 is not attributable to down-regulation of NO synthesis because the plasma concentrations of nitrite + nitrate (NO end-products) were still significantly elevated in rats with cirrhosis treated with AM251 whereas L-NAME significantly decreased nitrate/nitrite concentrations in both groups. It seems that CB1 receptors might have a role in the pathogenesis of cirrhosis-associated cardiac chronotropic incompetence in cirrhosis and this effect appeared to be independent of nitric oxide signalling and changes in autonomic nervous system as determined by analysis of heart rate variability

This study confirms the observation that cardiac chronotropic function is abnormal in rats with biliary cirrhosis. More importantly, it demonstrates that this abnormality is associated with increased levels of protein-bound nitrotyrosine in cardiac tissue. The administration of either L-NAME or N-acetylcysteine, both of which decrease the tissue levels of nitrotyrosine, led to normalization of heart rate as well as cardiac responsiveness to adrenergic stimulation in rats with biliary cirrhosis. In patients with cirrhosis, although resting tachycardia is part of the feature of the hyperdynamic circulation, manoeuvres leading to sympathetic activation (*e.g.*, ice-cold skin stimulation, mental stress, tilting and physical exercise), do not evoke an adequate acceleration of heart rate compared with healthy subjects (Bernardi et al. 1987; Bernardi et al 1991, Wong 2001). Conversely, when the sympathetic responses to tilting or exercise are assessed by the plasma concentrations of norepinephrine, the sympathetic response is enhanced (Bernardi et al. 1987; Bernardi et al 1991). This finding suggests the defect in cardiac responsiveness is located at the receptor and/or post receptor level. This notion is supported by the findings of several studies

assessing the effects of ß-adrenergic agents. For example, in patients with cirrhosis, the ED_{25} of isoproterenol is reported to be threefold higher than healthy controls (Ramond et al. 1986). Rats with biliary cirrhosis are bradycardic, and this condition is owing to a significant hypo-responsiveness to the chronotropic effect of catecholamines (Nahavandi et al. 1999; Mani et al. 2002). In the present study, we showed that two independent treatments (N-acetylcysteine and L-NAME), both of which can normalize chronotropic responses to adrenergic stimulation *in vitro*, also led to normalization of heart rate *in vivo* (Fig. 4.4). Moreover spectral analysis of HRV showed increased cardiac sympathetic activity in rats with cirrhosis, which was unchanged following either L-NAME or N-acetylcysteine treatment in rats with cirrhosis (Mani et al. 2006b). These data suggest impaired end-organ responsiveness to adrenergic stimulation may have a role in pathogenesis of cardiac chronotropic dysfunction in cirrhosis and the effects of L-NAME and N-acetylcysteine are independent of changes in autonomic nervous system activity.

The mechanism of tyrosine nitration in proteins under pathological conditions is an area of active investigation. It can occur through the formation of peroxynitrite or nitryl chloride, formed by the reaction of nitric oxide and hypochlorous acid, both of which can react with tyrosine in proteins to form nitrotyrosine (Baldus et al. 2001). Biliary cirrhosis is associated with enhanced nitric oxide production (Liu et al. 2000). Nitric oxide reacts rapidly with superoxide anion (O_2^-) to form peroxynitrite which can nitrate tyrosine residues in proteins. There is now good evidence that liver disease is associated with oxidative stress and increased formation of reactive oxygen species (Marley et al. 1999; Ljubuncic 2000). Ljubuncic et al. (2000) reported an increased formation of lipid peroxidation products in the cardiac tissue of rats with biliary cirrhosis compared with controls. This finding may be partly owing to enhanced generation of superoxide by NADPH oxidase in response to angiotensin II (Pagano et al. 1997), endothelin (Barton et al. 1997), or bile acids (Bomzon et al. 1997). The observation that there is increased tyrosine nitration in cirrhosis in liver as well as cardiac tissue, but not in brain suggests that nitrative stress is a generalized phenomenon in cirrhosis, which can involve different organs including liver and cardiovascular system. In the liver, for instance, it has recently been shown that

tyrosine nitration contributes to inactivation of hepatic glutamine synthetase which in turn leads to the development of hyperammonemia in rats with cirrhosis and sepsis (Gorg et al. 2005).

Fernando et al. (1998) have previously observed that administration of N-acetylcysteine normalizes the systemic haemodynamic abnormalities in rats with portal hypertension, and lipoic acid (another low molecular weight thiol antioxidant) had a similar effect in rats with chronic bile duct ligation (Marley et al. 1999). Therefore, we investigated whether N-acetylcysteine could improve cardiac function in rats with biliary cirrhosis, and made the critical observation that administration of N-acetylcysteine led to normalization of bradycardia *in vivo,* as well as improved cardiac responses to adrenergic stimulation *in vitro* (Figs. 4.4 and 4.8). These data are of interest, because they have therapeutic implications, even though the mechanisms involved remain poorly understood. We observed that both N-acetylcysteine and L-NAME can each markedly decrease the levels of tissue nitrotyrosine. Because nitration of tyrosine can alter the protein's function, these data suggest nitration of cardiac proteins may lead to abnormal cardiac responses in cirrhosis. Reactive nitrogen species can also react with cysteine residues in proteins to form S-nitrosated proteins. Therefore, we also measured the levels of S-nitrosothiols in cardiac tissue of rats with biliary cirrhosis; however there were no significant differences in cardiac levels of S-nitrosothiols between controls and rats with cirrhosis.

Both L-NAME and N-acetylcysteine can modulate the cardiac function and decrease cardiac nitrotyrosine levels in biliary cirrhosis. However, the effects of N-acetylcysteine is not attributable to downregulation of NO synthesis because the plasma concentrations of nitrite + nitrate (NO end-products) were still significantly elevated in rats with cirrhosis treated with N-acetylcysteine whereas L-NAME significantly decreased nitrate/nitrite concentrations in both groups (Fig. 4.6). The decrease of protein-bound nitrotyrosine after N-acetylcysteine treatment may be related to the ability of N-acetylcysteine, to either inhibit the formation of reactive nitrogen species or to increase the proteolytic degradation of the nitrated proteins. Using [$^2H_6$]PHPA as a probe to study formation of reactive nitrogen species *in vivo*, we could initially show enhanced nitration reactions *in vivo* and a corresponding increased formation of its nitrated product [$^2H_5$]NHPA in rats with cirrhosis.

However, based on this approach, we were unable to show decreased reactive nitrogen species formation following N-acetylcysteine administration as the urinary levels of [$^2H_5$]NHPA were un-changed in N-acetylcysteine treated animals (Fig. 4.12). Because these data suggest N-acetylcysteine does not scavenge reactive nitrogen species in our model, the effect of N-acetylcysteine on nitrotyrosine levels could be explained if it enhances the degradation of nitrated proteins. Souza et al. have shown that nitration of tyrosine residue(s) in proteins is sufficient to induce an accelerated degradation of the modified proteins to release free amino acids as well as free nitrotyrosine (Souza et al. 2000). This study suggested that if N-acetylcysteine increased proteolysis of nitrated proteins then free nitrotyrosine levels may be increased in animals treated with N-acetylcysteine. This finding was confirmed when the levels of free nitrotyrosine were measured in cardiac ventricular tissue and found to be increased (Fig. 4.11). This outcome suggests that N-acetylcysteine may upregulate proteolytic degradation of proteins containing nitrotyrosine leading to a decrease in protein-bound nitrotyrosine content and corresponding to an increase in free nitrotyrosine levels, and is consistent with reports that cellular redox state is a major modulator of proteosme activity both *in vivo* and *in vitro* (Jahngen-Hodge et al. 1997; Obin et al. 1998).

The mechanism by which protein nitration leads to abnormal cardiac function in cirrhosis is not clear, however a very similar mechanism has been recently postulated in cardiac dysfunction associated with high aldosterone levels (Sun et al. 2002). Sun et al. (2002) have recently shown that chronic aldosterone/salt treatment is associated with a time-dependent generation of nitrotyrosine in cardiomyocytes, which was attenuated by the administration of N-acetylcysteine. The concept that nitration of cardiac proteins leads to cardiac dysfunction has also been described in AIDS-related cardomyopathy (Chaves et al. 2003), and diabetes-associated cardiac dysfunction (Turko et al. 2003). Therefore, the development of new therapies, which prevent or modify nitration of cardiac proteins in cirrhosis, may have important implications in other types of cardiac dysfunction associated with systemic inflammation such as sepsis. Whereas the observation that increased nitration of cardiac proteins in cirrhosis is of interest, the question arises which proteins are nitrated and are they functionally important? In a recent report, Kanski et al. (2005) employed a proteomic approach to identify the cardiac proteins that undergo age-dependent protein tyrosine nitration.

Among the identified proteins are important mitochondrial enzymes responsible for ATP production and metabolism; desmin, which is involved in sliding of myocardial filaments and cardiac contraction, is also included (Kanski et al. 2005). Although we have tried to identify which proteins are nitrated in the current study (data not shown), we have not been able to obtain reproducible data, and at present the identity of the nitrated proteins remains unknown. However, the immunogold studies also suggest that cytoskeletal and mitochondrial proteins are targets for nitration in the atria of rats with cirrhosis. We conclude that cirrhosis leads to increased nitration of cardiac proteins, oxidation of cardiac lipids, and abnormal cardiac function. The observation that two independent treatments, which decrease cardiac nitrotyrosine levels, also lead to normalization of cardiac function, suggests nitration of cardiac proteins may lead to abnormal cardiac function.

Chapter 5. Decreased heart rate variability in patients with cirrhosis

5.1 Introduction

Decreased heart rate variability (HRV), or increased regularity of the cardiac rhythm, has been reported in number of clinical settings associated with increased production of inflammatory cytokines, for example sepsis, systemic inflammation and ischaemic heart disease, (Aronson et al. 2001; Griffin et al. 2005; Hamaad et al. 2005; Lanza et al. 2006) and in several neuropsychiatric conditions, for example, depression (Kim et al. 2005; Vigo et al. 2004) dementia (Kim et al. 2006; Zulli et al. 2005) and symptomatic relapse in major psychoses (Kim et al. 2004).

HRV is also decreased in patients with chronic liver disease (Hendrickse et al. 1992; Lazzeri et al. 1997; Fleisher et al. 2000; Coelho et al. 2001; Ates et al. 2006) and is a negative predictor of outcome in this patient population (Hendrickse et al. 1992; Ates et al. 2006). Plasma concentrations of inflammatory cytokines are increased in patients with cirrhosis, even in the absence of active infection (Tilg et al. 1992; Genesca et al. 1999) and this activation of inflammatory mediators might explain the decrease in HRV observed in these patients. However, while there is a clear positive correlation between plasma levels of the inflammatory cytokines and the degree of hepatic dysfunction (Tilg et al. 1992; Genesca et al. 1999) the relationship between HRV and the degree of hepatic decompensation is much less robust.

The possibility that the changes in HRV observed in patients with cirrhosis might relate to the presence and degree of hepatic encephalopathy does not seem to have been considered in the studies undertaken to date. The pathogenesis of hepatic encephalopathy remains unknown but recent interest has focused on the potential role of inflammatory mediators (Blei 2004; Shawcross et al. 2004; Jover et al. 2006; O'Beirne et al. 2006). Indeed serum levels of inflammatory cytokines have been shown to positively correlate with the severity of hepatic encephalopathy in this patient population (Genesca et al. 1999; Odeh et al. 2004; Odeh et al. 2005).

In this chapter, the relationship between HRV, assessed using both linear and non-linear dynamics, and neuropsychiatric performance, was assessed in patients with

cirrhosis to test the following hypotheses:

1. The decreased in HRV correlates with the presence and degree of hepatic encephalopathy, independently of the degree of hepatic impairment.
2. The relationship between HRV and hepatic encephalopathy is based on a common pathogenic mechanism, mediated by inflammatory cytokines.

5.2. Materials and methods IV

Study Subjects

The patient population comprised 75 individuals (51 men: 24 women) of mean (± SD) age 55 ± 9 years, with biopsy-proven cirrhosis. The aetiology of the liver lesion was determined on the basis of clinical, laboratory, radiological and histological variables. Patients were excluded from the study if they were under 16 or over 80 years of age; could not speak English or obey spoken commands; had misused alcohol in the preceding three months; had a history of insulin-dependent diabetes mellitus, significant head injury, cardiovascular/cerebro-vascular disease or arterial hypertension; or were taking neuroactive drugs or drugs known to affect the cardiac rhythm, other than propranolol. The reference population comprised eight healthy volunteers (three men: five women) of mean age 40 ± 12 years. None had a history, clinical or laboratory evidence of alcohol misuse, chronic liver disease or heart disease; none drank alcohol in excess of 20 g/day or took prescription medication.

Ethics

The study was conducted according to the Declaration of Helsinki (Hong Kong Amendment) and Good Clinical Practice (European guidelines). The protocol was approved the Royal Free Hampstead NHS Trust Ethics Committee. All participating subjects, or their appropriately appointed guardian, provided written, informed consent for study participation.

Assessment of the severity of hepatic dysfunction (Child score)

The functional severity of the liver injury was assessed using Pugh's modification of the Child's grading system (Pugh et al., 1973). The Child score is a grading system which was originally developed by Child and Turocotte (1964) to predict mortality during surgery in patients with cirrhosis. It is now widely used to determine the functional severity of the liver injury, as well as the necessity of liver transplantation. The score employs five clinical measures of liver disease. Each measure is scored 1-3, with 3 indicating most severe derangement as shown in Table 5.1. Chronic liver disease is classified into Child class A, B and C, employing the added score from the table. When the total score is 6 or less, the patient is classified as Child A. When the score is more than 6 and less than 10, the patients in classified into Child B category and patients with Child C usually represent a score equal to or above 10.

Table 5.1. Modified Child Classification of severity of liver disease according to the degree of ascites, the plasma concentrations of bilirrubin and albumin, the prothrombin time (NIR), and the degree of encephalopathy (HE).

Measure	1 point	2 points	3 points
Bilirubin (μmol/L)	<34	34-50	>50
Serum albumin (g/L)	>3.5	2.8-3.5	<2.8
INR (international normalized ratio)	<1.7	1.71-2.20	>2.20
Ascites	None	Suppressed with medication	Refractory
Clinical HE	None	Overt HE grade I-II	Overt HE grade III-IV

Assessment of neuropsychiatric status

Patients' mental state was evaluated using the West Haven criteria (Conn et al., 1977a). Psychometric performance was assessed, under standardized conditions, by the same observer, using Number Connection Tests A (NCT-A) and B (NCT-B) (Conn et al., 1977b), the Digit Symbol (DS) subtest of the Wechsler Adult Intelligence Scale (Wechsler, 1955) and the Line Tracing (LT) and Serial Dotting (SDot) tests (Hamster, 1983; Schomerus et al., 1999). Psychometric test results were scored in relation to age- and education-adjusted reference values (Weissenborn et al., 2001; Amodio et al., 2002) and were considered abnormal if they exceeded two standard deviations of the mean reference values. Psychometric performance was classified as impaired if the sum of the standard deviations equalled or exceeded four. Electroencephalograms (EEGs) were recorded, eyes closed, in a condition of relaxed wakefulness, using silver-silver chloride electrodes placed according to the International 10-20 system (Walter-Graphtec system equipment). The traces were analysed visually to exclude abnormal focal activity; they were then subjected to automated spectral analysis and classified according to Amodio et al. (Amodio et al., 1999). Neuropsychiatric status was classified as (i) *unimpaired:* individuals who had no clinical evidence of hepatic encephalopathy and no defining EEG or psychometric abnormalities; (ii) *minimal hepatic encephalopathy:* individuals who showed no clinical evidence of hepatic encephalopathy but had an abnormal EEG and/or

impaired psychometric performance; (iii) *overt hepatic encephalopathy:* individuals with clinically evident neuropsychiatric disturbances (Conn et al., 1977a).

Assessment of HRV

Data acquisition

A 10-minute, single channel electrocardiogram (ECG) was recorded simultaneously with the EEG by placing one silver-silver chloride electrode on each wrist (WG PLEEG system). The ECG data were exported - sampling rate 256 Hz - and an *ad hoc* computer program was used to detect the R peaks and to generate the R-R interval series. Visual inspection of all R-R intervals was performed and artefacts removed by careful manual editing by a single observer. Five-minute, artefact-free continuous R-R interval sections were selected for further analysis (Task Force report on HRV, 1996).

Linear analysis of HRV

The standard deviation of the R-R intervals (SDNN) was calculated on the selected artefact-free traces and used as a measure of total HRV. *Spectral analysis* of the R-R interval time series was carried out by fast Fourier transformation on 1024 sample points, applying Welch's window, using software developed by Niskanen et al. (Niskanen et al. 2004). Two bands were identified: i) a *low frequency component* (LF: 0.04-0.15 Hz), which reflects the oscillatory pattern of the baroreflex loop and is jointly mediated by sympathetic and parasympathetic activities (Altimiras 1999) and ii) a *high frequency component* (HF: 0.15-0.40 Hz), which reflects the inhibition of the vagal tone during inspiration (Altimiras, 1999). The *LF/HF ratio* was calculated and used as a measure of sympatho-vagal balance (Altimiras 1999).

Non-linear analysis of HRV

While linear measures of HRV simply describe the amount of variability, nonlinear HRV analysis attempts to capture the structure or complexity of the R-R time series. Thus, a physiological series of heart beats, a random series of beats, and a totally periodic series of beats might have the same SDNN, but their underlying structure of the series will be completely different.

Poincaré plot: The Poincaré plot is a graphical representation of the correlation between consecutive R-R intervals [x axis: $R\text{-}R_{(n)}$; y axis: $R\text{-}R_{(n+1)}$: Fig. 4.2]. If the cardiac rhythm is regular, the points on the Poincaré plot are located close to the line of identity. The standard deviation of the points perpendicular to the line-of-identity (SD1) describes short-term variability, which is mainly related to respiratory sinus arrhythmia (Tulppo et al. 1996); the standard deviation along the line-of-identity (SD2) describes the long-term R-R interval variations and accounts for all other heart rate changes, including those associated with sympathetic oscillations, barorefelx loop, thermoregulation and fluctuations in humoral factors (Tulppo et al. 1996). The parameters SD1 and SD2 were calculated using the software developed by Niskanen et al. (Niskanen et al. 2004).

Sample entropy: The sample entropy (SampEn) is a parameter that quantifies the degree of regularity versus the degree of unpredictability of a time series. SampEn is the logarithmic likelihood of the repetition of patterns in the time series; it calculates the probability that an epoch of window length m, with a degree of tolerance r, will be repeated at later time points. Regular time series are characterised by low SampEn, while random time series are characterised by high SampEn. In the present study, m was fixed at 2 and r at 0.2 ms. (Richman and Moorman, 2000).

Measurement of Cytokines Concentration

Plasma samples were collected from a subgroup of 22 patients with cirrhosis and varying degrees of hepatic encephalopathy and were kept at -80 until analysed for TNF-α, IL-6, IL-10 and IL-12 using eBioscience ELISA kits (San Diego, CA, USA) on Nunc Maxisorb ELISA plates according to the manufacturer's instructions by a single investigator, in duplicate, on a single plate for each cytokine to reduce assay variability. A standard curve provided by the manufacturer and a quality control serum were included on each ELISA plate.

Statistical analysis

The results are presented as mean ± SD. The distributions of variables were tested for normality using the Shapiro-Wilk's W test. Differences between normally distributed variables were examined by one way ANOVA/ANCOVA, including, where

necessary, adjustments for the degree of vagal modulation (SD1, HF); subsequent between group comparisons were performed using the Tukey test. Differences between non-normally distributed variables were examined using the Kruskal-Wallis tests; subsequent between group comparisons were performed using Dunn's test. Factorial ANOVA was used to examine the extent to which variable sets differed according to the degree of hepatic and neuropsychiatric impairment. Correlations between HRV indices, psychometric performance, EEG spectral variables and cytokine levels were tested using the Spearman's R coefficient of correlation. The relationship between HRV indices and survival was examined using Cox's proportional hazards model

5.3. Results IV

The aetiology of the cirrhosis was alcohol in 60 (80%); alcohol plus HBV, HCV infection in five (7%), cryptogenic in three (4%); non alcoholic steatohepatitis in two (3%); primary biliary cirrhosis in two (3%) and chronic hepatitis C infection, chronic autoimmune hepatitis and haemochromatosis in one each (1%). Functionally, 43 (57%) of the patients were classified as Child's Grade A, 12 (16%) as Child's Grade B, and 20 (27%) as Child's Grade C. On the day of study, 37 (49%) of the 75 patients were classified as neuropsychiatrically unimpaired, eight (11%) as having minimal hepatic encephalopathy and 30 (40%) as having overt hepatic encephalopathy.

There were no significant differences in mean heart rate between patients and healthy controls (Table 5.2). However, HRV was significantly decreased in the patient population, whether assessed using linear (SDNN $P<0.01$; LF $P<0.05$) or non-linear indices (SD1 $P<0.05$, SD2 $P<0.001$, SampEn $P<0.001$) (Table 5.2). Sympathovagal balance (as assessed be measuring LF/HF) was significantly increased in the patients with cirrhosis compared to the healthy controls, $P<0.05$ (Table 5.2).

As shown in Table 5.2, we found that among all HRV parameters, SD2 (long-term HRV) showed the strongest correlation with degree of HE. The striking observation was that when we applied multiple analysis of variance, the association between SD2 and the degree of hepatic encephalopathy was independent of the degree of hepatic dysfunction ($F_{Child}=0.267$, $P=0.76$; $F_{HE}=4.801$, $P<0.05$; $F_{Child\ and\ HE}=0.415$, $P=0.79$). Details of this finding are illustrated in Figs. 5.1, 5.2 and 5.3.

Table 5.2. Heart rate variability indices in healthy volunteers and patients with cirrhosis by degree of hepatic encephalopathy (HE) and degree of hepatic dysfunction (Pugh et al, 1973).

	Age (yr)	Pugh's score	HR-Mean (beat/min)	SDNN (ms)	LF (ms^2)	HF (ms^2)	LF/HF	SD1 (ms)	SD2 (ms)	SampEn
Healthy volunteers (n=8)	40 ± 12	-	67.4 ± 11.0	36.2 ± 11.3	184 ± 113	199 ± 226	1.4 ± 0.8	23.4 ± 12.1	56.1 ± 11.8	2.90 ± 0.33
Patients with cirrhosis (n=75)	55 ± 9 ^{aa}	7.5 ± 2.5	75.8 ± 12.9	19.4 ± 9.5 ^{aa}	58 ± 60 ^{a}	48± 69	2.2 ± 1.7 ^{a}	11.3 ± 7.8 ^{a}	31.8 ± 15.5 ^{aaa}	2.25 ± 0.61 ^{aaa}
Unimpaired (n=37)	53 ± 6 ^{a}	5.7 ± 1.8	74.4 ± 12.1	22.5 ± 10.3 ^{aa}	74 ± 72	66 ± 85	2.0 ± 1.2	13.2 ± 8.5 ^{aa}	37.6 ± 15.2 ^{aa}	2.42 ± 0.61
Minimal HE (n=8)	61 ± 6 ^{aaa}	6.1 ± 1.7	71.6 ± 12.2	23.8 ± 9.6 ^{a}	77 ± 56	46 ± 56	3.6 ± 3.1	12.6 ± 7.3 ^{a}	35.9 ± 13.3 ^{a}	2.40 ± 0.73
Overt HE (n=30)	55 ± 11 ^{a}	10.0 ± 2.7 ^{bbb}	78.5 ± 14.2	14.3 ± 7.1 ^{aaa,bb}	33 ± 49 ^{aaa,bb}	26 ± 38 ^{aaa}	2.1 ± 2.1	8.5 ± 6.0 ^{aaa}	23.5 ± 11.5 ^{aaa,bbb}	2.01 ± 0.54 ^{aa,b}
R			0.11	**-0.40*****	**-0.39*****	**-0.28***	-0.06	**-0.30****	**-0.44*****	**-0.29***
Child A (n=43)	56 ± 7 ^{aaa}	5.2 ± 0.65	74.4 ± 11.8	21.7 ± 9.8 ^{aa}	65 ± 65 ^{aa}	59 ± 78 ^{a}	2.4 ± 2.0	12.6 ± 8.5 ^{aa}	39.9 ± 14.4 ^{aa}	2.38 ± 0.65
Child B (n=12)	59 ± 10 ^{aaa}	8.2 ± 0.34 ^{ccc}	74.2 ± 11.1	18.4 ± 10.0 ^{aaa}	70 ± 59 ^{aa}	47 ± 59 ^{a}	2.7 ± 2.4	10.6 ± 6.6 ^{aa}	28.9 ± 13.8 ^{aaa}	2.10 ± 0.48 ^{a}
Child C (n=20)	50 ± 9 ^{a}	11.9 ± 0.9 ^{ccc}	79.6 ± 16.1	14.9 ± 8.5 ^{aaa}	36 ± 67 ^{aaa}	24 ± 31 ^{aa}	1.5 ± 1.3	8.7 ± 5.8 ^{aaa}	24.6 ± 15.2 ^{aaa}	2.06 ± 0.58 ^{aa}
R			0.12	**-0.32***	**-0.38*****	-0.18	-0.20	-0.22	**-0.32*****	-0.21

Significance of the differences between the patient population/subpopulations and the healthy volunteers: $^{a}P < 0.05$; $^{aa}P < 0.01$; $^{aaa}P < 0.001$
Significance of the differences between the patients with no HE and those with minimal/overt HE: $^{b}P < 0.05$; $^{bb}P < 0.01$; $^{bbb}P < 0.001$
Significance of the differences between the patients with Child C and those with Child A/B: $^{c}P < 0.05$; $^{cc}P < 0.01$; $^{ccc}P < 0.001$
R: Spearman's R correlation coefficient between the degree of HE/hepatic failure and heart rate variability indices in patients with cirrhosis: $^{*}p<0.05$; $^{**}P<0.01$, $^{***}P<0.001$

The relationship between long-term HRV (SD2) and the degree of neuropsychiatric impairment held firm even when data were adjusted for indicators of vagal modulation, namely SD1 and LF (Table 5.3).

As shown in Fig 5.4, significant correlations were observed between HRV indices and individual psychometric and spectral EEG variables.

Table 5.3. The relationship between long-term HRV (SD2) and the degree of neuropsychiatric impairment in patients with cirrhosis adjusted for indicators of vagal modulation of HRV. Data are expressed as covariate-adjusted.

HRV Parameter	Corrected for	Covariate mean	HE Classification			F (2,71)	P-value
			Unimpaired	Minimal HE	Overt HE		
SD2	**SD1**	11.28 (ms)	35.2 ± 1.7	34.3 ± 3.6	26.9 ± 1.9	5.39	**0.006**
SD2	**HF**	47.76 (ms^2)	35.5 ± 1.7	35.5 ± 3.8	26.6 ± 1.9	5.88	**0.004**

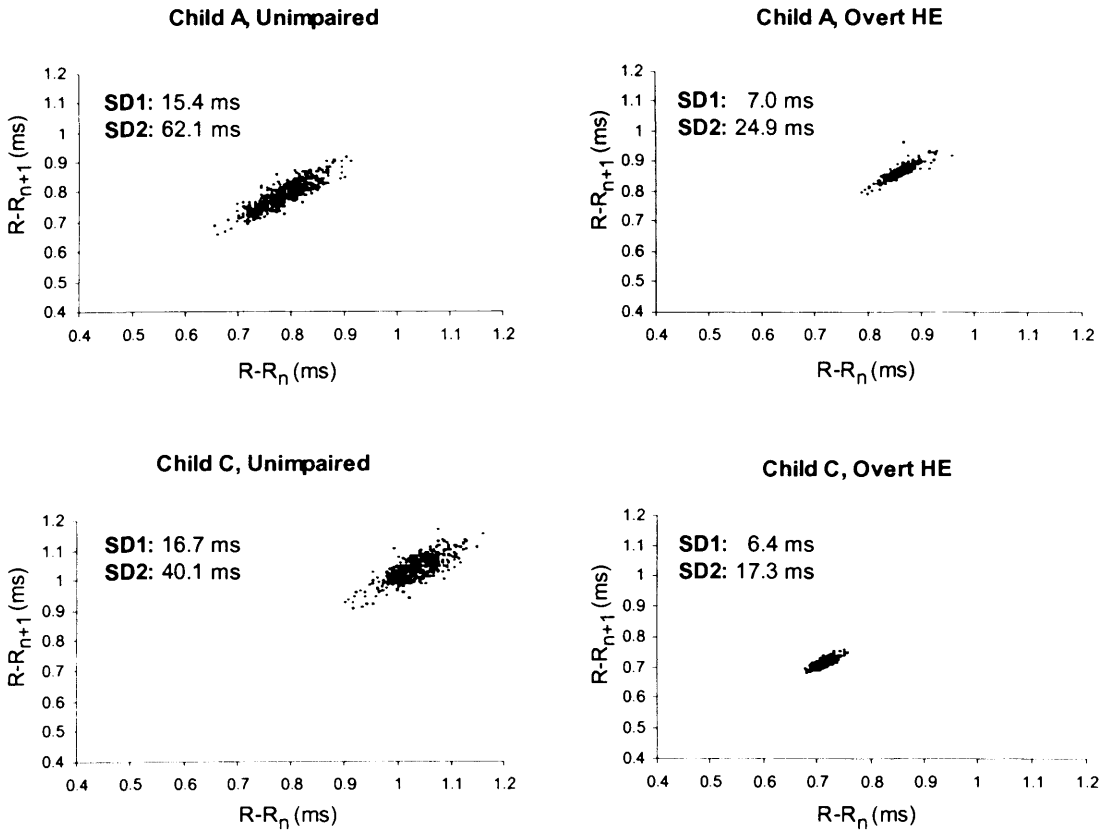

Figure 5.1. Poincaré plots depicting the correlation between consecutive R-R intervals, in four representative patients with cirrhosis, by degree of hepatic dysfunction and neuropsychiatric status. SD1 and SD2 represent the length and width of the Poincaré plot along the line-of-identity, respectively. Diminished scattering of the plot is the hallmark of a decrease in HRV. The Poincaré plot is less scattered in patients with overt hepatic encephalopathy (right panel) compared with patients who are neuropsychiatrically unimpaired (left panel), independently of the degree of hepatic dysfunction.

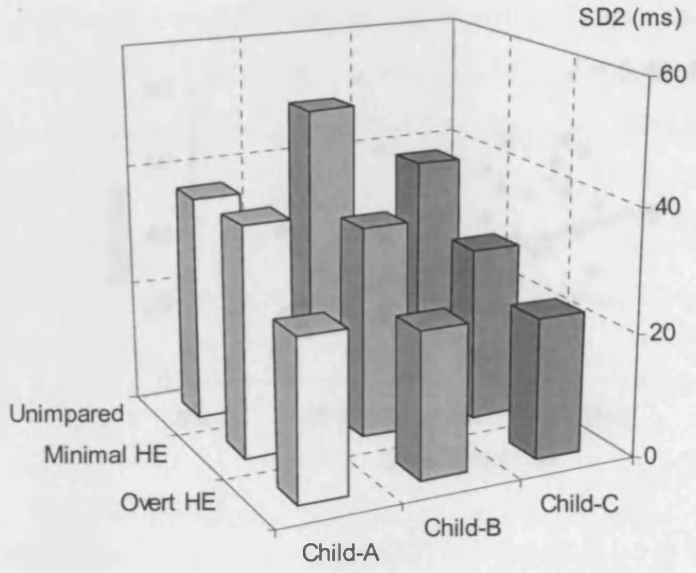

Figure 5.2. Long-term heart rate variability (SD2, Mean values) in patient with liver cirrhosis. Patients are categorized based on both degree of liver dysfunction (child) and hepatic encephalopathy (HE).

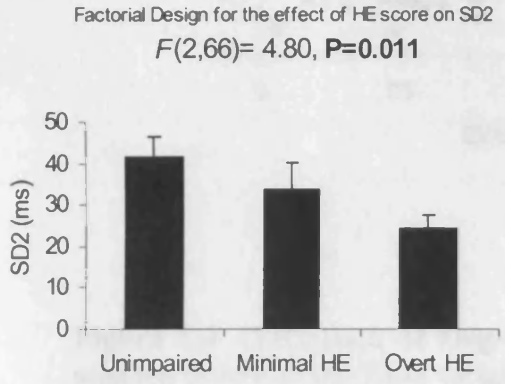

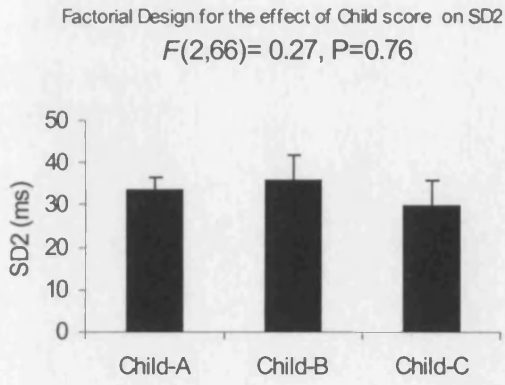

Figure 5.3. Factorial analysis of long-term HRV (SD2) in patients with cirrhosis adjusted for neuropsychiatric status (HE) or degree of liver dysfunction (Child).

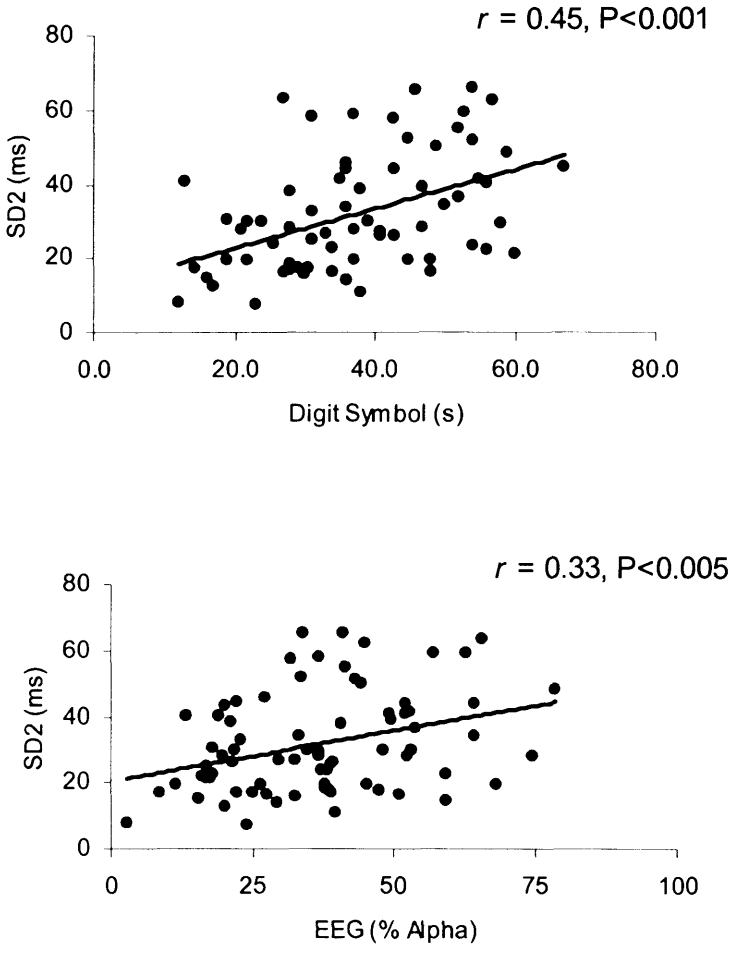

Figure 5.4. Correlation of long-term heart rate variability index (SD2) and selected psychometric/EEG variables in patients with cirrhosis.

Significant correlations were observed, in the patients with cirrhosis, between both linear and non-linear HRV indices and plasma concentrations of IL-6 ($P<0.05$; Table 5.4). Similarly, significant correlations were observed between psychometric variables and plasma TNF-α and IL-6 concentrations ($P<0.05$; Table 5.4).

Nine patients died during the follow-up period and two underwent orthotopic liver transplantation. There was a significant relationship between SD2 and survival ($P = 0.01$); the relative risk of death increased by 7.7% (95% CI, 1.8-13.6) for every ms drop in SD2.

Table 5.4. Correlations between plasma cytokine levels and heart rate variability/hepatic encephalopathy indices in patients with cirrhosis.

	TNF-α	IL-6	IL-10	IL-12
Psychometric performance				
NCT-A (s)	0.36	**0.45**	0.24	-0.06
NCT-B (s)	**0.46**	0.32	0.29	-0.22
SDot (s)	0.18	**0.48**	0.084	-0.14
HRV index				
SDNN (ms)	-0.34	**-0.43**	-0.34	-0.00
SD1 (ms)	-0.33	-0.28	-0.20	-0.09
SD2 (ms)	-0.35	**-0.49**	-0.40	0.07
SampEn	-0.38	-0.25	-0.28	0.02

NOTE: Values are correlation coefficients (Spearman's R); values in bold typeface are significant, $P<0.05$

5.4. Discussion IV

Healthy, physiological control of cardiovascular function is the result of complex interactions between multiple regulatory processes that operate over different time scales. Techniques derived from non-linear dynamics are now being adapted to quantify the behaviour of physiologic time series and to study their changes with age and disease (Goldberger et al. 2002). In the present study both linear and non-linear methods were used to analyse heart rate dynamics in patients with cirrhosis and showed that: 1) HRV is markedly decreased in this patient population compared with the healthy controls; 2) Changes in HRV is patients with cirrhosis correlate significantly with the severity of their neuropsychiatric impairment and this correlation is independent of the degree of hepatic dysfunction; 3) Non-linear measures of HRV correlate significantly with stand-alone EEG and psychometric variables; 4) Plasma levels of IL-6 correlate significantly with both indices of heart rate variability and neuropsychiatric variables in this patient population.

The relationship between decreased HRV and the degree of hepatic failure is well established (Fleisher et al. 2000; Ates et al. 2006). It has also been reported that reduced HRV is an independent risk factor for death in cirrhotic patients (Hendrickse et al. 1992, Fleisher et al 2000, Ates et al. 2006). The present study demonstrates that degree of neuropsychiatric impairment is more strongly correlated with HRV parameters than the degree of hepatic dysfunction. When the patients were categorized by both the Child score and the degree of hepatic encephalopathy, the correlation between reduced HRV and the degree of hepatic failure disappeared, while that between reduced HRV and HE remained significant (Fig 5.2 and 5.3). To our knowledge, this is the first study to show that reduced HRV is an independent predictor of HE in patients with cirrhosis. This is in line with a recent study by Newton et al. (2006), showing that HRV was significantly lower in fatigued than in non-fatigued patients with primary biliary cirrhosis (Newton et al. 2006). There were significant correlations between HRV indices and EEG spectral parameters, psychometric variables as well as plasma cytokine levels in patients with cirrhosis. These data further support a relationship between neuropsychiatric status and decreased HRV in this patient population. These findings are also consistent with those of previous studies showing a correlation between HRV parameters and neuropsychiatric abnormalities in different clinical settings, such as depression in

patients with ischemic heart disease (Vigo et al 2004), postmenopausal women (Kim et al. 2005) and negative symptoms in patients with schizophrenia (Kim et al. 2004).

The physiological mechanism underlying reduced HRV during systemic inflammatory response is not known but seems likely to represent dysfunction of the autonomic nervous system or of intracellular signal transduction processes, perhaps by circulating cytokines (Kuster et al. 1998, Pavlov et al. 2006). Malave et al. (2003) have recently shown that circulating levels of cytokines correlate with indices of depressed HRV in patients with congestive heart failure (Malave et al. 2003). Since inflammatory cytokines can potentially blunt ß-adrenergic signalling (Chung et al., 1990), Malave et al. have also suggested the possibility that over-expression of TNF-α and subsequent loss of ß-adrenergic responsiveness contributes to the decrease in HRV observed in heart failure (Malave et al., 2003). However, our recent report has shown that decreased HRV following endotoxin challenge is independent of impaired cardiac ß-adrenergic signalling in septic mice (Mani et al. 2006a). In addition our recent report suggests that loss of HRV in animal models of cirrhosis is not related to impaired cardiac ß-adrenergic responsiveness observed in cirrhotic rats (Mani et al. 2006b, Chapter 4). Here we have shown that plasma levels of IL-6 correlate significantly with both indices of heart rate variability and neuropsychiatric variables in patients with cirrhosis. This data do not provide an explicit mechanism for the association between IL-6 and slow R-R oscillations. However it is line with a study by Aronson et al. (2001) who showed that plasma IL-6, and not TNF-α, levels inversely correlated with indices of reduced HRV in patients with decompensate heart failure. Other groups have also shown that amongst the cytokines, IL-6 exhibit the strongest correlation with the indices of depressed HRV during inflammation (Gonzalez-Clemente et al. 2007, Tateishi et al. 2007). However the mechanism by which IL-6 might affect autonomic control of cardiac cycle needs further inverstigation.

Although great strides in the last decade have helped to elucidate the mechanism of inflammatory response, the precise mechanism by which inflammation induces 'regularisation' of heart rate variability remains elusive. Systemic inflammatory response is an example of a self-regulating complex system, with multiple cascading non-linear interactions and feedbacks, acting in series and in parallel, to form a 'scale-free' network. Alteration of heart rate dynamics during inflammation can be

considered to be a reflection of these non-linear interactions in the cardiovascular regulatory system. Regardless of the mechanism, these findings are important in clinical medicine, as HRV can potentially be considered a candidate measure for monitoring at risk patients, either alone or as part of a multivariable scheme.

HRV analysis has extensively been used to assess autonomic neuropathy in difference clinical settings (see Task Force report 1996 on heart rate variability for review). Because HE is frequently precipitated by constipation, it has been proposed that autonomic dysfunction may contribute to the development of HE by decreasing gut motility and increasing exposure to gastrointestinal bacteria (Maheshwari et al. 2004). To address this issue most researchers has assessed autonomic neuropathy by looking at heart rate response to deep breathing or Valsalva manoeuvre, which are indirect measures of vagal activity. These studies have shown that vagal neuropathy is common in cirrhosis regardless of the aetiology of liver disease (Hendrickse et al, 1992, Fleisher et al. 2000, Maheshwari et al. 2004). In addition, there is a trend towards a higher incidence of HE in patients with autonomic neuropathy (Maheshwari et al. 2004). In the present study we employed Poincaré plots to distinguish between the effects of vagal modulation from other causes of heart rate variations (Tulppo et al. 1996). SD1 describes short-term fluctuation of R-R intervals reflecting vagal drive and SD2 describes the long-term R-R interval variations and accounts for all other heart rate changes, including those associated with sympathetic oscillations, barorefelx loop, thermoregulation and fluctuations in humoral factors (Tulppo et al. 1996). We found that among all HRV parameters, SD2 showed the strongest correlation with degree of HE (Table 5.2). In addition, the relationship between long-term HRV (SD2) and the degree of neuropsychiatric impairment held firm even when control was exercised for vagal drive (SD1). Since the relationship between SD2 and the degree of HE remained essentially unchanged after adjusting for SD1 (Table 5.2), we can conclude that the correlation between long-term HRV and the neuropsychiatric impairment in cirrhosis can not be simply explained by vagal dysfunction. It is likely that systemic inflammation and cytokine might influence the complex network of the autonomic nervous system during systemic inflammation. Recent report form Gonzalez-Clemente et al. (2005, 2007) has supported this hypothesis by showing that inflammatory cytokines are involved in the pathogenesis of neuropathy in patients with diabetes (Gonzalez-Clemente et al. 2005, 2007).

The molecular mechanism(s) underlying the pathogenesis of HE is poorly understood; there is evidence suggesting that inflammatory mediators might play a crucial role (Shawcross et al., 2004, O'Beirne et al., 2006, Jover et al., 2006). Infection (e.g. sepsis or spontaneous bacterial peritonitis) is a well-known precipitating factor for the development of overt HE (Blei 2004). Furthermore, serum levels of TNF-α have been shown to correlate with severity of HE in chronic liver failure (Odeh et al., 2004, Odeh et al., 2005). More recent data suggest that the subtlest manifestation of HE, minimal encephalopathy, may also be associated with inflammation. For instance Shawcross et al. have reported a significant impairment of neuropsychiatric status following diet-induced hyperammonemia during the inflammatory state, but not after its resolution (Shawcross et al. 2004). The present study indicates that the changes observed in HRV and in neuropsychiatric status in patients with cirrhosis may have a common aetiology, possibly involving cytokines. In fact we could show a significant correlation between plasma levels of IL-6 and HRV parameters in patients with cirrhosis. This report adds evidence to the possible role of inflammatory responses in the aetiology of hepatic encephalopathy in patients with chronic liver disease.

6. Summary and conclusions

Ever since the discovery that nitric oxide (NO) can be generated enzymatically in biological systems and give rise to the formation of reactive nitrogen species (RNS), an extensive body of studies that address the involvement of reactive nitrogen species (RNS) in physiology and pathology have been published. The discovery that RNS can cause nitration or nitrosation within biological targets, such as tyrosine and thiols has also led to an expanding number of studies. Thus, detection of nitrotyrosine or related nitro adducts is often used as a footprint for the formation of RNS.

Despite the considerable progress that has been made over the years with respect to analytical methodology to determine endogenous protein nitration, which was often plagued by considerable sources of artifact (Frost et al. 2000, Moore and Mani 2002), one issue that has remained incompletely resolved to date is what is the most appropriate and convenient way to estimate overall protein tyrosine nitration *in vivo.* Measurement of protein-associated nitrotyrosine may not always provide an accurate estimation of the extent of protein nitration that has occurred *in vivo*, since most proteins, and oxidized proteins in particular, have finite life spans and undergo avid turnover by proteasomal degradation.

Therefore, analysis of accumulated breakdown products in serum or in urine might be a better approach to assess the formation of nitrotyrosine *in vivo*. We and others have identified 3-nitro-4-hydroxyphenylacetic acid (NHPA) as one of its major metabolites. In the present thesis, one of the major objectives was to evaluate the use of urinary NHPA as a biomarker for protein tyrosine nitration.

In one study performed in rats we addressed the possibility that the appearance of urinary NHPA could arise from nitration of endogenous *para*-hydroxyphenylacetic acid (PHPA), rather than tyrosine nitration followed by its metabolism. Using mass spectrometry in combination with isotopically labelled PHPA precursors, we demonstrated that nitration of endogenous PHPA accounts for the majority of NHPA in the urine. To confirm these data we carried out a similar study in human volunteers which showed that endogenous PHPA is nitrated *in vivo* and is the major source of urinary NHPA in humans (The data of nitration of PHPA in human volunteers is not shown here and is published elsewhere; see Panala et al. 2006).

Thus urinary NHPA arises from both metabolism of nitrotyrosine, and nitration of endogenous PHPA. In chapter 2 we showed that measurement of [$^2H_5$]NHPA after infusing [$^2H_6$]PHPA may be used as an index of RNS formation *in vivo*. Our observation that endotoxaemia causes a significant increase in [$^2H_5$]NHPA excretion (Fig. 2.6) supports the validity of this novel approach.

We also used this method to examine nitration reactions in experimental cirrhosis and demonstrated a significant increase in [$^2H_5$]NHPA formation following intravenous injection of [$^2H_6$]PHPA in rats with biliary cirrhosis (Fig. 4.12). In order to investigate if enhanced nitration reaction plays a role in cardiac dysfunction is cirrhosis; we measured free and protein-bound nitrotyrosine in cardiac tissue of bile duct ligated rats following pharmacological manipulations. This confirmed the observation that cardiac chronotropic function is abnormal in rats with biliary cirrhosis. More importantly, it demonstrates that this abnormality is associated with increased levels of protein-bound nitrotyrosine in cardiac tissue. The administration of either L-NAME or N-acetylcysteine, both of which decrease the tissue levels of nitrotyrosine, led to normalization of heart rate as well as cardiac responsiveness to adrenergic stimulation in rats with biliary cirrhosis.

Both L-NAME and N-acetylcysteine can improve cardiac function and decrease cardiac nitrotyrosine levels in biliary cirrhosis. However, the effects of N-acetylcysteine are not attributable to down-regulation of NO synthesis since the plasma concentrations of nitrite + nitrate (NO end-products) remained significantly elevated in rats with cirrhosis treated with N-acetylcysteine whereas L-NAME led to a significant decrease in plasma nitrate + nitrite concentrations in both groups. The decrease of protein-bound nitrotyrosine after N-acetylcysteine treatment may be related to the ability of N-acetylcysteine, to either inhibit the formation of reactive nitrogen species or to increase the proteolytic degradation of the nitrated proteins. Using [$^2H_6$]PHPA as a probe to study formation of reactive nitrogen species *in vivo*, we could initially show enhanced nitration reactions *in vivo* and a corresponding increased formation of its nitrated product [$^2H_5$]NHPA in rats with cirrhosis. However, based on this approach, we were unable to show decreased reactive nitrogen species formation following N-acetylcysteine administration as the urinary levels of [$^2H_5$]NHPA were un-changed in N-acetylcysteine treated animals (Fig. 4.12).

Because these data suggest N-acetylcysteine does not scavenge reactive nitrogen species in our model, the effect of N-acetylcysteine on nitrotyrosine levels could be explained if it enhances the degradation of nitrated proteins. Thus, whereas these data suggest N-acetylcysteine leads to increased proteolysis of nitrated proteins, the mechanism remains unclear and needs further investigation.

Whereas the observation that increased nitration of cardiac proteins in cirrhosis is of interest, the question arises which proteins are nitrated and are they functionally important? Although we initially tried to use proteomic methods to identify the nitrated proteins in the current study, we were unable to obtain reproducible data, and at present the identity of the nitrated proteins remains unknown. One group has successfully employed proteomic methods to identify the cardiac proteins that undergo age-dependent tyrosine nitration (Kanski et al. 2005). Among the identified proteins are mitochondrial enzymes as well as desmin which is involved in the sliding of myocardial filaments.

Apart from identification of nitrated proteins it is important to know what proportion of the candidate protein is modified by nitration. Because the overall extent of tyrosine nitration *in vivo* may only amount to one nitrotyrosine per 10^3 tyrosine residues, it appears unlikely that tyrosine nitration *in vivo* significantly impairs cardiac function unless specific tyrosine substrates are preferential targets for nitration. Cytoskeletal proteins such as actin have been suggested to represent important targets for tyrosine nitration reactions (Aslan et al. 2003). In fact chemical nitration of actin or neurofilaments has been shown to disrupt assembly of these proteins, and modification of only a few protein subunits appears necessary to cause disruption of a structure involving thousands of subunits (Beckman 1996; Aslan et al. 2003). The immunogold studies presented in Fig. 4.13 suggest that cytoskeletal and mitochondrial proteins are targets for nitration in the atria of rats with cirrhosis. However, further studies are required in future to examine whether such modifications contribute significantly to the pathobiology of cardiac chronotropic dysfunction in cirrhosis.

There can be little doubt that NOS activity is of considerable importance physiologically, or that overproduction of NO or increased NOS activity has the potential to cause harm either through nitration of proteins or through enhancement of

cGMP-dependent mechanisms (*e.g.* inhibition of L-type calcium channels in the cardiomyocytes). However, part of the problem in turning scientific discovery into useful therapeutics has been the sheer range of processes in which NO has been implicated, and the opposing effects of NO even within a single disease. A good example is provided in the field of liver cirrhosis: High-output NO generation in systemic vasculature can induce cardiac dysfunction and haemodynamic instability. However, decreased NO formation within the hepatic microcirculation promotes portal hypertension and its complications. Any systemic administration of NOS inhibitors (e.g. L-NAME) will have a marked and detrimental effect on hepatic microcirculation than a beneficial effect on systemic circulation. In the past, NOS inhibitors have been used in humans to explore the physiological mechanisms or as potential treatment. For instance, in patients with septic shock, the isoform non-specific NOS inhibitor, N^G-monomethyl-arginine, restores blood pressure and seems to improve haemodynamics. However, the largest study so far showed an adverse effect on outcome (Vallance and Leiper 2002). Even in genetically modified animals, although iNOS knockout mice are reported to be resistant to circulatory dysfunction in experimental sepsis (Funakoshi et al., 2002), disruption of iNOS does not improve the survival following a lethal dose of endotoxin or cytokines (Nicholson et al., 1999 and Funakoshi et al., 2002). Likewise, both iNOS and eNOS knockout mice are reported to develop cardiovascular dysfunction in a mouse model of portal hypertension (Iwakiri et al. 2002). This means that developing even isoform specific NOS inhibitors might not be a good strategy for management of cardiovascular abnormalities in patients with liver disease.

The spontaneous variations which occur in heart rate result from a series of complex interactions between multiple regulatory processes which operate over different time scales. Decreased variability and increased regularity of cardiac rhythm have been reported in different clinical settings associated with increased production of inflammatory cytokines and have a negative prognostic value. Heart rate variability (HRV) is decreased in patients with chronic liver disease, and is a negative predictor of outcome in this patient population. The possibility that the changes in HRV observed in patients with cirrhosis might be associated with hepatic encephalopathy

has not been considered previously. This is surprising given that: (i) reductions in HRV are known to occur in a number of neuropsychiatric disorders (chapter 5); (ii) reductions in HRV are observed in situation associated with increased circulating inflammatory cytokines; inflammatory cytokines are increased in patient with cirrhosis and correlate positively with the severity of hepatic encephalopathy (chapter 5).

As described in chapter 5, HRV was significantly decreased in patients with cirrhosis in parallel with the degree of neuropsychiatric impairment, independently of the degree of hepatic dysfunction. Moreover, significant correlations were observed between HRV indices and individual EEG spectral parameters and psychometric variables. There are several possible explanations for the relationship between HRV and neuropsychiatric status in patients with cirrhosis. The two most likely are (i) the presence of an autonomic neuropathy or (ii) the presence of a mechanism involving circulating inflammatory cytokines. The physiological mechanism underlying the loss of HRV during the systemic inflammatory response is unknown but cytokine-induced autonomic dysfunction or disruption of intracellular signal transduction processes undoubtedly plays a role. Amongst the cytokines IL-6 exhibit the strongest correlation with the indices of depressed HRV during inflammation (Gonzalez-Clemente et al. 2007; Tateishi et al. 2007; chapter 5). Cytokines can potentially blunt ß-adrenergic signalling and thus it has been suggested that over-expression of cytokines and subsequent loss of ß-adrenergic responsiveness might contributes to the decrease in HRV during inflammation. Although this hypothesis is attractive within the context of 'cirrhotic cardiomyopathy', our recent study has shown that decreased HRV following endotoxin challenge is not related to alterations in cardiac ß-adrenergic signalling in endotoxaemic mice (Mani et al. 2006a). In addition, loss of HRV in bile duct ligated rat model of cirrhosis occurs independently of impaired cardiac ß-adrenergic responsiveness (chapter 4).

Previous studies have suggested that decreased HRV is an independent risk factor for death and has a negative prognostic value in this patient population (Hendrickse et al. 1992; Ates et al. 2006). This finding was confirmed in the present thesis; the relative risk of death increased by 7.7 % for every ms drop in SD2. Thus, whatever the causal link between changes in HRV and neuropsychiatric status in patients with cirrhosis, a

reduction in HRV identifies individuals who at risk of death and could be used to monitor patients over time and perhaps facilitate selection for transplantation. It could also be speculated that the decrease in HRV observed in several other neuropsychiatric conditions might relate to changes in inflammatory cytokines and this possibility should be explored.

7. References

Abraham E, Anzueto A, Gutierrez G, Tessler S, San Pedro G, Wunderink R, Dal Nogare A, Nasraway S, Berman S, Cooney R, Levy H, Baughman R, Rumbak M, Light RB, Poole L, Allred R, Constant J, Pennington J, Porter S. Double-blind randomised controlled trial of monoclonal antibody to human tumour necrosis factor in treatment of septic shock. NORASEPT II Study Group. Lancet. 1998; 351: 929-933.

Akaike T, Inoue K, Okamoto T, Nishino H, Otagiri M, Fujii S, Maeda H. Nanomolar quantification and identification of various nitrosothiols by high performance liquid chromatography coupled with flow reactors of metals and Griess reagent. J Biochem. 1997; 122: 459-466.

Akaike T. Mechanisms of biological S-nitrosation and its measurement. Free Radic Res. 2000; 33: 461-469.

Alderton WK, Cooper CE, Knowles RG. Nitric oxide synthases: structure, function and inhibition. Biochem J. 2001; 357: 593-615.

Altimiras J. Understanding autonomic sympathovagal balance form short-term heart rate variations: are we analyzing noise? Comp Biochem Physiol. 1999; 124: 447-460.

Amodio P, Marchetti P, Del Piccolo F, de Tourtchaninoff M, Varghese P, Zuliani C, Campo G, Gatta A, Guerit JM. Spectral versus visual EEG analysis in mild hepatic encephalopathy. Clin Neurophysiol. 1999; 110: 1334-1344.

Amodio P, Wenin H, Del Piccolo F, Mapelli D, Montagnese S, Pellegrini A, Musto C, Gatta A, Umiltá C. Variability of trail making test, symbol digit test and line trait test in normal people. A normative study taking into account age-dependent decline and sociobiological variables. Aging Clin Exp Res. 2002; 14:117-131.

Anand R, Harry D, Holt S, Milner P, Dashwood M, Goodier D, Jarmulowicz M, Moore K. Endothelin is an important determinant of renal function in a rat model of acute liver and renal failure. Gut. 2002; 50:111–117.

Aronson D, Mittleman MA, Burger AJ. Interleukin-6 levels are inversely correlated with heart rate variability in patients with decompensated heart failure. J Cardiovasc Electrophysiol. 2001; 12: 294-300.

Aronson D, Mittleman MA, Burger AJ. Measures of heart period variability as predictors of mortality in hospitalized patients with decompensated congestive heart failure. Am J Cardiol. 2004; 93: 59-63.

Aslan M, Ryan TM, Townes TM, Coward L, Kirk MC, Barnes S, et al. Nitric oxide-dependent generation of reactive species in sickle cell disease. Actin tyrosine induces defective cytoskeletal polymerization. J Biol Chem. 2003; 278: 4194-4204.

Ates F, Topal E, Kosar F, Karincaoglu M, Yildirim B, Aksoy Y, Aladag M, Harputluoglu MMM, Demirel U, Alan H, Hilmioglu F. The relationship of heart rate variability with severity and prognosis of cirrhosis. Dig Dis Sci. 2006; 51: 1614-1618.

Augusto O, Bonini MG, Amanso AM, Linares E, Santos CC, De Menezes SL. Nitrogen dioxide and carbonate radical anion: two emerging radicals in biology. Free Radic Biol Med. 2002; 32: 841–859.

Aulak KS, Miyagi M, Yan L, West KA, Massillon D, Crabb JW, Stuehr DJ. Proteomic method identifies proteins nitrated in vivo during inflammatory challenge. Proc Natl Acad Sci USA. 2001; 98: 12056-12061.

Baker PR, Schopfer FJ, Sweeney S, Freeman BA. Red cell membrane and plasma linoleic acid nitration products: synthesis, clinical identification, and quantitation. Proc Natl Acad Sci USA. 2004; 101: 11577–11582.

Bal JS, Thuluvath PJ. Prolongation of QTc interval: relationship with etiology and severity of liver disease, mortality and liver transplantation Liver Int. 2003; 23: 243-248.

Balabanli B, Kamisaki Y, Martin E, Murad F. Requirements for heme and thiols for the nonenzymatic modification of nitrotyrosine. Natl Acad Sci USA. 1999; 96: 13136-13141.

Baldus S, Eiserich JP, Mani AR, Castro L, Figueroa M, Chumley P, et al. Endothelial transcytosis of myeloperoxidase confers specificity to vascular ECM proteins as targets of tyrosine nitration. J Clin Invest. 2001; 108: 1759-1770.

Balligand JL, Cannon PJ. Nitric oxide synthases and cardiac muscle. Autocrine and paracrine influences. Arterioscler Thromb Vasc Biol. 1997; 17: 1846-1858.

Barton M, Shaw S, d'Uscio LV, Moreau P, Luscher TF. Angiotensin II increases vascular and renal endothelin-1 and functional endothelin converting enzyme activity in vivo: role of ETA receptors for endothelin regulation. Biochem Biophys Res Commun. 1997; 238: 861-865.

Batkai S, Jarai Z, Wagner JA, Goparaju SK, Varga K, Liu J, Wang L, Mirshahi F, Khanolkar AD, Makriyannis A, Urbaschek R, Garcia N Jr, Sanyal AJ, Kunos G. Endocannabinoids acting at vascular CB1 receptors mediate the vasodilated state in advanced liver cirrhosis. Nat Med. 2001; 7: 827-832.

Beal MF, Ferrante RJ, Browne SE, Matthews RT, Kowall NW, Brown RH Jr. Increased 3-nitrotyrosine in both sporadic and familial amyotrophic lateral sclerosis. Ann Neurol. 1997; 42:644–654.

Beckman JS. Oxidative damage and tyrosine nitration from peroxynitrite. Chem. Res. Toxicol. 1996; 9: 836-844.

Benoit JN, Zimmerman B, Premen AJ, Go VL, Granger DN. Role of glucagon in splanchnic hyperemia of chronic portal hypertension. Am J Physiol. 1986; 251: G674-677.

Bernardi M, Trevisani F, De Palma R, Ligabue A, Capani F, Baraldini M, et al. Chronobiological evaluation of sympathoadrenergic function in cirrhosis. Relationship with arterial pressure and heart rate. Gastroenterology. 1987; 93: 1178-1186.

Bernardi M, Rubboli A, Trevisani F, Cancellieri C, Ligabue A, Baraldini M, et al. Reduced cardiovascular responsiveness to exercise-induced sympatho-adrenergic stimulation in patients with cirrhosis. J Hepatol. 1991; 12: 207-216.

Bernardi M, Calandra S, Colantoni A, Trevisani F, Raimondo ML, Sica G, Schepis F, Mandini M, Simoni P, Contin M, Raimondo G. Q-T interval prolongation in cirrhosis: prevalence, relationship with severity, and etiology of the disease and possible pathogenetic factors. Hepatology. 1998; 27: 28-34.

Beasley D. Interleukin 1 and endotoxin activate soluble guanylate cyclase in vascular smooth muscle. Am J Physiol. 1990; 259: R38-R44.

Blei AT. Infection, inflammation and hepatic encephalopathy, synergism redefined. J Hepatol. 2004; 40: 327-30.

Bomzon A, Gali D, Better OS, Blendis LM. Reversible suppression of the obstructive vascular contractile response in rats with obstructive jaundice. J Lab Clin Med 1985; 105: 568–572.

Bomzon A, Holt S, Moore K. Bile acids, oxidative stress and renal function in biliary obstruction. Semin Nephrol .1997; 17: 549-562.

Bosch J, Garcia-Pagan JC. Complications of cirrhosis. I. Portal hypertension. J Hepatol. 2000; 32: 141-156.

Bosch J, D'Amico G, García-Pagán JC. Portal hypertension. In: Schiff ER, Sorrell MF, Maddrey WC, eds. Schiff's Diseases of The Liver. pp 419-483, Lippincott Williams & Wilkins 2007, Tenth edition.

Bredt DS, Snyder SH. Isolation of nitric oxide synthetase, a calmodulin-requiring enzyme. Proc Natl Acad Sci USA. 1990; 87: 682–685.

Calver A, Harris A, Maxwell JD, Vallance P. Effect of local inhibition of nitric oxide synthesis on forearm blood flow and dorsal hand vein size in patients with alcoholic cirrhosis. Clin Sci. 1994; 86: 203-208.

Cassina AM, Hodara R, Souza JM, Thomson L, Castro L, Ischiropoulos H, Freeman BA, Radi R. Cytochrome c nitration by peroxynitrite. J Biol Chem. 2000; 275: 21409-15.

Chaves AA, Mihm MJ, Schanbacher BL, Basuray A, Liu C, Ayers LW, et al. Cardiomyopathy in a murine model of AIDS: evidence of reactive nitrogen species and corroboration in human HIV/AIDS cardiac tissues. Cardiovasc Res. 2003; 60: 108-118.

Child CG, Turcotte JG. Surgery and portal hypertension. In: The liver and portal hypertension. Edited by CG Child. Philadelphia: Saunders 1964:50-64.

Chung MK, Gulick TS, Rotondo RE, Schreiner GF, Lange LG. Mechanism of action of cytokine inhibition of ß-adrenergic agonist stimulation of cyclic AMP in rat cardiac myocytes: impairment of signal transduction. Circ Res. 1990; 67:753-763

Coelho L, Saraiva S, Guimaraes H, Feitas D, Providencia LA. Autonomic function in chronic liver disease assessed by heart rate variability study. Rev Port Cardiol. 2001; 20: 25-36.

Conn HO, Leevy CM, Vlahcevic ZR, Rodgers JB, Maddrey WC, Seeff L, Levy LL. Comparison of lactulose and neomycin in the treatment of chronic portal-systemic encephalopathy: a double blind controlled trial. Gastroenterology. 1977; 72: 573-83.

Conn HO. Trailmaking and number-connection tests in the assessment of mental state in portal systemic encephalopathy. Am J Dig Dis. 1977; 22: 541-50.

Cooper CE. Nitric oxide and iron proteins. Biochim Biophys Acta. 1999; 1411:290–309.

Corson MA, James NL, Latta SE, Nerem RM, Berk BC, Harrison DG. Phosphorylation of

endothelial nitric oxide synthase in response to fluid shear stress. Circ. Res. 1996; 79: 984–991.

Crow JP. Measurement and significance of free and protein-bound 3-nitrotyrosine, 3-chlorotyrosine, and free 3-nitro-4-hydroxyphenylacetic acid in biologic samples: a high-performance liquid chromatography method using electrochemical detection. Methods Enzymol. 1999; 301:151–160.

Dagher L, Moore K. The hepatorenal syndrome. Gut. 2001; 49: 729-737.

Denicola A, Freeman BA, Trujillo M, Radi R. Peroxynitrite reaction with carbon dioxide/bicarbonate: kinetics and influence on peroxynitrite-mediated oxidations. Arch Biochem Biophys. 1996; 333: 49–58.

Dimmeler S, Fleming I, Fisslthaler B, Hermann C, Busse R, Zeiher AM. Activation of nitric oxide synthase in endothelial cells by Akt-dependent phosphorylation. Nature.1999; 399: 601–605.

Drab M, Verkade P, Elger M, Kasper M, Lohn M, Lauterbach B, Menne J, Lindschau C, Mende F, Luft FC, Schedl A, Haller H, Kurzchalia TV. Loss of caveolae, vascular dysfunction, and pulmonary defects in caveolin-1 gene-disrupted mice. Science. 2001 28; 293: 2449-2452.

Ducrocq C, Dendane M, Laprevote O, Serani L, Das BC, Bouchemal-Chibani N, Doan BT, Gillet B, Karim A, Carayon A, Payen D. Chemical modifications of the vasoconstrictor peptide angiotensin II by nitrogen oxides (NO, HNO2, HOONO)--evaluation by mass spectrometry. Eur J Biochem. 1998; 253: 146-153.

Eiserich JP, Hristova M, Cross CE, Jones AD, Freeman BA, Halliwell B, van der Vliet A. Formation of nitric oxide-derived inflammatory oxidants by myeloperoxidase in neutrophils. Nature. 1998; 391:393–397.

Eiserich JP, Patel RP, O'Donnell VB. Pathophysiology of nitric oxide and related species: free radical reactions and modification of biomolecules. Mol Aspects Med. 1998; 19: 221-357.

Eiserich, JP, Estévez, AG, Bamberg TV, Ye YZ, Chumley PH, Beckman JS, Freeman BA. Microtubule dysfunction by posttranslational nitrotyrosination of α-tubulin: A nitric oxide-dependent mechanism of cellular injury. Proc Natl Acad Sci USA. 1999; 96: 6365–6370.

Evans WH. Isolation and characterization of membranes and cell organelles. In: Rickwood, D., ed. Preparative centrifugation, a practical approach. pp. 233–270. Oxford University Press, Oxford, 1992.

Evelyn KA, Malloy HT. Microdetermination of oxyhemoglobin methemoglobin, and sulfhemoglobin in a single sample of blood. J Biol Chem. 1938; 126:655–662.

Fell V, Hoskins JA, Pollitt RJ. The labelling of urinary acids after oral doses of deuterated L-phenylalanine and L-tyrosine in normal subjects. Quantitative studies with implications for the deuterated phenylalanine load test in phenylketonuria. Clin Chim Acta. 1978; 83: 259–269.

Feron O, Belhassen L, Kobzik L, Smith TW, Kelly RA, Michel T. Endothelial nitric oxide synthase targeting to caveolae. Specific interactions with caveolin isoforms in cardiac myocytes and endothelial cells. J Biol Chem. 1996; 271: 22810–22814.

Feelisch M, Rassaf T, Mnaimneh S, Singh N, Bryan NS, Jourd'Heuil D, Kelm M. Concomitant S-, N-, and heme-nitros(yl)ation in biological tissues and fluids: implications for the fate of NO in vivo. FASEB J. 2002; 16:1775–1785.

Fernandez M, Garcia-Pagan JC, Casadevall M, Mourelle MI, Pique JM, Bosch J, Rodes J. Acute and chronic cyclooxygenase blockage in portal-hypertensive rats: influence in nitric oxide biosynthesis. Gastroenterology. 1996; 110: 1529-1535.

Fernandez M, Bonkovsky HL. Increased heme oxygenase-1 gene expression in liver cells and splanchnic organs from portal hypertensive rats. Hepatology. 1999; 29:1672-1679.
Fernandez M, Lambrecht RW, Bonkovsky HL. Increased heme oxygenase activity in splanchnic organs from portal hypertensive rats: role in modulating mesenteric vascular reactivity. J Hepatol. 2001; 34: 812-817.

Fernandez-Rodriguez CM, Prieto J, Quiroga J, Zozaya JM, Andrade A, Rodriguez-Ortigosa C. Enhanced urinary excretion of cGMP in liver cirrhosis. Relationship to hemodynamic changes, neurohormonal activation, and urinary sodium excretion. Dig Dis Sci. 1997; 42: 1416-1420.

Fernando B, Marley R, Holt S, Anand R, Harry D, Sanderson P, Smith R, Hamilton G, Moore K. N-acetylcysteine prevents development of the hyperdynamic circulation in the portal hypertensive rat. Hepatology. 1998; 28: 689-694.

Fleisher LA, Fleckenstein JF, Frank SM, Thuluvath PJ. Heart rate variability as a predictor of autonomic dysfunction in patients awaiting liver transplantation. Dig Dis Sci. 2000; 45: 340-344.

Friedman SL. Hepatic fibrosis In: Schiff ER, Sorrell MF, Maddrey WC, eds. Schiff's Diseases of The Liver. pp 395-410, Lippincott Williams & Wilkins 2007, Tenth edition.

Frost MT, Halliwell B, Moore KP. Analysis of free and protein-bound nitrotyrosine in human plasma by a gas chromatography/mass spectrometry method that avoids nitration artifacts. Biochem J. 2000; 345:453-458.

Fukuyama N, Takebayashi Y, Hida M, Ishida H, Ichimori K, Nakazawa H. Clinical evidence of peroxynitrite formation in chronic renal failure patients with septic shock. Free Radic Biol Med. 1997; 22: 771-774.

Funakoshi H, Kubota T, Kawamura N, Machida Y, Feldman AM, Tsutsui H, Shimokawa H, Takeshita A. Disruption of inducible nitric oxide synthase improves beta-adrenergic inotropic responsiveness but not the survival of mice with cytokine-induced cardiomyopathy, Circ. Res. 2002; 90: 959–965

Furchgott RF. Studies on relaxation of rabbit aorta by sodium nitrite: the basis for the proposal that the acid-activatable factor from bovine retractor penis is inorganic nitrite and the endothelium-derived relaxing factor is nitric oxide. In: Vasodilatation: Vascular Smooth Muscle, Peptides, Autonomic Nerves, and Endothelium, edited by Vanhoutte PM. p. 401–414. New York: Raven, 1988.

Gachhui R, Presta A, Bentley DF, Abu-Soud HM, McArthur R, Brudvig G, Ghosh DK Stuehr DJ. Characterization of the reductase domain of rat neuronal nitric oxide synthase generated in the methylotrophic yeast Pichia pastoris. Calmodulin response is complete within the reductase domain itself. J Biol Chem. 1996; 271: 20594–20602.

Gachhui R, Abu-Soud HM, Ghosha DK, Presta A, Blazing MA, Mayer B, George SE, Stuehr DJ. Neuronal nitric-oxide synthase interaction with calmodulin-troponin C chimeras. J Biol Chem. 1998; 273; 5451–5454.

Garcia-Cardena G, Oh P, Liu J, Schnitzer JE, Sessa WC. Targeting of nitric oxide synthase to endothelial cell caveolae via palmitoylation: implications for nitric oxide signaling. Proc Natl Acad Sci USA.1996; 93; 6448–6453.

Garcia-Cardena G, Fan R, Shah V, Sorrentino R, Cirino G, Papapetropoulos A, Sessa WC. Dynamic activation of endothelial nitric oxide synthase by Hsp90. Nature. 1998; 392: 821-824.

Garcia-Gonzalez M, Hernandez-Madrid A, Lopez-Sanroman A, Candela A, Nuno J, Barcena R. Reversal of QT interval electrocardiographic alterations in cirrhotic patients undergoing liver transplantation. Transplant Proc. 1999; 31: 2366-2367.

Gaskari SA, Liu H, Moezi L, Li Y, Baik SK, Lee SS. Role of endocannabinoids in the pathogenesis of cirrhotic cardiomyopathy in bile duct-ligated rats. Br J Pharmacol 2005; 146: 315-323.

Gaskari SA, Honar H, Lee SS. Therapy insight: Cirrhotic cardiomyopathy. Nat Clin Pract Gastroenterol Hepatol. 2006; 3: 329-337.

Genesca J, Gonzalez A, Segura R, Catalan, R, Marti R, Varela E, Cadelina G, Martinez M, Lopez-Talavera JC, Esteban R, Groszmann RJ, Guardia J. Interleukin-6, nitric oxide, and the clinical and hemodynamic alterations of patients with liver cirrhosis. Am J Gastroenterol. 1999; 94: 169-177.

Giles G, Bosworth C, Lancaster J, Kraus D. Hydrogen sulphide as a signalling molecule: liberation of NO from S-nitrosoglutathione. Free Radic Biol Med. 2004; 37: 596.

Gladwin MT, Ognibene FP, Pannell LK, Nichols JS, Pease-Fye ME, Shelhamerm JH, Schechter AN. Relative role of heme nitrosylation and beta-cysteine 93 nitrosation in the transport and metabolism of nitric oxide by hemoglobin in the human circulation. Proc Natl Acad Sci USA. 2000; 97:9943–9948.

Gladwin MT, Schechter AN, Kim-Shapiro DB, Patel RP, Hogg N, Shiva S, Cannon RO 3rd, Kelm M, Wink DA, Espey MG, Oldfield EH, Pluta RM, Freeman BA, Lancaster JR Jr, Feelisch M, Lundberg JO. The emerging biology of the nitrite anion. Nat Chem Biol. 2005; 1: 308-314.

Goldberger AL, Amaral LA, Hausdorff JM, Ivanov PCh, Peng CK, Stanley HE. Fractal dynamics in physiology: alterations with disease and aging. Proc Natl Acad Sci USA. 2002; 99: 2466-2472.

Goldberger AL. Giles F. Filley lecture. Complex systems. Proc Am Thorac Soc. 2006; 6: 467-471.

Goldman RK, Vlessis AA, Trunkey DD. Nitrosothiol quantification in human plasma. Anal Biochem. 1998; 259: 98-103.

Gomis R, Fernandez-Alvarez J, Pizcueta P, Fernandez M, Casamitjana R, Bosch J, Rodes J. Impaired function of pancreatic islets from rats with portal hypertension resulting from cirrhosis and partial portal vein ligation. Hepatology. 1994; 19:1257-1261.

Gonzalez-Clemente JM, Mauricio D, Richart C, Broch M, Caixas A, Megia A, Gimenez-Palop O, Simon I, Martinez-Riquelme A, Gimenez-Perez G, Vendrell J. Diabetic neuropathy is associated with activation of the TNF-alpha system in subjects with type 1 diabetes mellitus. Clin Endocrinol (Oxf). 2005; 63: 525-529.

Gonzalez-Clemente JM, Vilardell C, Broch M, Megia A, Caixas A, Gimenez-Palop O, Richart C, Simon I, Martinez-Riquelme A, Arroyo J, Mauricio D, Vendrell J. Lower heart rate variability is associated with higher plasma concentrations of IL-6 in type 1 diabetes. Eur J Endocrinol 2007; 157: 31-38.

Goodwin DC, Gunther MR, Hsi LC, Crews BC, Eling TE, Mason RP, Marnett LJ. Nitric oxide trapping of tyrosyl radicals generated during prostaglandin endoperoxide synthase turnover. Detection of the radical derivative of tyrosine 385. J Biol Chem. 1998; 273: 8903-8909.

Gorg B, Wettstein M, Metzger S, Schliess F, Haussinger D. Lipopolysaccharide-induced tyrosine nitration and inactivation of hepatic glutamine synthetase in the rat. Hepatology. 2005; 41: 1065-1073.

Gow AJ, Buerk DG, and Ischiropoulos H. A novel reaction mechanism for the formation of S-nitrosothiol in vivo. J Biol Chem. 1997; 272: 2841–2845.

Gow AJ, Farkouh CR, Munson DA, Posencheg MA, Ischiropoulos H. Biological significance of nitric oxide-mediated protein modifications. Am J Physiol Lung Cell Mol Physiol. 2004; 287: L262-L268.

Graebe M, Brond L, Christensen S, Nielsen S, Olsen NV, Jonassen TE. Chronic nitric oxide synthase inhibition exacerbates renal dysfunction in cirrhotic rats. Am J Physiol Renal Physiol. 2004; 286: F288-F297.

Griffin MP, Lake DE, Bissonette EA, Harrell FE Jr, O'Shea TM, Moorman JR. Heart rate characteristics: novel physiomakers to predict neonatal infection and death. Pediatrics. 2005; 116: 1070-1074.

Guarner C, Soriano G, Tomas A, Bulbena O, Novella MT, Balanzo J, Vilardell F, Mourelle M, Moncada S. Increased serum nitrite and nitrate levels in patients with cirrhosis: relationship to endotoxemia. Hepatology. 1993; 18: 1139-1143.

Hamaad A, Sosin M, Blann AD, Patel J, Lip GY, MacFadyen RJ. Markers of inflammation in acute coronary syndromes: association with increased heart rate and reductions in heart rate variability. Clin Cardiol. 2005; 28: 570-576.

Hamster W. Neuropsychologie der latenten hepatischen enzephalopathie. Habilitationsschrift, Universität Tübingen, Tübingen. 1983

Hare JM, Stamler JS. NO/redox disequilibrium in the failing heart and cardiovascular system. J Clin Invest. 2005; 115: 509-517.

Harry D, Anand R, Holt S, Davies S, Marley R, Fernando B, Goodier D, Moore K. Increased sensitivity to endotoxemia in the bile duct-ligated cirrhotic rat. Hepatology. 1999; 30:1198–1205.

Hayashi Y, Nishio M, Naito Y, Yokokura H, Nimura Y, Hidaka H, Watanabe Y. Regulation of neuronal nitric-oxide synthase by calmodulin kinases. J Biol Chem. 1999; 274: 20597–20602.

Hemmens B, Woschitz S, Pitters E, Klosch B, Volker C, Schmidt K, Mayer B. The protein inhibitor of neuronal nitric oxide synthase (PIN): characterization of its action on pure nitric oxide synthases. FEBS Lett. 1998; 430: 397–400.

Hendrickse MT, Thuluvath PJ, Triger DR. Natural history of autonomic neuropathy in chronic liver disease. Lancet 1992; 339: 1462-1464.

Henriksen JH, Bendtsen F, Hansen EF, Moller S. Acute non-selective beta-adrenergic blockade reduces prolonged frequency-adjusted Q-T interval (QTc) in patients with cirrhosis. J Hepatol. 2004; 40: 239-246.

Henriksen JH, Gotze JP, Fuglsang S, Christensen E, Bendtsen F, Moller S. Increased circulating pro-brain natriuretic peptide (proBNP) and brain natriuretic peptide (BNP) in patients with cirrhosis: relation to cardiovascular dysfunction and severity of disease. Gut. 2003; 52: 1511-1517.

Herring N, Danson EJ, Paterson DJ. Cholinergic control of heart rate by nitric oxide is site specific. News Physiol Sci. 2002; 17: 202-206.

Hess DT, Matsumoto A, Kim SO, Marshall HE, Stamler JS. Protein S-nitrosylation: purview and parameters. Nat Rev Mol Cell Biol. 2005; 6: 150-66.

Hobbs AJ. Soluble guanylate cyclase: the forgotten sibling. Trends Pharmacol Sci. 1997; 18: 484–491.

Hogg N, Singh RJ, Konorev E, Joseph J, Kalyanaraman B. S-Nitrosoglutathione as a substrate for gamma-glutamyl transpeptidase. Biochem J. 1997; 323:477–481.

Holt S, Goodier D, Marley R, Patch D, Burroughs A, Fernando B, Harry D, Moore K. Improvement in renal function in hepatorenal syndrome with N-acetylcysteine. Lancet. 1999; 353: 294-295.

Hori N, Wiest R, Groszmann RJ. Enhanced release of nitric oxide in response to changes in flow and shear stress in the superior mesenteric arteries of portal hypertensive rats. Hepatology. 1998; 28: 1467-1473.

Hou Y, Guo Z, Li J, Wang PG. Seleno compounds and glutathione peroxidase Catalyzed decomposition of S-nitrosothiols. Biochem Biophys Res Commun. 1996; 228: 88–93.

Ignarro LJ, Buga GM, Wood KS, Byrns RE, and Chaudhuri G. Endothelium-derived relaxing factor produced and released from artery and vein is nitric oxide. Proc Natl Acad Sci USA. 1987; 84: 9265–9269.

Inserte J, Perello A, Agullo L, Ruiz-Meana M, Schluter KD, Escalona N, Graupera M, Bosch J, Garcia-Dorado D. Left ventricular hypertrophy in rats with biliary cirrhosis. Hepatology. 2003; 38: 589-598.

Irie Y, Saeki M, Kamisaki Y, Martin E, Murad F. Histone H1.2 is a substrate for denitrase, an activity that reduces nitrotyrosine immunoreactivity in proteins. Proc Natl Acad Sci USA. 2003; 100: 5634-5639.

Ischiropoulos H. Biological tyrosine nitration: a pathophysiological function of nitric oxide and reactive oxygen species. Arch Biochem Biophys. 1998; 356: 1–11.

Iwakiri Y, Cadelina G, Sessa WC, Groszmann RJ. Mice with targeted deletion of eNOS develop hyperdynamic circulation associated with portal hypertension. Am J Physiol Gastrointest Liver Physiol. 2002; 283: G1074-G1081.

Iwakiri Y, Tsai MH, McCabe TJ, Gratton JP, Fulton D, Groszmann RJ, Sessa WC. Phosphorylation of eNOS initiates excessive NO production in early phases of portal hypertension. Am J Physiol Heart Circ Physiol. 2002; 282: H2084-H2090.

Jaffrey SR, Snyder SH. PIN: an associated protein inhibitor of neuronal nitric oxide synthase. Science. 1996; 274: 774–777.

Jaffrey SR, Erdjument-Bromage H, Ferris CD, Tempest P, Snyder SH. Protein S-nitrosylation: a physiological signal for neuronal nitric oxide. Nat Cell Biol. 2001; 3:193–197.

Jahngen-Hodge J, Obin MS, Gong X, Shang F, Nowell TR Jr, Gong J, et al. Regulation of ubiquitin-conjugating enzymes by glutathione following oxidative stress. J Biol Chem 1997; 272: 28218-28226.

Janssen BJ, De Celle T, Debets JJ, Brouns AE, Callahan MF, Smith TL. Effects of anesthetics on systemic hemodynamics in mice. Am J Physiol Heart Circ Physiol. 2004; 287:H1618-H1624.

Jourd'Heuil D, Mai CT, Laroux FS, Wink DA, Grisham MB. The reaction of S-nitrosoglutathione with superoxide. Biochem Biophys Res Commun. 1998; 246:525-530.

Jourd'Heuil D, Hallen K, Feelisch M, Grisham MB. Dynamic state of S-nitrosothiols in human plasma and whole blood. Free Radic Biol Med. 2000; 28:409–417.

Jover R, Rodrigo R, Felipo V, Insausti R, Saez-Valero J, Garcia-Ayllon MS, Suarez I, Candela A, Compan A, Esteban A, Cauli O, Auso E, Rodriguez E, Gutierrez A, Girona E, Erceg S, Berbel P, Perez-Mateo M. Brain edema and inflammatory activation in bile duct ligated rats with diet-induced hyperammonemia: a model of hepatic encephalopathy in cirrhosis. Hepatology. 2006; 43: 1257-66.

Ju H, Zou R, Venema VJ, Venema RC. Direct interaction of endothelial nitric-oxide synthase and caveolin-1 inhibits synthase activity. J Biol Chem. 1997; 272: 18522–18525.

Kamisaki Y, Wada K, Bian K, Balabanli B, Davis K, Martin E, Behbod F, Lee YC, Murad F. An activity in rat tissues that modifies nitrotyrosine-containing proteins. Proc Natl Acad Sci USA. 1998; 95: 11584-11589.

Kanski J, Behring A, Pelling J, Schoneich C. Proteomic identification of 3-nitrotyrosine-containing rat cardiac proteins: effects of biological aging. Am J Physiol Heart Circ Physiol. 2005; 288: H371-H381.

Kharitonov VG, Sundquist AR, and Sharma VS. Kinetics of nitrosation of thiols by nitric oxide in the presence of oxygen. J Biol Chem. 1995; 270: 28158–28164.

Kim JH, Yi SH, Yoo CS, Yang SA, Yoon SC, Lee KY, Ahn YM, Kang UG, Kim YS. Heart rate dynamics and their relationship to psychotic symptom severity in clozapine-treated schizophrenic subjects. Prog Neuropsychopharmacol Biol Psychiatry. 2004; 28: 371-378.

Kim CK, McGorray SP, Bartholomew BA, Marsh M, Dicken T, Wassertheil-Smoller S, Curb JD, Oberman A, Hsia J, Gardin J, Wong ND, Barton B, McMahon RP, Sheps DS. Depressive symptoms and heart rate variability in postmenopausal women. Arch Intern Med 2005; 165: 1239-1244.

Kim DH, Lipsitz LA, Ferrucci L, Varadhan R, Guralnik JM, Carlson MC, Fleisher LA, Fried LP, Chaves PH. Association between reduced heart rate variability and cognitive impairment in older disabled women in the community: Women's Health and Aging Study I. J Am Geriatr Soc 2006; 54: 1751-1757.

King SM, Barbarese E, Dillman JF, Patel-King RS, Carson JH, Pfister KK. Brain cytoplasmic and flagellar outer arm dyneins share a highly conserved Mr 8,000 light chain. J Biol Chem 1996; 271: 19358–19366.

Knowles ME, McWeeny DJ, Couchman L, Thorogood M. Interaction of nitrite with proteins at gastric pH. Nature.1974; 247: 288-289.

Komeima K, Hayashi Y, Naito Y, Watanabe Y. Inhibition of neuronal nitric-oxide synthase by calcium/calmodulin-dependent protein kinase IIalpha through Ser847 phosphorylation in NG108–NG115 neuronal cells. J Biol Chem 2000; 275: 28139–28143.

Kostka P, Xu B, Skiles EH. Degradation of S-nitrosocysteine in vascular tissue homogenates: role of divalent ions. J Cardiovasc Pharmacol. 1999; 33: 665–670.

Kowalski HJ, Abelmann WH. The cardiac output at rest in Laennec's cirrhosis. J Clin Invest. 1953; 32: 1025–1033.

Kravetz D, Bosch J, Arderiu MT, Pizcueta MP, Casamitjana R, Rivera F, Rodes J.
Effects of somatostatin on splanchnic hemodynamics and plasma glucagon in portal hypertensive rats. Am J Physiol. 1988; 254:G322-G328.

Krylatov AV, Maslov LN, Ermakov SY, Barzakh EI, Lasukova OV, Crawford D, Ghadessy R, Serebrov VY. Negative chronotropic effect of cannabinoids and their water-soluble emulsion is related to activation of cardiac CB1 receptors. Bull Exp Biol Med. 2006;142: 450-453.

Kuster H, Weiss M, Willeitner AE, Detlefsen S, Jeremias I, Zbojan J, Geiger R, Lipowsky G, Simbruner G. Interleukin-1 receptor antagonist and interleukin-6 for early diagnosis of neonatal sepsis 2 days before clinical manifestation. Lancet. 1998; 352: 1271-1277.

Kuwahara M, Yayou K, Ishii K, Hashimoto S, Tsubone H, Sugano S. Power spectral analysis of heart rate variability as a new method for assessing autonomic activity in the rat. J Electrocardiol. 1994; 27: 333-337.

Lanza GA, Sgueglia GA, Cianflone D, Rebuzzi AG, Angeloni G, Sestito A, Infusino F, Crea F, Maseri A; SPAI (Stratificazione Prognostica dell'Angina Instabile) Investigators. Relation of heart rate variability to serum levels of C-reactive protein in patients with unstable angina pectoris. Am J Cardiol. 2006; 97: 1702-1706.

Lazzeri C, La Vila G, Laffi G, Vecchiarino S, Gambilonghi F, Gentilini P, Franchi F. Autonomic regulation of the heart and QT interval in non-alcoholic cirrhosis with ascites. Digestion. 1997; 58: 580-586.

Lee SS, Girod C, Braillon A, Hadengue A, Lebrec D. Hemodynamic characterization of chronic bile duct-ligated rats: effects of pentobarbital sodium. Am J Physiol 1986; 251: G176–G180.

Lee SS, Marty J, Mantz J, Samain E, Braillon A, Lebrec D. Desensitization of myocardial beta-adrenergic receptors in cirrhotic rats. Hepatology. 1990; 12: 481-485.

Lee RF, Glenn TK, Lee SS. Cardiac dysfunction in cirrhosis. Best Pract Res Clin Gastroenterol. 2007; 21: 125-140.

Leivas A, Jiménez W, Bruix J, Boix L, Bosch J, Arroyo V, Rivera F, Rodés J. Gene expression of endothelin-1 and ET(A) and ET(B) receptors in human cirrhosis: relationship with hepatic hemodynamics. J Vasc Res. 1998; 35: 186-193.

Lim DG, Sweeney S, Bloodsworth A, White CR, Chumley PH, Krishna NR, Schopfer F, O'Donnell VB, Eiserich JP, Freeman BA. Nitrolinoleate, a nitric oxide-derived mediator of cell function: synthesis, characterization, and vasomotor activity. Proc Natl Acad Sci USA. 2002; 99: 15941-1596.

Liu H, Ma Z, Lee SS. Contribution of nitric oxide to the pathogenesis of cirrhotic cardiomyopathy in bile duct-ligated rats. Gastroenterology. 2000; 118: 937-944.

Liu H, Song D, Lee SS. Role of heme oxygenase-carbon monoxide pathway in pathogenesis of cirrhotic cardiomyopathy in the rat. Am J Physiol Gastrointest Liver Physiol. 2001; 280: G68-G74.

Liu L, Hausladen A, Zeng M, Que L, Heitman J, Stamler JS. A metabolic enzyme for S-nitrosothiols conserved from bacteria to humans. Nature. 2001; 410:490–494.

Ljubuncic P, Tanne Z, Bomzon A. Evidence of a systemic phenomenon for oxidative stress in cholestatic liver disease. Gut. 2000; 47: 710-716.

Loureiro-Silva MR, Cadelina GW, Groszmann RJ. Deficit in nitric oxide production in cirrhotic rat livers is located in the sinusoidal and postsinusoidal areas. Am J Physiol Gastrointest Liver Physiol. 2003; 284: G567-G574.

Lumsden AB, Henderson JM, Kutner MH. Endotoxin levels measured by a chromogenic assay in portal, hepatic and peripheral venous blood in patients with cirrhosis. Hepatology. 1988; 8: 232-236.

Lymar SV, Hurst JK. Rapid reaction between peroxynitrite ion and carbon dioxide: implications for biological activity. J Am Chem Soc. 1995; 117: 8867–8868.

Ma Z, Miyamoto A, Lee SS. Role of altered beta-adrenoceptor signal transduction in the pathogenesis of cirrhotic cardiomyopathy in rats. Gastroenterology. 1996; 110: 1191-1198.

MacMillan-Crow LA, Crow JP, Kerby JD, Beckman JS, Thompson JA. Nitration and inactivation of manganese superoxide dismutase in chronic rejection of human renal allografts. Proc Natl Acad Sci USA. 1996; 93: 11853-11858.

Maheshwari A, Thomas A, Thuluvath PJ. Patients with autonomic neuropathy are more likely to develop hepatic encephalopathy. Dig Dis Sci. 2004; 49: 1584-1588.

Malave HA, Taylor AA, Nattama J, Deswal A, Mann DL. Circulating levels of tumor necrosis factor correlate with indexes of depressed heart rate variability: a study in patients with mild-to-moderate heart failure. Chest. 2003; 123: 716-724.

Mani AR, Nahavandi A, Moosavi M, Safarinejad R, Dehpour AR. Dual nitric oxide mechanisms of cholestasis-induced bradycardia in the rat. Clin Exp Pharmacol Physiol. 2002; 29: 905-908.

Mani AR, Moore KP. Dynamic assessment of nitration reactions in vivo. Methods Enzymol. 2005; 396: 151-159.

Mani AR, Ollosson R, Mani Y, Ippolito S, Moore KP. Heart rate dynamics in iNOS knockout mice. Life Sci. 2006a; 79: 1593-1599.

Mani AR, Ippolito S, Ollosson R, Moore KP. Nitration of cardiac proteins is associated with abnormal cardiac chronotropic responses in rats with biliary cirrhosis. Hepatology. 2006b; 43: 847-856.

Mannick JB. Hausladen A, Liu L, Hess DT, Zeng M, Miao QX, Kane LS, Gow AJ, Stamler JS. Fas-induced caspase denitrosylation. Science. 1999; 284:651–654.
Mannick J, Schonhoff C, Papeta N, Ghafourifar P, Szibor M, Fang K, Gaston B. S-Nitrosylation of mitochondrial caspases. J Cell Biol .2001; 154, 1111–1116.

Marley R, Holt S, Fernando B, Harry D, Anand R, Goodier D, et al. Lipoic acid prevents development of the hyperdynamic circulation in anesthetized rats with biliary cirrhosis. Hepatology. 1999; 29: 1358-1363

Marley R, Feelisch M, Holt S, Moore K. A chemiluminescence-based assay for S-nitrosoalbumin and other plasma S-nitrosothiols. Free Radic Res. 2000; 32: 1–9.

Marley R, Patel RP, Orie N, Ceaser E, Darley-Usmar V, Moore K. Formation of nanomolar concentrations of S-nitroso-albumin in human plasma by nitric oxide. Free Radic Biol Med 2001; 31:688–696.

Moezi L, Gaskari SA, Liu H, Baik SK, Dehpour AR, Lee SS. Anandamide mediates hyperdynamic circulation in cirrhotic rats via CB(1) and VR(1) receptors. Br J Pharmacol. 2006; 149: 898-908.

Morrow JD, Awad JA, Boss HJ, Blair IA, Roberts LJ 2nd. Non-cyclooxygenase-derived prostanoids (F2-isoprostanes) are formed in situ on phospholipids. Proc Natl Acad Sci USA. 1992; 89: 10721-10725.

Marshall HE, Stamler JS. Inhibition of NF-kappa B by S-nitrosylation. Biochemistry. 2001; 40: 1688-1693.

Marshall HE, Stamler JS. Nitrosative stress-induced apoptosis through inhibition of NF-kappa B. J Biol Chem 2002; 277:34223–34228.

Mason MG, Nicholls P, Wilson MT, Cooper CE. Nitric oxide inhibition of respiration involves both competitive (heme) and noncompetitive (copper) binding to cytochrome c oxidase. Proc Natl Acad Sci USA. 2006; 103: 708-713.

Mata-Greenwood E, Jenkins C, Farrow KN, Konduri GG, Russell JA, Lakshminrusimha S, Black SM, Steinhorn RH. eNOS function is developmentally regulated: uncoupling of eNOS occurs postnatally. Am J Physiol Lung Cell Mol Physiol. 2006; 290: L232-L241.

McCabe TJ, Fulton D, Roman LJ, Sessa WC. Enhanced electron flux and reduced calmodulin dissociation may explain "calcium-independent" eNOS activation by phosphorylation. J Biol Chem. 2000; 275: 6123–6128.

Michel JB, Feron O, Sacks D, Michel T. Reciprocal regulation of endothelial nitric-oxide synthase by Ca^{2+}-calmodulin and caveolin. J Biol Chem. 1997; 272: 15583–15586.

Miyajima H, Nomura M, Muguruma N, Okahisa T, Shibata H, Okamura S, Honda H, Shimizu I, Harada M, Saito K, Nakaya Y, Ito S. Relationship between gastric motility, autonomic activity, and portal hemodynamics in patients with liver cirrhosis. J Gastroenterol Hepatol 2001; 16: 647-59.

Mihm MJ, Yu F, Weinstein DM, Reiser PJ, Bauer JA. Intracellular distribution of peroxynitrite during doxorubicin cardiomyopathy: evidence for selective impairment of myofibrillar creatine kinase. Br J Pharmacol. 2002; 135: 581-588.

Misra HP. Reaction of copper–zinc superoxide dismutase with diethyldithiocarbamate. J Biol Chem. 1979; 254:11623–11628.

Mohr S, Stamler JS, Brune B. Posttranslational modification of glyceraldehyde-3-phosphate dehydrogenase by S-nitrosylation and subsequent NADH attachment. J Biol Chem. 1996; 271: 4209-4214.

Moncada S, Erusalimsky JD. Does nitric oxide modulate mitochondrial energy generation and apoptosis? Nat Rev Mol Cell Biol. 2002; 3: 214-220.

Moore KP, Darley-Usmar V, Morrow J, Roberts LJ II. Formation of F2-isoprostanes during oxidation of human low-density lipoprotein and plasma by peroxynitrite. Circ Res. 1995; 77: 335-341.

Moore KP, Mani AR. Measurement of protein nitration and S-nitrosothiol formation in biology and medicine. Methods Enzymol. 2002; 359:256–268.

Nahavandi A, Dehpour AR, Mani AR, Homayounfar H, Abdoli A, Abdolhoseini MR. The role of nitric oxide in bradycardia of rats with obstructive cholestasis. Eur J Pharmacol. 2001; 411: 135-141.

Newton JL, Allen J, Kerr S, Jones DEJ. Reduced heart rate variability and baroreflex sensitivity in primary biliary cirrhosis. Liver Int. 2006; 26: 197-202.

Nicholson SC, Hahn RT, Grobmyer SR, Brause JE, Hafner A, Potter S, Devereux RB, Nathan CF. Echocardiographic and survival studies in mice undergoing endotoxic shock: effects of genetic ablation of inducible nitric oxide synthase and pharmacologic antagonism of platelet-activating factor. J. Surg. Res. 1999; 86: 198–205.

Nikitovic D, Holmgren A. S-Nitrosoglutathione is cleaved by the thioredoxin system with liberation of glutathione and redox regulating nitric oxide. J Biol Chem. 1996; 271: 19180–19185.

Niskanen JP, Tarvainen MP, Ranta-Aho PO, Karjalainen PA. Software for advanced HRV analysis. Comput Methods Programs Biomed. 2004; 76: 73-81.

Nucaro E, Jodra M, Russell E, Anderson L, Dennison P, Dufton M. Conversion of tyrosine to phenolic derivatives by Taiwan cobra venom. Toxicon. 1998; 36: 1173–1187.

O'Beirne JP, Chouhan M, Hughes RD. The role of infection and inflammation in the pathogenesis of hepatic encephalopathy and cerebral edema in acute liver failure. Nature Clin Pract Gastroenterol Hepatol. 2006; 3: 118-119.

Obin M, Shang F, Gong X, Handelman G, Blumberg J, Taylor A. Redox regulation of ubiquitin-conjugating enzymes: mechanistic insights using the thiol-specific oxidant diamide. FASEB J. 1998; 12: 561-569.

Odeh M, Sabo E, Srugo I, Oliven A. Serum levels of tumor necrosis factor-alpha correlate with severity of hepatic encephalopathy due to chronic liver failure. Liver Int 2004; 24: 110-116.

Odeh M, Sabo E, Srugo I, Oliven A. Relationship between tumor necrosis factor-alpha and ammonia in patients with hepatic encephalopathy due to chronic liver failure. Ann Med. 2005; 37: 603-612.

O'Donnell VB, Freeman BA. Interactions between nitric oxide and lipid oxidation pathways: implications for vascular disease. Circ Res. 2001; 88: 12-21.

Ohshima H, Friesen M, Brouet I, Bartsch H. Nitrotyrosine as a new marker for endogenous nitrosation and nitration of proteins. Food Chem Toxicol. 1990; 28: 647–652.

Orie NN, Vallance P, Jones DP, Moore KP. S-nitroso-albumin carries a thiol-labile pool of nitric oxide, which causes venodilation in the rat. Am J Physiol Heart Circ Physiol. 2005; 289: H916-H923.

Pagano PJ, Clark JK, Cifuentes-Pagano ME, Clark SM, Callis GM, Quinn MT. Localization of a constitutively active, phagocyte-like NADPH oxidase in rabbit aortic adventitia: enhancement by angiotensin II. Proc Natl Acad Sci USA. 1997; 94: 14483-14488.

Palmer RM, Ferrige AG, and Moncada S. Nitric oxide release accounts for the biological activity of endothelium-derived relaxing factor. Nature. 1987; 327: 524–526.

Pannala AS, Mani AR, Rice-Evans CA, Moore KP. pH-dependent nitration of para-hydroxyphenylacetic acid in the stomach. Free Radic Biol Med. 2006; 41: 896-901.

Paolocci N, Ekelund UE, Isoda T, Ozaki M, Vandegaer K, Georgakopoulos D, et al. cGMP-independent inotropic effects of nitric oxide and peroxynitrite donors: potential role for nitrosylation. Am J Physiol Heart Circ Physiol. 2000; 279: H1982-H1988.

Pavlov VA, Ochani M, Gallowitsch-Puerta M, Ochani K, Huston JM, Czura CJ, Al-Abed Y, Tracey KJ. Central muscarinic cholinergic regulation of the systemic inflammatory response during endotoxemia. Proc Natl Acad Sci USA. 2006; 103: 5219-5223.

Perez-Mato I, Castro C, Ruiz FA, Corrales FJ, Mato JM. Methionine adenosyltransferase S-nitrosylation is regulated by the basic and acidic amino acids surrounding the target thiol. J Biol Chem. 1999; 274: 17075-17079.

Petersson, H. Steen, D.E. Kalume, K. Caidahl, and P. Roepstorff, J. Investigation of tyrosine nitration in proteins by mass spectrometry. Mass Spectrom. 2001; 36: 616-625.

Petros A, Bennett D, Vallance P. Effect of nitric oxide synthase inhibitors on hypotension in patients with septic shock. Lancet. 1991; 338: 1557-1558.

Pizcueta MP, Garcia-Pagan JC, Fernandez M, Casamitjana R, Bosch J, Rodes J. Glucagon hinders the effects of somatostatin on portal hypertension. A study in rats with partial portal vein ligation. Gastroenterology. 1991; 101: 1710-1715.

Ponikowski P, Anker SD, Chua TP, Szelemej R, Piepoli M, Adamopoulos S, Webb-Peploe K, Harrington D, Banasiak W, Wrabec K, Coates AJ. Depressed heart rate variability as an independent predictor of death in chronic congestive heart failure secondary to ischaemic or idiopathic dilated cardiomyopathy. Am J Cardiol. 1997; 79: 1645-1650.

Pozzi M, Carugo S, Boari G, Pecci V, de Ceglia S, Maggiolini S, Bolla GB, Roffi L, Failla M, Grassi G, Giannattasio C, Mancia G. Evidence of functional and structural cardiac abnormalities in cirrhotic patients with and without ascites. Hepatology. 1997; 26: 1131-1137.

Pryor WA, Squadrito GL. The chemistry of peroxynitrite: a product from the reaction of nitric oxide with superoxide. Am J Physiol. 1995; 268: L699-L722.

Pryor WA, Houk KN, Foote CS, Fukuto JM, Ignarro LJ, Squadrito GL, Davies KJ. Free radical biology and medicine: it's a gas, man! Am J Physiol Regul Integr Comp Physiol. 2006; 291: R491-R511.

Pugh RN, Murray-Lyon IM, Dawson JL, Pietroni MC, Williams R. Transection of the oesophagus for bleeding oesophageal varices. Br J Surg 1973; 60: 646-649.

Radi R. Nitric oxide, oxidants, and protein tyrosine nitration. Proc Natl Acad Sci USA 101; 2004: 4003–4008.

Ramond MJ, Comoy E, Lebrec D. Alterations in isoprenaline sensitivity in patients with cirrhosis: evidence of abnormality of the sympathetic nervous activity. Br J Clin Pharmacol. 1986; 21: 191-196.

Rasaratnam B, Connelly N, Chin-Dusting J. Nitric oxide and the hyperdynamic circulation in cirrhosis: is there a role for selective intestinal decontamination? Clin Sci. 2004; 107: 425-434.

Regan TJ, Levinson GE, Oldewurtel HA, Frank MJ, Weisse AB, Moschos CB. Ventricular function in noncardiacs with alcoholic fatty liver: role of ethanol in the production of cardiomyopathy. J Clin Invest. 1969; 48: 397-407.

Richman JS, Moorman JR. Physiological time-series analysis using approximate entropy and sample entropy. Am J Physiol Heart Circ Physiol. 2000; 278: H2039-H2049.

Ridnour LA, Thomas DD, Mancardi D, Espey MG, Miranda KM, Paolocci N, et al. The chemistry of nitrosative stress induced by nitric oxide and reactive nitrogen oxide species: putting perspective on stressful biological situations. Biol Chem. 2004; 385: 1-10.

Riordan SM, Skinner N, Nagree A, McCallum H, Mc Iver CJ, Kurtovic J, Hamilton JA, Bengmark S, Williams R, Visvanathan K. Peripheral blood mononuclear cell expression of toll-like receptors and relation to cytokine levels in cirrhosis. Hepatology. 2003; 37: 1154-1164.

Ros J, Claria J, To-Figueras J, Planaguma A, Cejudo-Martin P, Fernandez-Varo G, Martin-Ruiz R, Arroyo V, Rivera F, Rodes J, Jimenez W. Endogenous cannabinoids: a new system involved in the homeostasis of arterial pressure in experimental cirrhosis in the rat. Gastroenterology. 2002; 122: 85-93.

Rossi R, Giustarini D, Milzani A, Colombo R, Dalle-Donne I, Di Simplicio P. Physiological levels of S-nitrosothiols in human plasma. Circ Res. 2001; 89: E47.

Ruiz-del-Arbol L, Monescillo A, Jimenez W, Garcia-Plaza A, Arroyo V, Rodes J. Paracentesis-induced circulatory dysfunction: mechanism and effect on hepatic hemodynamics in cirrhosis. Gastroenterology. 1997; 113: 579-586.

Ruiz-del-Arbol L, Urman J, Fernandez J, Gonzalez M, Navasa M, Monescillo A, Albillos A, Jimenez W, Arroyo V. Systemic, renal, and hepatic hemodynamic derangement in cirrhotic patients with spontaneous bacterial peritonitis. Hepatology. 2003; 38: 1210-1218.

Ruiz-del-Arbol L, Monescillo A, Arocena C, Valer P, Gines P, Moreira V, Milicua JM, Jimenez W, Arroyo V. Circulatory function and hepatorenal syndrome in cirrhosis. Hepatology. 2005; 42: 439-447.

Shishehbor MH, Aviles RJ, Brennan ML, Fu X, Goormastic M, Pearce GL, Gokce N, Keaney Jr. JF, Penn MS, Sprecher DL, Vita LA, Hazen SL. Association of nitrotyrosine levels with cardiovascular disease and modulation by statin therapy. JAMA 2003; 289: 1675–1680

Schomerus, H., Weissenborn, K., Hamster, W., Rückert, N., Hecker, H. PSE-Syndrom-Test, Swets Test. Services, Swets & Zeitlinger BV, Frankfurt. 1999

Schopfer FJ, Baker PR, Freeman BA. NO-dependent protein nitration: a cell signaling event or an oxidative inflammatory response? Trends Biochem Sci. 2003; 28: 646-654.

Schrier RW, Arroyo V, Bernardi M, Epstein M, Henriksen JH, Rodés J. Peripheral arterial vasodilation hypothesis: a proposal for the initiation of renal sodium and water retention in cirrhosis. Hepatology. 1988; 8: 1151–1157.

Shah V, Wiest R, Garcia-Cardena G, Cadelina G, Groszmann RJ, Sessa WC. Hsp90 regulation of endothelial nitric oxide synthase contributes to vascular control in portal hypertension. Am J Physiol. 1999; 277: G463-G468.

Shawcross DL, Davies NA, Williams R, Jalan R. Systemic inflammatory response exacerbates the neuropsychological effects of induced hyperammonaemia in cirrhosis. J Hepatol 2004; 40: 247-54.

Sherlock S. Cirrhosis of the liver. Oxford Textbook of Medicine. Oxford, Oxford University Press, 1986.

Sherlock S, Dooley J. Diseases of the Liver and Biliary System. Blackwell, London, 2002.

Shimamura M, Kamada S, Hayashi T, Naruse H, Iida Y. Sensitive determination of tyrosine metabolites, p-hydroxyphenylacetic acid, 4-hydroxy-3-methoxyphenyl-acetic acid and 4-

hydroxy-3-methoxymandelic acid, by gas chromatography-negative-ion chemical-ionization mass spectrometry. Application to a stable isotope-labelled tracer experiment to investigate their metabolism in man. J Chromatogr. 1986; 374: 17–26.

Shimokawa T, Kulmacz RJ, DeWitt DL, Smith WL. Tyrosine 385 of prostaglandin endoperoxide synthase is required for cyclooxygenase catalysis. J Biol Chem. 1990; 265: 20073-20076.

Sieber CC, Groszmann RJ. In vitro hyporeactivity to methoxamine in portal hypertensive rats: reversal by nitric oxide blockade. Am J Physiol. 1992a; 262: G996-G1001.

Sieber CC, Groszmann RJ. Nitric oxide mediates hyporeactivity to vasopressors in mesenteric vessels of portal hypertensive rats. Gastroenterology. 1992b; 103: 235-239.

Sokolovsky M, Riordan JF, Vallee BL. Conversion of 3-nitrotyrosine to 3-aminotyrosine in peptides and proteins. Biochem Biophys Res Commun. 1967; 27: 20–25.

Song D, Sharkey KA, Breitman DR, Zhang Y, Lee SS. Disordered central cardiovascular regulation in portal hypertensive and cirrhotic rats. Am J Physiol Gastrointest Liver Physiol. 2001; 280: G420-G430.

Souza JM, Choi I, Chen Q, Weisse M, Daikhin E, Yudkoff M, Obin M, Ara J, Horwitz J, Ischiropoulos H. Proteolytic degradation of tyrosine nitrated proteins. Arch Biochem Biophys. 2000; 380: 360–366.

Spencer NY, Zeng H, Patel RP, Hogg N. Reaction of S-nitrosoglutathione with the heme group of deoxyhemoglobin. J Biol Chem. 2000; 275: 36562–36567.

Stamler JS, Jaraki O, Osborne J, Simon DI, Keaney J, Vita J, Singel D, Valeri CR, Loscalzo J. Nitric oxide circulates in mammalian plasma primarily as an S-nitroso adduct of serum albumin. Proc Natl Acad Sci USA. 1992; 89:7674-7677.

Stipanuk MH, Beck PW. Characterization of the enzymic capacity for cysteine desulphhydration in liver and kidney of the rat. Biochem J. 1982; 206: 267–277.

Strieter RM, Remick DG, Ward PA, Spengler RN, Lynch JP 3rd, Larrick J, Kunkel SL. Cellular and molecular regulation of tumor necrosis factor-alpha production by pentoxifylline. Biochem Biophys Res Commun. 1988; 155: 1230-1236

Suffredini AF, Fromm RE, Parker MM, Brenner M, Kovacs JA, Wesley RA, Parrillo JE. The cardiovascular response of normal humans to the administration of endotoxin. N Engl J Med. 1989; 321: 280-287.

Sun J, Xin C, Eu, JP, Stamler JS, Meissner G. Proc Natl Acad Sci USA 2001; 98: 11158-11162.

Sun Y, Zhang J, Lu L, Chen SS, Quinn MT, Weber KT. Aldosterone-induced inflammation in the rat heart : role of oxidative stress. Am J Pathol 2002; 161: 1773-1781.

Tabrizi-Fard MA, Maurer TS, Fung HL. In vivo disposition of 3-nitro-L-tyrosine in rats: implications on tracking systemic peroxynitrite exposure. Drug Metab Dispos. 1999; 27: 429–431.

Takahama U, Oniki T, Murata H. The presence of 4-hydroxyphenylacetic acid in human saliva and the possibility of its nitration by salivary nitrite in the stomach. FEBS Lett. 2002; 518: 116–118.

Task force report. Heart rate variability. Standards of measurement, physiological interpretation, and clinical use. Task Force of the European Society of Cardiology and the North American Society of Pacing and Electrophysiology. Eur Heart J. 1996; 17: 354-81.

Tateishi Y, Oda S, Nakamura M, Watanabe K, Kuwaki T, Moriguchi T, Hirasawa H. Depressed heart rate variability is associated with high IL-6 blood level and decline in the blood pressure in septic patients. Shock 2007 (in press).

Tavakoli S, Hajrasouliha AR, Jabehdar-Maralani P, Ebrahimi F, Solhpour A, Sadeghipour H, Ghasemi M, Dehpour AR. Reduced susceptibility to epinephrine-induced arrhythmias in cirrhotic rats: the roles of nitric oxide and endogenous opioid peptides. J Hepatol. 2007; 46: 432-439.

Tilg H, Wilmer A, Vogel W, Herold M, Nolchen B, Judmaier G, Huber C. Serum levels of cytokines in chronic liver diseases. Gastroenterology. 1992; 103: 264-74.

Trevisani F, Merli M, Savelli F, Valeriano V, Zambruni A, Riggio O, Caraceni P, Domenicali M, Bernardi M. QT interval in patients with non-cirrhotic portal hypertension and in cirrhotic patients treated with transjugular intrahepatic porto-systemic shunt. J Hepatol. 2003; 38: 461-467.

Trujillo M, Alvarez MN, Peluffo G, Freeman BA, Radi R. Xanthine oxidase-mediated decomposition of S-nitrosothiols. J Biol Chem. 1998; 273: 7828–7834.

Tulppo MP, Makikallio TH, Takala TE, Seppanen T, Huikuri HV. Quantitative beat-to-beat analysis of heart rate dynamics during exercise. Am J Physiol. 1996; 271: H244-H252.

Turko IV, Li L, Aulak KS, Stuehr DJ, Chang JY, Murad F. Protein tyrosine nitration in the mitochondria from diabetic mouse heart: implications to dysfunctional mitochondria in diabetes. J Biol Chem. 2003; 278: 33972-33977.

Uppu RM, Squadrito GL, Pryor WA. Acceleration of peroxynitrite oxidations by carbon dioxide. Arch Biochem Biophys. 1996; 327: 335–343.

Vallance P, Moncada S. Hyperdynamic circulation in cirrhosis: a role for nitric oxide? Lancet. 1991; 337: 776-778.

Vallance P, Leiper J. Blocking NO synthesis: how, where and why? Nat Rev Drug Discov. 2002; 1: 939-50.

Van der Vliet A, Eiserich JP, Halliwell B, Cross CE. Formation of reactive nitrogen species during peroxidase-catalyzed oxidation of nitrite. A potential additional mechanism of nitric oxide-dependent toxicity. J Biol Chem. 1997; 272: 7617–7625.

Van der Vliet A. Tyrosine nitration: who did it, and how do we prove it? A commentary on "pH dependent nitration of para-hydroxyphenylacetic acid in the stomach". Free Radic Biol Med. 2006; 41: 869-871

Van Obbergh L, Vallieres Y, Blaise G. Cardiac modifications occurring in the ascitic rat with biliary cirrhosis are nitric oxide related. J Hepatol. 1996; 24: 747-752.

Varga K, Wagner JA, Bridgen DT, Kunos G. Platelet- and macrophage-derived endogenous cannabinoids are involved in endotoxin-induced hypotension. FASEB J. 1998; 12:1035-1044.

Venema VJ, Ju H, Zou R, Venema RC. Interaction of neuronal nitric-oxide synthase with caveolin-3 in skeletal muscle. Identification of a novel caveolin scaffolding/inhibitory domain. J Biol Chem. 1997; 272; 28187–28190.

Vigo DE, Nicola Siri L, Ladrón De Guevara MS, Martínez-Martínez JA, Fahrer RD, Cardinali DP, Masoli O, Guinjoan SM. Relation of depression to heart rate nonlinear dynamics in patients > or =60 years of age with recent unstable angina pectoris or acute myocardial infarction. Am J Cardiol. 2004; 93: 756-760.

Viner RI, Ferrington DA, Williams TD, Bigelow DJ, Schoneich C. Protein modification during biological aging: selective tyrosine nitration of the SERCA2a isoform of the sarcoplasmic reticulum Ca^{2+}-ATPase in skeletal muscle. Biochem J. 1999; 340: 657-669.

Wechsler D. Wechsler Adult Intelligence Scale. Psychological Corporation. New York, 1955.

Weissenborn K, Ennen JC, Schomerus H, Rückert N, Hecker H. Neuropsychological characterization of hepatic encephalopathy. J Hepatol. 2001; 34: 768-773.

Wiest R, Shah V, Sessa WC, Groszmann RJ. NO overproduction by eNOS precedes hyperdynamic splanchnic circulation in portal hypertensive rats. Am J Physiol. 1999; 276: G1043-G1051.

Wiest R, Das S, Cadelina G, Garcia-Tsao G, Milstien S, Groszmann RJ. Bacterial translocation in cirrhotic rats stimulates eNOS-derived NO production and impairs mesenteric vascular contractility. J Clin Invest. 1999; 104: 1223-1233.

Wiest R, Tsai MH, Groszmann RJ. Octreotide potentiates PKC-dependent vasoconstrictors in portal-hypertensive and control rats. Gastroenterology. 2001; 120: 975-983.

Wiest R, Garcia-Tsao G. Bacterial translocation (BT) in cirrhosis. Hepatology. 2005 41: 422-433.

Williams DL. The chemistry of S-nitrosothiols. Acc Chem Res. 1999; 32: 869–876.

Wink DA, Nims RW, Darbyshire JF, Christodoulou D, Hanbauer I, Cox GW, Laval F, Laval J, Cook JA, and Krishna MC. Reaction kinetics for nitrosation of cysteine and glutathione in aerobic nitric oxide solutions at neutral pH. Insights into the fate and physiological effects of intermediates generated in the NO/O2 reaction. Chem Res Toxicol. 1994; 7: 519–525.

Wong F, Girgrah N, Graba J, Allidina Y, Liu P, Blendis L. The cardiac response to exercise in cirrhosis. Gut. 2001; 49: 268-275.

Wu CT, Eiserich JP, Ansari AA, Coppel RL, Balasubramanian S, Bowlus CL, et al. Myeloperoxidase-positive inflammatory cells participate in bile duct damage in primary biliary cirrhosis through nitric oxide-mediated reactions. Hepatology. 2003; 38: 1018-1025.

Yoshioka K, Kakumu S, Arao M, Tsutsumi Y, Inoue M. Tumor necrosis factor alpha production by peripheral blood mononuclear cells of patients with chronic liver disease. Hepatology. 1989; 10: 769-773.

Zambruni A, Trevisani F, Caraceni P, Bernardi M. Cardiac electrophysiological abnormalities in patients with cirrhosis. J Hepatol. 2006; 44: 994-1002.

Zhang Y, Hogg N. Formation and stability of S-nitrosothiols in RAW 264.7 cells. Am J Physiol Lung Cell Mol Physiol. 2004; 287: L467–L474.

Zulli R, Nicosia F, Borroni B, Agosti C, Prometti P, Donati P, De Vecchi M, Romanelli G, Grassi V, Padovani A. QT dispersion and heart rate variability abnormalities in Alzheimer's disease and in mild cognitive impairment. J Am Geriatr Soc. 2005; 53: 2135-2139.

8. Abbreviation

ANOVA: analysis of variance

ANCOVA: analysis of co-variance

BDL: bile duct-ligated

CB1: cannabinoid receptor 1

CGRP: calcitonin gene-related polypeptide

CTR: control

CysNO: *S*-nitrosocysteine

DS: digit symbol

DTPA: diethylenetriamine pentaacetic acid

ECG: electrocardiogram

EDTA: ethylenediamine tetraacetic acid

EEG: electroencephalogram

eNOS: endothelial nitric oxide synthase

GC: gas chromatography

GC/MS: gas chromatography mass spectrometry

GSNO: *S*-nitrosoglutathione

HE: hepatic encephalopathy

HF: high frequency

HRV: heart rate variability

IL-1: interleukin-1

IL-6: interleukin-6

IL-10: interleukin-10

IL-12: interleukin-12

iNOS: inducible nitric oxide synthase

INR: international normalized ratio

LF: low frequency

L-NAME: N^G-L-nitro-arginine methyl ester

LPS: lipopolysaccharide

LT: line tracing

MS: mass spectrometry

ms: millisecond

NAC: N-acetylcysteine

NCT-A: Number Connection Tests A

NCT-B: Number Connection Tests B

NEO: neomycin

NEM: *N*-ethylmaleimide

NF-κB: nuclear factor κB

NHPA: 3-nitro-4-hydroxyphenylacetic acid

[$^{13}C_8$]NHPA: [1,2,1′,2′,3′,4′,5′,6′-^{13}C]NHPA

[$^{2}H_5$]NHPA: [2,2,2′,5′,6′-^{2}H]NHPA

NICI: negative-ion chemical ionization

NO: nitric oxide

NO_2: nitrogen dioxide

NO_2^-: nitrite

NO_3^-: nitrate

N_2O_3: dinitrogen trioxide

NOS: nitric oxide synthase

nNOS: neuronal nitric oxide synthase

nu: normalized units

$O_2^{\cdot}$: superoxide anion

$ONOO^-$: peroxynitrite

PBS: phosphate buffered saline solution

PGI_2: prostacyclin

PHPA: *para*-hydroxyphenylacetic acid

[$^{13}C_8$]PHPA: [1,2,1′,2′,3′,4′,5′,6′-^{13}C]PHPA

[$^{2}H_6$]PHPA: [2,2,2′,3′,5′,6′-^{2}H]PHPA

POLYB: polymixin B

PTXF: pentoxyfylline

PVDF: polyvinylidene fluoride

RNS: reactive nitrogen species

SampEn: sample entropy

SD: standard deviation

SDNN: standard deviation of beat to beat interval

SDot: serial dotting

SDS: sodium dodecyl sulphate

SDS-PAGE: sodium dodecyl sulphate polyacrylamide gel electrophoresis

SEM: standard error of mean

SOD: superoxide desmutase

TFA: trifluoroacetic acid

TNF-α: tumor necrosis alpha

[$^{13}C_9$]tyrosine: [1,2,3,1′,2′,3′,4′,5′,6′-^{13}C]tyrosine.

UV: ultraviolet

VLF: very low frequency

VR1: vanilloid receptot 1

9. Appendix 1. Publications extracted from this thesis

1. **Mani AR**. Montagnese S, Jackson C, Jenkins CW, Head IM, Stephens RC, Moore KP, Morgan MY. The relationship between decreased heart rate variability and hepatic encephalopathy in patients with cirrhosis. *Gut* 2007 (submitted).

2. **Mani AR**, Ippolito S, Ollosson R, Moore KP. Nitration of cardiac proteins is associated with abnormal cardiac chronotropic responses in rats with biliary cirrhosis. *Hepatology* 2006; 43: 847-856.

3. **Mani AR**, Ollosson R, Mani Y, Ippolito S, Moore KP. Heart rate dynamics in iNOS knockout mice. *Life Sciences* 2006; 79: 1593-9.

4. Pannala AS, **Mani AR**, Rice-Evans CA, Moore KP. pH-dependent nitration of para-hydroxyphenylacetic acid in the stomach. *Free Radicals in Biology and Medicine* 2006; 41: 896-901.

5. **Mani AR**, Ebrahimkhani MR, Ippolito S, Ollosson R, Moore KP. Metalloprotein-dependent decomposition of S-nitrosothiols: Studies on the stabilization and measurement of S-nitrosothiols in tissues. *Free Radiclas in Biology and Medicine* 2006; 40: 1654-1563.

6. Ebrahimkhani MR, Kiani S, Oakley F, Kendall T, Shariftabrizi A, Tavangar SM, Moezi L, Payabvash S, Karoon A, Hoseininik H, Mann DA, Moore KP, **Mani AR** , Dehpour AR. Naltrexone, an opioid receptor antagonist, attenuates liver fibrosis in bile duct ligated rats. *Gut* 2006; 55: 1606-16.

7. Kingdon EJ, **Mani AR**, Frost MT, Denton CP, Powis SH, Black CM, Moore KP. Low plasma protein nitrotyrosine levels are a biochemical hallmark of primary Raynaud's phenomenon. *Annals of Rheumatic Diseases* 2006; 65(7): 952-4.

8. **Mani AR**, Moore KP. Dynamic assessment of nitration reactions in vivo. *Methods in Enzymology* 2005: 396; 151-159.

9. Ebrahimkhani MR, **Mani AR**, Moore K. Hydrogen sulphide and the hyperdynamic circulation in cirrhosis: a hypothesis. *Gut* 2005; 54: 1668-71.

10. Klocke R, **Mani AR**, Moore KP, Morris CJ, Blake DR, Mapp PI. Inactivation of xanthine oxidoreductase is associated with increased joint swelling and nitrotyrosine formation in acute antigen-induced arthritis. *Clinical and Experimental Rheumatology* 2005: 23; 345-350.

11. Dhamrait SS, Stephens JW, Cooper JA, Acharya J, **Mani AR**, Moore K, Miller GJ, Humphries SE, Hurel SJ, Montgomery HE. Cardiovascular risk in healthy men and markers of oxidative stress in diabetic men are associated with common variation in the gene for uncoupling protein II. *European Heart Journal* 2004; 25: 468-75.

12. **Mani AR**, Pannala AS, Orie NN, Ollosson R, Harry D, Rice-Evans CA, Moore KP. Nitration of endogenous *para*-hydroxyphenylacetic acid and the metabolism of nitrotyrosine. *Biochemical Journal* 2003; 374: 521-7.

13. Pannala AS, **Mani AR**, Spencer JP, Skinner V, Bruckdorfer KR, Moore KP, Rice-Evans CA . The effect of dietary nitrate on salivary, plasma, and urinary nitrate metabolism in humans. *Free Radicals in Biology and Medicine* 2003; 34: 576-84.

14. Moore KP, **Mani AR**. Measurement of protein nitration and S-nitrosothiol formation in biology and medicine. *Methods in Enzymology* 2002; 359: 256-68.

15. Baldus S, Eiserich JP, **Mani A**, Castro L, Figueroa M, Chumley P, Ma W, Tousson A, White CR, Bullard DC, Brennan ML, Lusis AJ, Moore KP, Freeman BA. Endothelial transcytosis of myeloperoxidase confers specificity to vascular ECM proteins as targets of tyrosine nitration. *Journal of Clinical Investigation* 2001; 108:1759-70.